UNIVERSITY OF OKLAHOMA

GRADUATE COLLEGE

MONITORING NORMAN, OKLAHOMA FOR TEMPORAL VARIATION IN SARS-CoV-2 USING WASTEWATER DURING UNIVERSITY OF OKLAHOMA FOOTBALL GAMES

A THESIS

SUBMITTED TO GRADUATE FACULTY

in partial fulfillment of the requirements for the degree of

MASTER OF ENVIRONMENTAL SCIENCE

By

EMILY RHODES
Norman, Oklahoma
2022

MONITORING NORMAN, OKLAHOMA FOR TEMPORAL VARIATION IN SARS-CoV-2 USING WASTEWATER DURING UNIVERSITY OF OKLAHOMA FOOTBALL GAMES

A THESIS APPROVED FOR THE
SCHOOL OF CIVIL ENGINEERING AND ENVIRONMENTAL SCIENCE

BY THE COMMITTEE CONSISTING OF

Dr. Jason Vogel, Chair

Dr. Bryce Lowery

Dr. Keith Strevett

Acknowledgments

First, I would like to thank Dr. Vogel for believing in me and guiding me throughout this research and my graduate studies. I am so grateful for the knowledge I have gained from this research, my graduate studies, and numerous other opportunities I have had during my years with the Oklahoma Water Survey. I would like to thank my committee members, Dr. Bryce Lowery, and Dr. Keith Strevett for their expertise and advice during this process.

Next, I would like to thank Dr. Bradley Stevenson, Erin Jefferies, and all the members of the SARS-CoV-2 microbiology laboratory for agreeing to process the additional samples from this project. I know it was a tremendous effort. I would also like to thank Dr. Madison Swayne and Dr. Bryce Lowery for their efforts to access the population data. I also want to thank Ryan Bart, and the rest of the staff at the Norman Water Reclamation Facility for allowing me to sample at the wastewater treatment plant, providing me with additional composite samples, and giving me access to their flow data. Without the help of these groups, this research could not be completed. I also must thank my fellow students and staff at the Oklahoma Water Survey for their help, advice, and comradery during this time.

Finally, I must thank my friends and family who supported me on this path. You all have been there to celebrate every victory and to offer support in times of stress. I could not have done this without you.

Table of Contents

List of Figures

List of Tables

Abstract

Coronavirus Disease 2019, more commonly referred to as COVID-19, is the disease caused by the virus Severe Acute Respiratory Syndrome Coronavirus 2 (SARS-CoV-2). It is difficult to then get an accurate measure of cases through typical epidemiological methods such as clinical testing because many people do not know they have the disease. However, SARS-CoV-2 viral particles are often excreted by infected hosts, including those who are asymptomatic, and can be tracked through wastewater in a process called wastewater-based epidemiology (WBE). A problem that complicates WBE is that humans are not static and move in and out of sewer drainages throughout the day. One way to track human movement anonymously is through their cell phones and a software called StreetLight®. Football games at the University of Oklahoma provided an opportunity to combine WBE with StreetLight software to determine if there was an increase in the amount of SARS-CoV-2 in the wastewater due to large events. To determine this, wastewater samples were taken hourly at the City of Norman Water Reclamation Facility (NWRF) beginning on Saturday mornings and ending on Sunday mornings. To compare the amount of SARS-CoV-2 in the wastewater on gamedays was different than other days, composite samples were collected from the NWRF representing weekdays as well as two control Saturdays were selected to sample (one per football season). Finally, population data was collected at hourly intervals on Saturdays to normalize the SARS-CoV-2 concentrations, resulting in a measure we called the viral load per person and make the amount of SARS-CoV-2 in the wastewater comparable between seasons. This study can inform decision makers about hosting large-scale events throughout the rest of the pandemic, as well as during other disease outbreaks. Furthermore, the viral load per person is a novel way of presenting this data that makes comparing sewer drainages possible.

CHAPTER 1

INTRODUCTION, BACKGROUND, HYPOTHESES AND OBJECTIVES

Coronavirus Disease 2019, more commonly referred to as COVID-19, is the disease caused by the virus Severe Acute Respiratory Syndrome Coronavirus 2 (SARS-CoV-2) (Chakraborty & Maity, 2020). The disease, which broke out in December 2019 in Wuhan, Hubei Province, China, and spread around the globe is a novel coronavirus, which had never been seen before this outbreak (Hu, Guo, Zhou, & Shi, 2020). Since its discovery and declaration as a pandemic, SARS-CoV-2 has continued to spread around the globe, infecting millions of people through at least December 2021 (World Health Organizaton, 2021). With new variants emerging and drastically varying vaccination rates globally, the end of the pandemic may be long off (The Lancet Microbe, 2021). While social distancing, isolating, and other public health strategies are effective at reducing spread, they can be associated with loss of economic revenue and other societal challenges (Bliss, Musikanski, Phillips, & Davidson, 2020). Understanding more about how large events can impact community spread can be beneficial to ending the COVID-19 pandemic and guide decision makers as new diseases emerge.

SARS-CoV-2 has many distinct characteristics. For example, symptoms of COVID-19 range from fever, fatigue, and dry cough, to gastrointestinal troubles, and more severe respiratory disease; however, a sizable portion of those who contract COVID-19 will have mild symptoms or even be asymptomatic – particularly in young people (Hu, Guo, Zhou, & Shi, 2020). It is difficult to then get an accurate measure of cases through typical epidemiological methods such as clinical testing because many people do not know they have the disease. Despite the challenges the large percentage of asymptomatic cases mounts, SARS-CoV-2 viral particles are

often excreted by infected hosts, including those who are asymptomatic, and can be tracked through wastewater in a process called wastewater-based epidemiology (WBE) (Ahmed, et al., 2020).

However, one problem that further complicates matters is that humans are not static, and many people might engage in high-risk activities that were common before the pandemic, such as attending college football games. One way to track human movement anonymously is through their cell phones and a software called StreetLight. Using WBE to measure SARS-CoV-2 concentration as well as anonymously tracking the movement of humans using their cell phones, we can approximate a SARS-CoV-2 viral load per person per hour in wastewater. Given both technologies, football games at the University of Oklahoma (OU) provided an opportunity to calculate a viral load per person starting the morning of the football game through the next morning to track the temporal variability of COVID-19 and human activity through the wastewater. This ability is useful for planning for reducing community spread of the disease, particularly among populations that are less likely to engage in mitigation practices, as well as provide guidance about hosting large events in future disease outbreaks.

1.1 Literature Review

1.1.1 COVID-19 Disease and Pandemic

Coronavirus disease 2019 (COVID-19) is the disease caused by the virus, severe acute respiratory syndrome coronavirus 2 (SARS-CoV-2), a member of the *Coronaviridae* family, which cause diseases ranging from the common cold to severe acute respiratory syndrome (Kitajima, et al., 2020). SARS-CoV-2 is a single-stranded, positive-sense RNA enveloped virus (Polo, et al., 2020). SARS-CoV-2 is in the family of two other well-known coronavirus outbreaks: severe acute respiratory syndrome (SARS) which occurred in 2002 and 2003 and

Middle East Respiratory Syndrome (MERS) which occurred in 2012 (Chakraborty & Maity, 2020). In fact, SARS-CoV-2 shares 79% of its genomic sequence with SARS and 50% with MERS. SARS-CoV-2 is also quite similar to coronaviruses found in bats, particularly a bat coronavirus called RaTG13, with which SARS-CoV-2 shares at least 90% of its sequence identity. Another wildlife species that carries coronaviruses is the pangolin, which has a coronavirus that shares approximately 92% of its sequence identity with SARS-CoV-2. Despite efforts to determine if human encounters with these species lead to current pandemic, the origin of SARS-CoV-2 is still unknown (Hu, Guo, Zhou, & Shi, 2020).

A virus that predominantly impacts the respiratory system, it is spread mostly through inhalation of droplets from an infected person (Chakraborty & Maity, 2020), (Cevik, Kuppalli, Kindrachuk, & Peiris, 2020). The structure of SARS-CoV-2 has three major components, the spike protein, the envelope, and the membrane. It is the spike protein which binds to the host's cells, which is the first step in infection (Cevik, Kuppalli, Kindrachuk, & Peiris, 2020). Once in the host, SARS-CoV-2 may incubate for 2.2 to 11.5 days, with a median of 5.1 days before a person feels symptoms (Lauer, et al., 2020). The reproductive number (R_0) indicates how efficient a virus is at spreading, where greater numbers indicate more efficiency. The R_0 of SARS-CoV-2 ranges from 2.3 (Sunjaya & Jenkins, 2020) to 2.79 (Liu & Rocklöv, 2021). The R_0 of SARS-CoV-2 is greater than that of SARS-CoV-1 (SARS), making it more transmissible (Cevik, Kuppalli, Kindrachuk, & Peiris, 2020). While all age groups are susceptible to being infected by COVID-19, the median age of patients is 50 years old (Hu, Guo, Zhou, & Shi, 2020). In the respiratory tract, the greatest load of SARS-CoV-2 RNA is found at the time of symptom onset or the first week of the illness, thus indicating that a person is most infective during the first week of illness.

SARS-CoV-2 is also shed in the fecal matter of infected persons, though this is not really considered a major route of transmission (Cevik, Kuppalli, Kindrachuk, & Peiris, 2020). While not all people who actively have COVID-19 will shed RNA particles in their feces, approximately 43% will (Zhang, et al., 2021). The exact amount of SARS-CoV-2 shed per infected person is still subject to more investigation but could even vary geographically (Ahmed, et al., 2020). This difference in shedding in feces could be impacted by variants, manifestations or symptoms of the disease, or differences in the populations infected. Furthermore, SARS-CoV-2 RNA particles in the stool commonly are present after shedding has stopped through the respiratory tract (Cevik, Kuppalli, Kindrachuk, & Peiris, 2020).

The symptoms of this disease are typically fever, cough, chest discomfort, fatigue, headache, and diarrhea, among many others (Pullen, et al., 2020). There are several preexisting factors that increase the risk of more severe disease. These preexisting factors include advanced age, hypertension (high blood pressure), cardiovascular disease, chronic obstructive pulmonary disease (COPD), obesity, and diabetes (Cevik, Kuppalli, Kindrachuk, & Peiris, 2020). However, a sizable portion of those infected will have mild symptoms, or may even be asymptomatic, making clinical confirmation of cases difficult (Polo, et al., 2020). The percentage of asymptomatic cases may even be as high as 65% (Yu, et al., 2020). It is possible for asymptomatic persons to spread COVID-19 to healthy individuals, making spread from asymptomatic persons a problem (Yu & Yang, 2020). Getting an accurate count of infections with traditional clinical testing in a timely manner is also difficult due to the volume of cases around the world, shortages of supplies, and a lack of understanding of the disease by medical and academic experts (Lu, Huang, Zhang, & Sha, 2020).

What began as an outbreak of SARS-CoV-2 in Wuhan, China in December 2019 was classified as a pandemic by the world health organization (WHO) in March, 2020 and remains classified as such today (Hu, Guo, Zhou, & Shi, 2020, Lauer, et al., 2020). This disease is the "most consequential infectious disease since the 1918 influenza pandemic" (Polo, et al., 2020). The rapid spread of this disease impacted almost every person on earth in some way (Tarkar, 2020). Beyond the devastating human health impacts this pandemic has had globally, it also has disrupted the global economy and politics. At the start of the pandemic, global travel and, in many cases, domestic travel was stopped. Many companies also took precautions to limit exposure, causing an increase in unemployment and decrease in production (Chakraborty & Maity, 2020).

Public health experts have recommended many ways to limit the spread of COVID-19. These methods range from keeping a distance of at least six feet away from others, to wearing masks or other face coverings, among many others. Table 1 shows the major strategies to reduce spread, as well as community level actions to implement the strategies.

Table 1: Public health strategy and community level actions to prevent spread of COVID-19, adapted from Honein, et al. 2020

Strategy	Action
Universal Masking	Mandate the universal use of masks in indoor settings.
Physical Distancing and Limiting Contacts	Create physical barriers and visual reminders might promote adherence to maintaining physical distance
Avoiding nonessential indoor spaces and crowded outdoor settings	Promote flexible working methods (e.g., telework); restrict the number of people allowed in indoor spaces
Increased testing, diagnosis, and isolation	Increase access to rapid, affordable testing
Prompt case investigation and contact tracing to identify, quarantine, and test close contacts	Prioritize contact tracing and quarantining
Safeguarding persons most at risk for severe illness or death	Identify at-risk persons; increase access to rapid, affordable testing
Protecting essential workers	Create policies to protect essential workers by preventing them from getting exposed
Postponing travel	Require masks for travel and encourage people to postpone non-essential travel
Increased room air ventilation, enhanced hand hygiene, and cleaning and disinfection	Provide hand sanitation stations; enhance ventilation and cleaning procedures
Widespread availability and use of effective vaccines	Incentivize vaccination with rewards; ensure that mitigation efforts are still followed after vaccination

1.1.2 Wastewater Based Epidemiology

Wastewater based epidemiology (WBE) is the process of using wastewater to track diseases and other human health indicators through the sewage system. This method was named in 2001 when researchers used it to look at pharmaceutical concentrations in wastewater (Lu, Huang, Zhang, & Sha, 2020), but has been used as early as the polio eradication program in the twentieth century (Polo, et al., 2020). Wastewater-based epidemiology has proved useful to study the spread of many public health phenomena, from tracking the use of certain pharmaceuticals in a community (Nelson, Do, Lewis, & Carr, 2010), to enteric viruses (Farkas, et al., 2018), and salmonella (Yan, O'Brien, Shelton, Whelen, & Pagaling, 2018), to name a small few. So long as

the substance excreted by humans is stable in wastewater to some degree, it can be tracked in wastewater (Lu, Huang, Zhang, & Sha, 2020).

The collection of samples from within the sanitary sewer system that represents the shedding from the population of interest is a vital part of WBE and can be challenging to due to human and environmental factors (Polo, et al., 2020). The type of sample collected at a location will affect its representativeness. There are three major types of samples: grabs, time-weighted composites, and flow-weighted composites. A grab sample is a single sample taken at a moment in time and analyzed. While grabs are a convenient way to collect a sample, they provide only a snapshot of the entire day (Hayes, et al., 2021). A time-weighted composite is a series of grab samples taken at a certain time interval and combined. Flow-weighted composites are a series of samples taken after a certain amount of water has passed through the pipe and combined. Both time weighted and flow weighted composites have drawbacks. First, it is difficult to determine how large each aliquot within the entire sample should be. Furthermore, it is time consuming and costly to run an autosampler for long periods of time (Hayes, et al., 2021). While Curtis, Keeling, Yetka, Larson, and Gonzalez (2020) found that grab samples taken every two hours were appropriate in many circumstances, when looking at viral RNA, any differences between grabs and flow weighted composite samples were amplified when using the viral RNA concentration to calculate viral load – the total amount of RNA copies per the entire volume of water that passed through the pipe during sample collection. Ultimately, the goal of the project determines the type of samples to be collected.

The frequency at which samples are taken is dependent on the goals of the project and can be an important element of WBE. While using a flow-weighted sampling procedure can eliminate concerns about the frequency of sampling, however, it is not always an option,

particularly in instances of high or low flow. In situations where a time paced-sampling regime is used, the goals of the project must be kept in mind. In China (Zhang, et al., 2019), Belgium (Boogaerts, Covaci, Kinyua, Neels, & van Nuijs, 2016), and Croatia (Krizman, Senta, Ahel, & Terzic, 2016), 24-hour, time-paced samples were used to determine the temporal variation of alcohol consumption.

Another factor to consider for WBE is the desired population to be sampled, and therefore, the location samples are to be taken from. There are three major scales of WBE sampling – facility, neighborhood, and community. The facility level includes one or two individual buildings where a relatively small number of people congregate. Within the past year, many colleges and universities took to using the facility-level approach to monitor specific dormitories for SARS-CoV-2. Other applications of facility-level WBE include monitoring for illicit drugs during high school and collegiate basketball games in Kentucky (Montgomery, O'Rourke, & Subedi, 2021). Neighborhood level WBE includes several houses or facilities in a geographic unit. While lacking the specificity of the smaller-scale facility-level WBE monitoring, this is beneficial for public health officials to look at trends in certain areas for intervention while still maintaining individual privacy. This scale is smaller than community-level but larger than facility-level and typically involves sampling directly from the sewage system of a desired area. The final scale of WBE is community-level monitoring, this often means sampling wastewater of an entire city or town. One major benefit of community-level WBE is that for many communities in the United States, researchers can collect samples from wastewater treatment plants, rather than having to set up equipment at manholes or other vulnerable locations. While beneficial to use to track public health phenomenon at this level, it

does lack the specificity of the other scales, which makes it difficult to target resources to the areas that need it most.

1.1.3 Estimating Populations

One of the most difficult aspects of WBE is correlating the number of positive cases to the values detected in wastewater. The first step in this process is to have an accurate count of the population in the sampling area at all times, which makes having a good estimation of the contributing population paramount. However, because humans are not static, it is difficult accurately estimate such a population. One way this is done is using biomarkers (Polo, et al., 2020). Biomarkers are compounds excreted by a large portion of the population that can be used to estimate the number of people in a sewershed (Chen, et al., 2014). A biomarker that is commonly used for WBE is the pepper mild mottle virus (PMMoV). Using WBE to detect SARS-CoV-2 in wastewater is a new practice, thus, researchers have used pepper mild mottle virus (PMMoV) to normalize SARS-CoV-2 concentrations (Wu, et al., 2020), (D'Aoust, et al., 2021). This is because PMMoV is the most abundant RNA virus found in human feces (Symonds, Rosario, & Breitbart, 2019), and is stable in wastewater, with little seasonal variation (Wu, et al., 2020). Although PMMoV concentrations vary over space and time, 106 to 1010 gene copies per liter of domestic wastewater are consistently detected (Symonds, Rosario, & Breitbart, 2019). Researchers in San Francisco, using WBE to monitor for SARS-CoV-2, found that PMMoV was one of the most consistent biomarkers, but found that it was a less promising than other biomarkers due to its diet-dependency and large range in concentrations (Greenwald, et al., 2021). The dependence upon diet and range of concentrations makes PMMoV an unsuitable biomarker for this study.

There has long been need for devices that provide the high-resolution data that cell phones now provide in the study of epidemiology. With the technology available, there are other

ways to estimate the contributing population is a sewer drainage beyond biomarkers, such as using cell phones to estimate the population in a drainage for a given time frame. Some have turned to using both biomarkers and mobile device-based population estimation. For instance, researchers in Oslo, Norway found strong agreement between population fluxes in the city, measured with mobile-device data and the biomarker ammonium (Baz-Lomba, Di Ruscio, Amador, Reid, & Thomas, 2019). While this is an ideal situation, it is not feasible in many circumstances.

Understanding the movement of humans during an epidemic is critical for disease control (Tizzoni, et al., 2014), but until recently there has been a lack in detailed data about human movement. Using smartphones and their GPS capabilities allows researchers to track the movement of people at fine temporal and spatial resolutions (Couture, Dingel, Green, Handbury, & Williams, 2020), (Chaix, 2018), (Deville, et al., 2014). This practice is also beneficial because it does not require that participants self-report movement and activities, (Chaix, 2018) and provide a more timely estimate of the population and its geographical flux than the US Census Bureau is capable of (Deville, et al., 2014), (Lee, Sohn, & Heo, 2018). Specifically, as Chaix (2018) points out with high-resolution movement tracking data, researchers can put travel into context, such as the particular reason for a person to be in a certain place at a certain time. The pings generated from using cell phone data are anonymous and are also easily mapped (Couture, Dingel, Green, Handbury, & Williams, 2020). Mobile device data has been used to estimate park visitation in Orange County, California (Monz, Mitrovich, D'Antonio, & Sisneros-Kidd, 2019). In Oslo, Norway, researchers used WBE combined with mobile device population data to monitor for illicit drug use (Thomas, Amador, Baz-Lomba, & Reid, 2017).

However, there are limitations to such datasets, for instance, not all members of the population have a smartphone (Couture, Dingel, Green, Handbury, & Williams, 2020). With the use of these devices also comes questions about the ethics of technology tracking human locations. StreetLight, the software used in this study, was originally designed to provide information about traffic movement for mobility and transportation planning. Importantly, the data obtained from this software is deidentified and aggregated so it does do not contain any information that could be used to personally identify a person (StreetLight, 2020).

1.1.4 Event-Based Wastewater Based Epidemiology

One aspect of wastewater-based epidemiology is that it is scalable and can be used to monitor for certain analytes at specific events. To date, most event-based wastewater monitoring experiments have been focused on tobacco, alcohol, and illicit drug use during sporting events and concerts (Devault, Peyre, Jaupitre, Daveluy, & Karolak, 2020; Lemas, et al., 2021; Benaglia, et al., 2020). In Italy, researchers were able to see an increase in alcohol consumption during sporting events by collecting samples on an hourly basis (Salgueiro-Gonzalez, et al., 2021). In Florida, researchers at the University of Florida tracked the concentration of illicit drugs in the wastewater leaving the football stadium during a game. To achieve this, they sampled at two manholes and one pumping station on a 30-minute basis beginning one hour before the game and ending approximately 30 minutes after the end of the game (Lemas, et al., 2021).

1.1.5 Wastewater Based Epidemiology for SARS-CoV-2

In the past twenty years, WBE has gained popularity to track numerous public health phenomena, and now SARS-CoV-2. Researchers realized early on during this pandemic that SARS-CoV-2 was shed in the feces of infected individuals, making WBE an effective way to track COVID-19 in an area (Kitajima, et al., 2020; Silverman & Boehm, 2020; Wu, et al., 2020;

Polo, et al., 2020). There are a multitude of reasons that experts have turned to WBE to track COVID-19, one reason being the high rate of asymptomatic or not clinically confirmed cases that would otherwise go undetected (Kitajima, et al., 2020 and Wu, et al., 2020). In fact, Wu et al. (2020) found that in Massachusetts, viral titers in wastewater were orders of magnitude higher than what would be expected based on confirmed cases. Hayes, et al. (2020) also report that SARS-CoV-2 RNA was found in wastewater before any cases had been confirmed by individual testing. Because SARS-CoV-2 (and all other viruses) does not replicate outside of the human body and is viable for up to two to four days in wastewater, WBE proves to be an effective way to track the spread of disease (Polo, et al., 2020). Using WBE, researchers can track the temporal variability of SARS-CoV-2 (Bivins, et al., 2021b).

Despite the promise WBE shows for tracking COVID-19, there remain hurdles which make it difficult to correlate the viral numbers in the wastewater to an accurate count of infected individuals. Firstly, the period of time over which the virus can be shed in the feces can range from one to 33 days with peak shedding occurring from 0.22 to 2.6 days (Miura, Kitajima, & Omori, 2021), some patients have been shown to continue shedding in feces after a negative nasopharyngeal test result (Chen, et al., 2020), and in some cases, have shed viral particles up to seven weeks after symptom onset (Kitajima, et al., 2020). Another complication is that the quantity of virus found in feces varies from person to person. For instance, Miura, Kitajima and Omori (2021) found that the median concentration over the entire shedding period was 0.22 to 4.8 log copies/gram of feces, with the maximum ranging from 4.1 to 5.5 log copies/gram of feces. Meanwhile, through their review, Kitajima et al. (2020) reported approximately 107 copies of SARS-CoV-2 per mL in wastewater. Furthermore, due to a lack of clinical testing, there is no

complete count of infected individuals in a community, making it difficult to correlate the amount of SARS-CoV-2 in the sewage to individual cases.

Another challenge that researchers have faced, is what sampling method to use for SARS-CoV-2 WBE, grabs, time-paced, or flow-weighted composites. Bivins, et al. (b) (2020) found agreement between flow-weighted and time-paced samples but emphasized that researchers should try to avoid sampling directly after low flow events, particularly the early morning hours. It should be noted that Bivins et al. did not collect flow weighted samples, rather they estimated what the concentration of flow-weighted samples would be based on the flow through the sampling area. Polo, et al. (2020) point out that the type of sample is less important than the period in which sampling is carried out. For instance, it may make sense for certain situations to use daily, flow-weighted samples, however, the most important thing is to collect those samples for long enough to see trends and even predict cases in the future. Beyond the physical parameters required to collect representative samples, the concentration and extraction process must be effective and efficient (Lu, Huang, Zhang, & Sha, 2020). Table 2 lists many of the recent SARS-CoV-2 WBE studies, the sample type and sample frequency, as well as the scale the study was monitoring.

Table 2: List of SARS-CoV-2 wastewater-based epidemiology studies organized by sampling scale.

Study Title	Sample Type	Sample Frequency	Objective	Scale
COVID-19 containment on a college campus via wastewater-based epidemiology, targeted clinical testing and an intervention (Betancourt, et al., 2021)	Grabs	Daily, transitioned to twice a week	Outbreak detection	Facility*
Implementing building-level SARS-CoV-2 wastewater surveillance on a university campus (Gibas, et al., 2021)	Grabs	Three times a week	Outbreak detection	Facility
High-resolution within-sewer SARS-CoV-2 surveillance facilitates informed intervention (Reeves, et al., 2021)	24-hour time-weighted samples	Daily	Outbreak detection	Facility
Enumerating asymptomatic COVID-19 cases and estimating SARS-CoV-2 fecal shedding rates via wastewater-based epidemiology (Schmitz, et al., 2021)	Grabs	Twice weekly	Determining number of asymptomatic cases, viral shedding rates	Facility
Targeted wastewater surveillance of SARS-CoV-2 on a university campus for COVID-19 outbreak detection and mitigation (Scott, et al., 2021)	Grabs	Weekly	Outbreak detection	Facility
Providing a safe, in-person, residential college experience during the COVID-19 pandemic (Travis, et al., 2021)	24-hour time-weighted composite samples	Weekdays	Outbreak detection	Facility
The first case study of wastewater-based epidemiology of COVID-	3-hour time-weighted composite samples	Undetermined	Outbreak detection	Facility and Community

19 in Hong Kong (Xu, et al., 2021)	(facility scale), 24-hour time-weighted composite samples (community scale)			
Detection of SARS-CoV-2 RNA in hospital wastewater from a low COVID-19 disease prevalence area (Gonçalves, et al., 2021)	Grabs	Daily	Outbreak detection	Neighborhood**
Sensitivity of wastewater-based epidemiology for detection of SARS-CoV-2 RNA in a low prevalence setting (Hewitt, et al., 2022)	24-hour time-weighted samples	Daily	Outbreak detection	Neighborhood
Wastewater-based epidemiology for tracking COVID-19 trend and variants of concern in Ohio, United States (Ai, et al., 2022)	24-hour time-weighted composite samples	Twice weekly	Outbreak detection	Community***
Wastewater Virus Detection Complements Clinical COVID-19 Testing to Limit Spread of Infection at Kenyon College (Barich & Slonczewski, 2021)	Grabs, transitioned to 24-hour time-weighted samples	Twice weekly	Outbreak detection	Community
COVID-19 surveillance in Southeastern Virginia using wastewater-based epidemiology (Gonzalez, et al., 2020)	Grabs, 24-hour flow-weighted composite samples	Weekly	Outbreak and trend detection	Community
SARS-CoV-2 RNA in Wastewater Settled Solids Is Associated with COVID-19 Cases in a Large Urban Sewershed (Graham, et al., 2021)	24-hour time-weighted samples	Daily	Comparing WBE using the wastewater to extract viral RNA versus using settled solids to	Community

			extract viral RNA	
Detection of SARS-CoV-2 in wastewater in Japan by multiple molecular assays-implication for wastewater-based epidemiology (WBE) (Hata, Honda, Hara-Yamamura, & Meuchi, 2020)	Grab	Weekly and biweekly	Outbreak detection	Community
Comprehensive Surveillance of SARS-CoV-2 Spread Using Wastewater-based Epidemiology Studies (Hemalatha, et al., 2020)	Grabs	A few times at each site over a couple month long period	Trend detection	Community and Neighborhood
Monitoring SARS-CoV-2 Circulation and Diversity through Community Wastewater Sequencing, the Netherlands and Belgium (Izquierdo-Lara, et al., 2021)	24-hour flow-weighted samples	Weekly	Observing trends, variant detection	Community
COVID-19 wastewater based epidemiology: long-term monitoring of 10 WWTP in France reveals the importance of the sampling context (Lazuka, et al., 2021)	24-hour flow-weighted samples	Weekly, transitioned to twice weekly	Determining trends, providing context to sampling	Community
Monitoring changes in COVID-19 infection using wastewater-based epidemiology: A South African Perspective (Pillay, et al., 2021)	Grabs	Weekly	Outbreak detection	Community
Wastewater-based epidemiology as a useful tool to track SARS-CoV-2 and support public health policies at municipal level in Brazil (Prado, et al., 2021)	Grabs	Weekly	Outbreak and trend detection	Community and Neighborhood
Emergence of SARS-CoV-2 Alpha lineage and its correlation with	24-hour flow-	Twice weekly	Variant detection,	Community

quantitative wastewater-based epidemiology data (Radu, et al., 2022)	weighted samples		outbreak detection	
Sewage, Salt, Silica, and SARS-CoV-2 (4S): An Economical Kit-Free Method for Direct Capture of SARS-CoV-2 RNA from Wastewater (Whitney, et al., 2021)	24-hour time-weighted samples	One time	Testing new method to quantify SARS-CoV-2 in wastewater	Community
SARS-CoV-2 Titers in Wastewater Are Higher than Expected from Clinically Confirmed Cases (Wu, et al., 2020)	Grabs	One time	Confirm WBE can be used to quantify SARS-CoV-2, compare to clinical cases	Community
*Facility scale collects samples from one or two buildings, smallest scale **Neighborhood scale collects samples from several buildings or facilities, intermediate scale ***Community scale collects samples from an entire community or municipality, largest scale				

1.1.6 Wastewater Sampling for SARS-CoV-2 on College Campuses

From the start of March through mid-December 2020, there were nearly 3 million cases of COVID-19 in people aged 0-24, and nearly 60% of those cases were in college-aged persons (18-24). However, the cases in this age group that required hospitalization, ICU admission, or resulted in death were nearly 50 times less likely when compared to adults of all ages greater than 25 years old (Leidman, et al., 2021). However, given the greater likelihood that there were many asymptomatic carriers in this age group during that went undetected using traditional clinical testing (Scott, et al., 2021). Because of this, it is prudent to monitor college campuses.

As of August 2020, college and university campuses were determined to be places of increased COVID-19 incidence, despite general declines in the number of cases at the time in all other age groups (Leidner, et al., 2021). Furthermore, in the immediate 21 days before and after the start of the fall semester in August 2020, universities that held in-person instruction saw in

increase of COVID-19 prevalence, compared to a decrease in prevalence at universities that held classes remotely (Leidner, et al., 2021). Thus, monitoring universities that are holding in-person instruction is valuable. Specifically, it is beneficial to monitor the wastewater at the building level at universities that have congregate living situations, there is evidence of asymptomatic transmission, or where student behavior is not conducive to slow spread of disease (Bivins, et al., 2021).

1.1.7 COVID-19 in Oklahoma in Autumn 2020

The trends in reported cases in Oklahoma for each football season are nearly opposite of each other. The highest reported cases for the 2020 season occurred later in the season, while the greatest number of cases for the 2021 season was at the start of the season. For the purposes of this document the 2020 football season is defined as August 1 – December 5, 2020, which is the final home game of the season, while the 2021 football season is defined as August 1 – December 1, 2021. Figure 1 displays the number of new reported from the United States Centers for Disease Control and Prevention (CDC) cases per day for each season. The peak for the 2020 season occurred on November 24, 2020, with approximately 4,300 new cases reported that day. The 2021 peak occurred on August 25, 2021, with approximately 4,100 cases reported that day. Possible reasons for these differences are outlined in this and the following section.

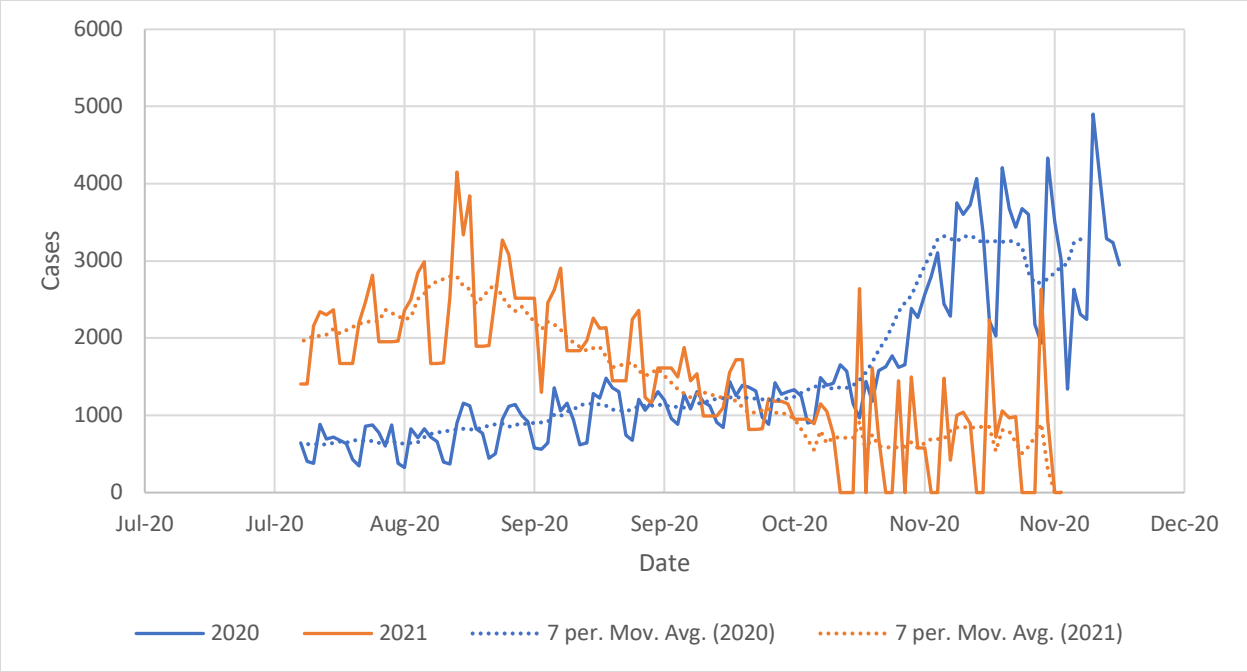

Figure 1: New cases per day in Oklahoma during football season (August 1- December 5, 2020 and August 1 - December 1, 2021). Data from the CDC: https://covid.cdc.gov/covid-data-tracker/#trends_dailycases&territory-select=40&leftAxis=New_case&rightAxis=select

The COVID-19 response in the U.S. has varied state by state, city by city, and even institution by institution. In the State of Oklahoma, as a state-wide policy, masks and social distancing were recommended only in "red or orange" counties for individuals eleven and older in work or public spaces, and restaurants (Frye, 2020). A county is classified as orange by the Oklahoma State Department of Health when it exceeds 14.29 new cases per 100,000 people per day, and Cleveland County, the home of the City of Norman and The University of Oklahoma has been classified as orange since at least September 24, 2020 through the end of 2020 (State of Oklahoma Department of Health, n.d.).

In many ways, college campuses provide an environment for diseases to spread, as they bring together thousands of students from all over the globe and keep them in a relatively confined space. Colleges and universities utilize many congregate living areas, such as dormitories and apartments to house large number of students relatively affordably. These

residential settings provide settings that pose a significant risk for spread (Walke, Honein, & Redfield, 2020). Leidman et al. (2021) found that for the autumn of 2020 weekly case incidence in the United States was highest the week of December 6, 2020. For the ages 0-17, this peak followed the trends of adults older than 25, however, for college-aged 18 to 24-year-olds, a greater peak was noticed the week of September 6, which could potentially indicate transmission on college campuses just after the start of the semester. Furthermore, they found that counties that were home to universities who hosted in-person events had an increase of approximately 56% in cases immediately following the start of the Fall 2020 semester (Leidman, et al., 2021).

Given the guidance of the CDC, along with mask mandates in place at both the University and the City of Norman, Oklahoma, The University of Oklahoma allowed 25% occupancy at home football games in 2020, resulting in 22,700 people in attendance at each for five games in total (2020 Football Season, n.d.). Masks were required at these events, though there were limits to how well mask usage was enforced. However, there were no restrictions about domestic travel into the City of Norman, Oklahoma, where many people traditionally travel to during football games, even if they are not attending the game in person. Because COVID-19 incubation times range from 2.2 to 11.5 days, with a median of 5.1 days (Lauer, et al., 2020) and a high percentage of asymptomatic cases (Hu, Guo, Zhou, & Shi, 2020), there remains a possibility that people engaged in high-risk activity such as not wearing proper face masks, social distancing, attending large indoor or outdoor gatherings, or traveling, to attend football games in Norman, Oklahoma. Engaging in these types of high-risk activities can increase community spread (Honein, et al., 2020).

The COVID-19 pandemic continued to produce new cases throughout the autumn of 2020 for many reasons. There is an element of seasonality associated with COVID-19

prevalence, where transmission is reduced during warmer weather (Notari, 2021). Throughout the 2020 football season, the temperature in Oklahoma was decreasing, as is typical for that time of year in this region. Another reason for the peak in cases at the end of the 2020 football season was due to travel for the holidays, particularly Thanksgiving (Mehta, Clipman, Wesolowski, & Solomon, 2021). Though the University of Oklahoma held classes entirely online after the Thanksgiving vacation (OU Announces Calendar Updates to Fall, Spring Semesters , 2020), the number of cases throughout the state was still increasing, likely due in part to travel for the holiday.

1.1.7 COVID-19 in Oklahoma in Autumn 2021

The state legislature in Oklahoma passed Senate Bill 658 which reads: "Schools; requiring provision of certain information to parents; prohibiting certain entities from implementing specified requirements; establishing criteria for implementation of mask mandate" in May of 2021, effectively disallowing schools to mandate masking in light of the ongoing COVID-19 pandemic (Bill Information for SB 658, 2021). In many ways, the passage of this law represents the sentiments about the pandemic and mitigation measures of many people in the state. Because of this and other circumstances, the Fall 2021 football season was treated much differently than the season prior, with a return to full capacity and on-campus tailgating. Notably, there are no masking or vaccination requirements for the football games (OU Announces Return of Tailgating and Other Game Day Activities for 2021 Football Season, 2021). However, the CDC continues to recommend masking and social distancing for all institutions of higher education, but particularly for campuses where vaccination status varies, much like the University of Oklahoma (CDC, 2021).

Another reason for concern in 2021 is the emergence of new variants of SARS-CoV-2, that are more infective and dangerous. There have been several changes to the structure of the virus, particularly the spike protein, as this pandemic has carried on (Tao, et al., 2021). These variants often have a geographic signature (Cevik, Kuppalli, Kindrachuk, & Peiris, 2020) and typically originate in areas with high community circulation and low vaccination coverage (Liu & Rocklöv, 2021). The primary variants that were at play during this study were the alpha and delta variants. Alpha variant was first identified in the UK and some estimate that it was 50% more transmissible than the original virus and was associated with an estimated 50% increase in mortality (Tao, et al., 2021). The alpha variant was the more active variant in the state during the 2020 football season.

The major variant that was at its peak in the fall of 2021 across the globe is known as the delta variant. The delta variant has been the major variant circulating in the United States since June 2021 and is associated with another wave of COVID-19 outbreaks (Siegel, et al., 2021). In fact, there was an outbreak of this variant traced to a gymnastics facility in Oklahoma City (Dougherty, Mannell, Naqvi, Matson, & Stone, 2021). Oklahoma City, the capitol of the state, is only approximately 25 miles north of the University of Oklahoma. There are numerous reasons for concern about this variant; first, the household transmission risk is approximately 60% greater with the delta variant than the alpha, which already is more transmissible than the original version of SARS-CoV-2. This is because the amount of virus in the body during infection with the delta variant is greater, as evidenced by the lower cycle threshold (CT) value of delta (Mahase, 2021). As mentioned before, the R_0 of the original virus ranges from 2.3 to 2.79, with a higher R_0 indicating more ability to spread. The R_0 of delta is 5.08 (Liu & Rocklöv, 2021).

Another factor to consider about the autumn of 2021 compared to the autumn of 2020 is the existence of SARS-CoV-2 vaccines. As of October 15, 2021, the percentage of adults in Oklahoma who have received at least one dose of a vaccine is 71%, while 60% of adults in the state have both doses (Oklahoma State Department of Health, 2021). This may impact the feelings of individuals who are vaccinated to feel more comfortable attending OU football games. While vaccination does reduce the risk of hospitalization and severe disease from the delta variant, experts recommend other measures such as masking and social distancing should be continued to reduce spread and prevent further mutations of the virus (Bian, et al., 2021).

Because SARS-CoV-2 is a novel virus, there is new research emerging about it daily. While there is existing research about the use of WBE at sporting events to track other public health phenomena, such as the basketball games Montgomery, O'Rourke, & Subedi (2021) monitored for illicit drugs, there is not yet data available about the temporal variation of SARS-CoV-2 in wastewater at large sporting events. Sassano, McKee, Ricciardi, & Boccia (2020) speculated that European soccer matches were associated with the spread of SARS-CoV-2 in Italy and Spain. However, in regards to sports, much of the research has looked at spread of the virus amongst team members. For instance, researchers have studied whether SARS-CoV-2 is spread by players in professional rugby (Jones, et al., 2021), European professional soccer (Egger, Faude, Schreiber, Gärtner, & Meyer, 2021), and even American high school football (Siegel, Kloppenburg, Woerle, Sjoblom, & Danyluk, 2021). The information this research provides can be used to guide policy and inform decision makers in the face of our next public health crisis.

1.2 Hypotheses and Objectives

The overarching goal of this study is to determine if wastewater-based epidemiology can be used to measure temporal changes of SARS-CoV-2 in the wastewater of the city of Norman, Oklahoma. Secondary goals of this research are determining how much of the change in SARS-CoV-2 concentration is due to travel into the city of Norman for the football game and determining if StreetLight data can be used to measure changes in population in an entire city.

1.2.1 Hypotheses

The hypotheses for this research are:

- The concentration (viral load per person, relative viral load per person) of SARS-CoV-2 in the wastewater at the Norman wastewater treatment plant is statistically significantly greater on gamedays than the weekdays surrounding the games.
- The concentration (viral load per person, relative viral load per person) of SARS-CoV-2 in the wastewater is significantly greater on gamedays than controls.
- The concentration (viral load per person, relative viral load per person) of SARS-CoV-2 is statistically greatest around the start of the football game and the four hours comprising the football game compared to other times throughout the sampling period.
- The concentration (viral load per person, relative viral load per person) of SARS-CoV-2 is significantly greater in the 2021 football season than the 2020 season.
- The population in Norman is significantly greater on gamedays than the controls, indicating that people traveled into the city of Norman to attend and/or celebrate football games.

All hypotheses about the amount of SARS-CoV-2 are meant to test the concentration, viral load per person, and relative viral load per person.

1.2.2 Objectives

The objectives of this study were to determine if allowing limited in-person attendance of football games at the University of Oklahoma in the fall of 2020 and 2021, had an impact on the amount of SARS-CoV-2 found in the City of Norman, Oklahoma sewershed. To assess this, we analyzed wastewater for SARS-CoV-2, the flow of wastewater into the water treatment facility, and population. To ensure we stay on track, we developed several guiding questions. First, we asked several questions regarding the flow of wastewater measured at the wastewater treatment plant, such as: is the volume of sewage water significantly different on game weekends versus non-game weekends? Are the volumes measured during each game significantly different compared to each other? Is there a time that the flow is greatest – does that coincide with the football game?

Another question this study sought to answer was whether the average concentration of SARS-COV-2 on gamedays is significantly different than the concentrations from the time weighted composites from the Norman wastewater treatment plant on days close to the gameday, temporally. Samples were collected from the wastewater treatment plant representing Tuesdays, Thursdays, Fridays, and Saturdays. This is because the SARS-CoV-2 concentration would be greater on the gameday than surrounding days given the greater number of people in the contributing sewer drainage on gamedays.

The next set of guiding questions were applicable for the three methods we used to quantify SARS-CoV-2 – concentration, and viral load per person (the concentration multiplied by the average flow and divided by the number of people in the sewershed at the time), and relative viral load per person (the viral load per person with the value for the first sample subtracted from all remaining samples). These questions were: is viral concentration or load per

person significantly different on game weekends versus non-game weekend? And is there a significant difference in viral concentration or load per person before, during, immediately after the game, and late night (the time college students would be going out)?

The final guiding questions related to the cell phone data and were specifically: is there an influx of people into Norman on game weekends as determined through cell phone pings? And how does the population change throughout the day of the game? This was of interest both to normalize the amount of SARS-CoV-2 in the wastewater as well as confirm that the population in town increases due to football games.

CHAPTER 2

APPROACH AND METHODS

2.1 Approach

For the 2020 football season, five days were selected to sample, while seven days were selected for the 2021 football season. Table 4 shows specific information for each day. Because each game is different in terms of population dynamics, what is happening in town, or decisions from the University, knowing the context surrounding the football game is important, because it might impact the behaviors of fans, encouraging or discouraging them from certain behaviors. One example of this is how the activities going on in town impacted could impact how many people were there for the game, whether they stayed in town after the game, or even if they left the game early. Another reason we took this information into consideration is because, for instance, if an opponent is geographically nearer to Norman, Oklahoma, it is possible that more of their fans traveled into town for the game. Because we were tracking the change in population per hour in the sewershed, it felt important to try to understand more about the people represented in this study and why they behaved the way they did. The approach to this study is complete sampling at each game, track the number of people in the City of Norman sewershed per hour, and understand the atmosphere that day. Each season there were a small number of games that had circumstances surrounding them that could not be captured by only looking at the opponent, published attendance, or the result of the game that might have impacted the behavior of those in town.

Table 3: Date of home game, opponent, start time, published attendance, and result

2020					2021				
Date	**Opponent**	**Start Time**	**Attendance**	**Result**	**Date**	**Opponent**	**Start Time**	**Attendance**	**Result**
September 12	Missouri State	6:00 PM	22,700	48-0 (W)	September 4	Tulane	11:00 AM	42,206	40-35 (W)
November 7	Kansas	2:30 PM	22,700	62-9 (W)	September 11	Western Carolina	6:00 PM	83,538	76-0 (W)
November 14	Control	N/A	N/A	N/A	September 18	Nebraska	11:00 AM	84,659	23-16 (W)
November 21	Oklahoma State	6:30 PM	22,700	41-13 (W)	September 25	West Virginia	6:30 PM	84,353	16-13 (W)
December 5	Baylor	7:00 PM	22,700	27-14 (W)	October 16	Texas Christian	6:30 PM	84,391	52-31 (W)
					November 13	Control	N/A	N/A	N/A
					November 20	Iowa State	11:00 AM	82,685	28-21 (W)

2.1.1 2020 Football Season Context

There were a few games in the 2020 football season that had special context. For instance, the Missouri State game is the season opening game, with kickoff at 6:00 pm CST September 12, 2020. At this point in the pandemic, cases in Oklahoma were generally low, and sentiments were opposed to restrictions, as evidenced by the lack of social distancing and masking in the stadium at the football game (McCourry, 2020). Also, despite university policy prohibiting tailgating on campus for the 2020 football season (2020 Game Day Policies & Procedures, 2020) and the City of Norman mandate that bars and restaurants in the city be limited to 75% occupancy (Hayes J. , 2020), parties and tailgates occurred off campus, and had been occurring for the majority of the semester leading up to the game (Kyncl, 2020).

Another aspect that could impact fans' behavior is against Oklahoma State University when the University of Oklahoma hosted the prestigious ESPN College GameDay, for the first time since 2012 and for the eighth time in school history (McCourry, 2020).

The final game that to be sampled in the 2020 season is the December 5, 2020 game against Baylor. This game would have been the celebration for the senior players, though the celebrations were cancelled due to COVID-19 (Engelbrecht, 2020). Also, at this point in the

semester, the university had moved to an all-online class schedule through finals and encouraged students to stay home after traveling home for Thanksgiving break (OU Announces Calendar Updates to Fall, Spring Semesters , 2020).

2.1.2 2021 Football Season Context

The University of Oklahoma faced Tulane on Saturday September 4, 2021, in what should have been an away game played in New Orleans, Louisiana. Because of Hurricane Ida, which went through New Orleans early September, making impossible to hold the season-opener there, and the game was moved to Norman, Oklahoma (Hoover, 2021). Had the game been held at Tulane, attendees would have been required to show proof of COVID-19 vaccination or a negative test (Young, 2021), this was not enforced in Norman due to the last-minute nature of the game, however capacity was limited at the game instead.

The second of four home games in a row, the Sooners faced Western Carolina. In what should have been the first home game of the year, tailgating and full stadium capacity were allowed this day (OU Announces Return of Tailgating and Other Game Day Activities for 2021 Football Season, 2021).

Celebrating the fiftieth anniversary of the 1971 “game of the century,” the University of Oklahoma Sooners faced off against former conference rivals, the Nebraska Cornhuskers on September 18, 2021, at 11:00 am CST (Dix, 2020).

2.2 Methods

2.2.1 Sampling Method

Samples were collected at the Norman wastewater treatment plant for the days of four home football games and one day without a home football game during Autumn of 2020 and during six home football games and one day without a home football game during the Autumn of 2021. These days are selected to track the impact of football games on the temporal variation of

SARS-CoV-2 in wastewater. The samples were collected at the City of Norman, Oklahoma's wastewater treatment facility after initial grit screening but before any water treatment. The City of Norman water reclamation facility (NWRF) is an activated sludge treatment facility that serves a population of 107,500 individuals (City of Norman, OK, n.d.). Samples were collected at the NWRF (Figure 2) using Teledyne ISCO (Lincoln, NE) Avalanche refrigerated autosamplers, set to collect 700 mL samples every hour for 24 hours beginning Saturday between 8:00 and 9:00 am. Two sets of fourteen 950 mL plastic ISCO sample bottles were cleaned using a 10% percent bleach solution, rinsed with tap water, then washed with 2% detergent (citranox) and rinsed with DI water, and finally treated with sodium thiosulfate and rinsed again with DI water (adapted from US Geological Survey, 2003). Samples were kept between 1-6°C and processed around 24 hours after collection. Furthermore, 24-hour time weighted composite samples from the staff at NWRF for Friday and Saturday for each sampling event were collected and analyzed.

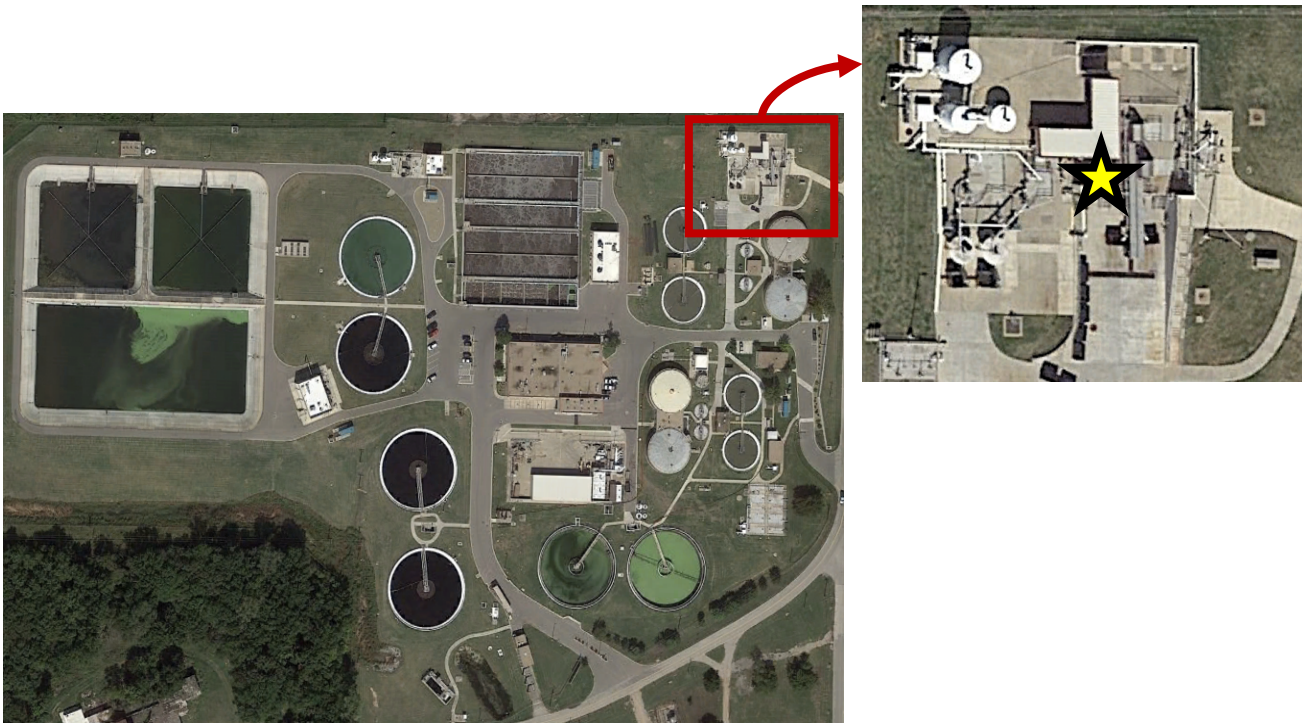

Figure 2: Sampling location at the City of Norman Water Reclamation Facility. The autosampler is located at the yellow star on the figure at the right.

2.2.2 SARS-CoV-2 Quantification

After samples are received, they were kept at 4 to 6°C until they could be processed (within 24 hours of receipt). After retrieval from the refrigerator, the samples were strained and divided into triplicates, mixed with polyethylene glycol (PEG 8000), and left to precipitate overnight at 6°C. In the morning (10 to 16 hours later), samples were spun at 14,600 Relative Centrifugal Force (RCF) to create pellets. The supernatant PEG solution is then carefully decanted from the pellets. The pellets were resuspended using a Guanidine Thiocyanate Lysis (GTC) buffer. Using magnetic beads, the viral RNA is extracted from the solution. Once RNA is extracted, the amount of SARS-CoV-2 RNA is calculated using quantitative reverse transcription polymerase chain reaction (RT-qPCR) (Kuhn, et al., 2022). The geometric mean of the triplicates was used in this analysis to normalize non-detections. Non-detections were assigned a value of 312 copies/L – approximately half of the detection level (Helsel, 2005). Microbiological analyses

were performed by Dr. Bradley Stevenson's laboratory in the University of Oklahoma's Department of Microbiology and Plant Biology.

2.2.3 Cell Phone Data

Data on the number of mobile devices entering and leaving the Norman sewershed, as determined from the City of Norman's sewer boundary shapefile, from StreetLight, San Francisco, California, (SL) Data (streetlightdata.com), a data analytics company that deidentifies and organizes location information from mobile technologies (e.g. phones, communication towers, and GPS-enabled devices). Community mobility patterns estimates were obtained along roadway corridors and between specific locations through an educational/research license. Origin-Destination (OD) analysis was used via the SL platform. Trip count data were aggregated using algorithmically transformed location point data and validated using embedded in-vivo road network sensors and traffic counters (StreetLight, 2020).

OD-IDs were generated into and out of the Norman sewershed every hour starting on Friday at 12:00 a.m. CST and ending at 11:59 p.m. CST on Sunday for five weekends in Autumn 2020: September 11-13, November 7-9, November 14-16, November 21-23, December 5-7 and seven weekends in 2021: September 3-5, September 10-12, September 17-19, September 24-26, October 15-17, November 12-14, and November 19-21. Each of the weekends were associated with a University of Oklahoma home football game except for November 14-16, 2020, and November 12-14, 2021, which were used as control weekends to understand typical traffic flows within the Norman sewershed. In addition to trip counts, SL also reports trip attributes including average trip duration and average trip length. The analysis was constrained to only include personal trips originating at a home. These data were tabulated using STATA 16.1.

Hourly population estimates within the Norman sewershed were calculated using 2019 census tract estimates from the American Community Survey (ACS) data. Census tract geographies (N=26) were clipped to the Norman sewershed boundary and aerial apportionment of census tract population were used to estimate the total population serviced within the sewershed. The total estimated population is 87,779. The US Census Bureau, which also manages the ACS, does try to include college students in their population estimates, aiming to count where "people where they live and sleep most of the time" (US Census Bureau, 2020). This total population is pinned to the 12:00-1:00 am hour. SL hourly traffic counts into and out of the sewershed were then iteratively added and subtracted from the estimated total population to generate hourly estimates of the population within the sewershed area.

2.2.4 Viral Loads

The viral load is, simply put, the amount of SARS-CoV-2 in the wastewater. Because the concentration of SARS-CoV-2 is presented as copies per liter, to get a measure without units, the concentration is multiplied by the flow, in liters. Equation 1 was used to calculate the SARS-CoV-2 viral load for each sample. The Q_{avg} is the average flow for the approximate hour the sample represents, for instance, if the sample was taken at 8:30 am, the flow was averaged from 8:00 am to 8:59 am, and so forth. Flow data was provided by the NWRF at fifteen-minute time intervals. To achieve a viral load per person, the viral load for each hour was divided by the population present in Norman for that hour as determined by the cell phone data. A relative viral load per person was calculated by subtracting the first value of each day from all subsequent samples. This method assumes that that the first sample of the day is representative of the SARS-CoV-2 levels already in the sewershed and all changes in the viral load per person are due to travel into or out of the area.

Equation 1: Viral load:

$$\text{Viral Load} = \sqrt[3]{C_1 \times C_2 \times C_3} \times Q_{avg}$$

Where:

C_n is the concentration of one of three triplicates
Q_{avg} is the average flow for the hour

Statistical analyses were performed in SPSS and Microsoft Excel to test the hypotheses of this project by testing the following variables: flow, population, concentration, viral load per person and relative viral load per person. The analyses occurred for each game, across games, and across seasons to test the hypotheses that there are differences at all these temporal scales. There were two ways these variables were compared between games. First, the variability of each variable for each day compared to each other was determined using one-way ANOVA tests. For the concentration, viral load per person, and relative viral load per person, there are fewer than 30 values for each day, and a Kruskal-Wallis H-test (or a nonparametric one-way ANOVA) was used. It is also worth looking at whether the mean value for each variable for the control (non-game) is statistically different from the mean value for the same variable for all the weekends with a game. To address the uneven sample size resulting from comparing variables of one day to variables of multiple days, a Welch's T-test was used. A T-test was used to compare these variables for two games to each other.

Within day variability was analyzed by breaking the day into subgroups consisting of before the game, during the game, after the game, and a final group called late night. The before game group consisted of the four hours directly before kickoff. During game consisted of the four hours in which the game was played. All games lasted longer than 3 hours but less than 4 hours for both seasons. Both the shortest and the longest game occurred in the 2020 season, the shortest was Missouri State at 3 hours and 6 minutes, while the longest was Kansas at 3 hours

and 46 minutes (https://soonersports.com/sports/football/stats). The after-game group consisted of the four hours directly after the end of the game, however, this category is only valid for some games because the four hours directly after evening games ran into the late-night category. The late-night category will consist of the hours 11:00 pm to 3:00 am. To compare these groups against each other, given their small sample size, a nonparametric test of means was used in SPSS and the software was allowed to select the most appropriate test given the data. This resulted in the use of a Mann-Whitney test to compare the values. These tests are not reported due to concerns about the power when only 8 samples are compared to each other.

Across all games, it is of interest to know if there are time groupings that are different from the others. To compare this, for instance, the flow, population, concentration, viral load per person, and relative viral load per person of the before group of all games were compared to the during game group of those variables for all games. This analysis was done within seasons as well as across seasons. The statistical tests for this analysis utilized T-tests to compare means.

The concentration of the gameday samples was compared to the concentration of samples from the NWRF collected on other days of the week to assess whether there is a change in the concentration associated with the football games. There are two ways this was tested, first, the days temporally near a gameday were compared to the gameday, again likely using a Mann-Whitney nonparametric test, given the small and uneven samples sizes. Within and across seasons, a similar analysis occurred, though likely a Welch's T-test was used to compare the two groups.

Regressions were utilized to understand the strength of the relationships between the data. Specifically, these regressions looked at how the flow and population are related to the amount of SARS-CoV-2 in the wastewater. To determine these relationships, flow and

population, concentration, viral load, viral load per person, and relative viral load per person were compared to each other. Similar regressions were run between population and concentration, viral load, viral load per person, and relative viral load.

CHAPTER 3

RESULTS

Samples were collected over the 24-hour period from Saturday morning to Sunday morning. Each season was analyzed individually as well as compared to each other. Analysis consisted of determining relationships between flow, population, concentration, and viral load per person over time, as well as relationships between these variables. Appendix A contains the raw flow data used for analysis, while Appendix B contains the raw population data, Appendix C contains the raw flow data, Appendix D contains the raw viral load per person data, and Appendix E contains the raw relative viral load per person data.

3.1 2020 Football Season

Results are broken into five categories for each game: flow, population, concentration, viral load per person, and relative viral load per person.

3.1.1 Flow

Flow data from the NWRF were compiled to calculate viral loads from approximately 8:00 am Saturday to approximately 8:00 am Sunday (Figure 3). The mean flow between each sampling event is significantly different, determined using an ANOVA test at the 95% confidence level, $P < 0.01$. The difference in flow for the control compared to Kansas and Baylor were not significant ($P = 0.19, 0.59$). Compared to Missouri State and Oklahoma State, however, the difference in flow was significant ($P < 0.01$, $P = 0.05$).

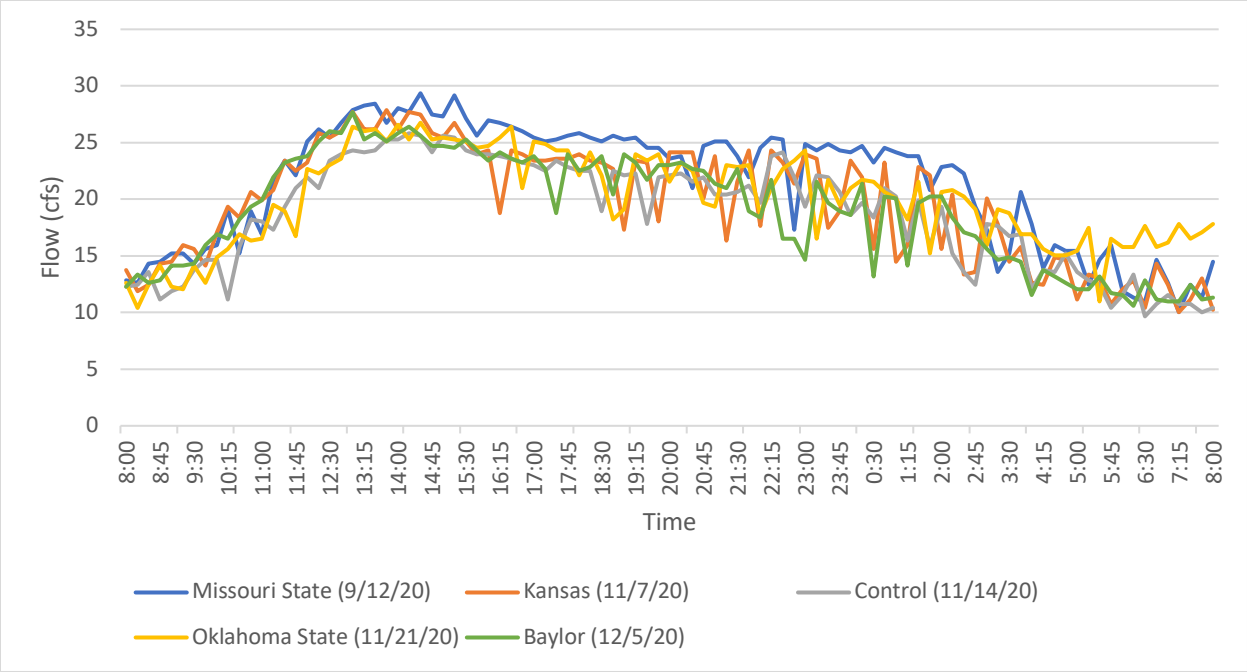

Figure 3: Flow for each gameday during the 2020 football season, City of Norman, OK.

The mean flow over the entire 24-hour period for each game as well as before, during, after-game, and late-night can be seen in Table 4. For most games, there was not a four-hour period between the end of the game and the start of the late-night group, thus the after-game group was excluded from analysis on those games. The control weekend has the smallest mean 24-hour flow. For all games, the flow before the game compared to during the game is significantly greater ($P < 0.01$). The same is true of the flow before the game compared to the late-night category ($P < 0.01$), and the during group compared to the late-night group ($P < 0.01$).

Table 4: Mean flow (cfs) by time group for all games in the 2020 football season. For each game (within columns) time categories with different letter superscripts are significantly different as determined by Mann-Whitney tests at the 95% confidence level. In the 24-hour row, games with different superscript Greek letters are significantly different.

	Missouri State (September 12, 2020)	**Kansas (November 7, 2020)**	**Control (November 14, 2020)**	**Oklahoma State (November 21, 2020)**	**Baylor (December 5. 2020)**
Before	26.8^{A}	24.4^{D}	N/A	24.5^{G}	23.3^{J}
During	24.4^{B}	24.2^{D}	N/A	21.7^{H}	20.9^{K}
After	N/A	21.9^{E}	N/A	N/A	N/A
Late-Night	23.1^{C}	19.2^{F}	18.4	19.9^{I}	18.3^{L}
24-hour	21.0^{α}	$19.3^{\beta,\chi}$	$18.7^{\beta,\chi,\varepsilon}$	$19.9^{\alpha,\chi,\delta,\phi}$	$19.0^{\beta,\chi,\delta,\phi}$

The flow over time for the Missouri State gameday (September 12, 2020) can be seen in Figure 4A. To further understand this relationship, all time groups (before, during, and late-night) were compared to each other using a Welch's test and were significantly different ($P < 0.01$). The results of the within game time group comparison can be seen in Table 5. The flow over time for the Kansas game (November 7, 2020) is shown in Figure 4B. When comparing all time groups (before, during, after, and late-night), the difference was significant ($P < 0.01$). Figure 4C displays the flow over time for the control day, November 14, 2020. Because there was no game that day, the flow could not be analyzed at different time steps, as they are based on the time of the football game. The flow over time for the Oklahoma State game (November 21, 2020) can be seen in Figure 4D. When comparing all time groups (before, during, and late-night) for the Oklahoma State game, each time group is significantly different ($P < 0.01$). Figure 4E displays the flow over time for the Baylor game, December 5, 2020. All time groups compared to each other (before, during, and late-night) have significantly different mean flow values ($P <$

0.01).

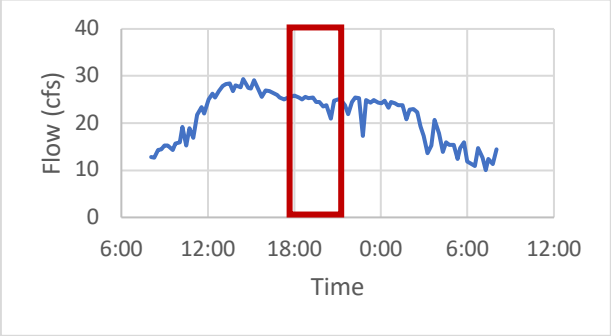

A: (Above) flow over time for Missouri State (September 12, 2020) game.

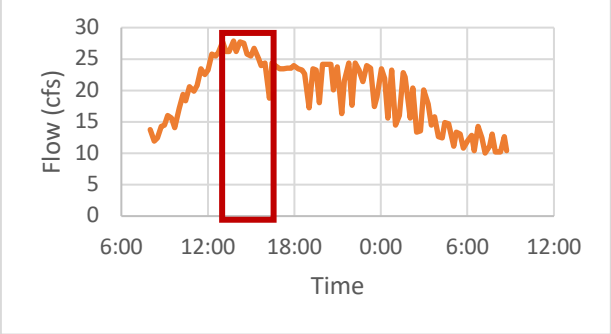

B: (Above) flow over time for Kansas (November 7,

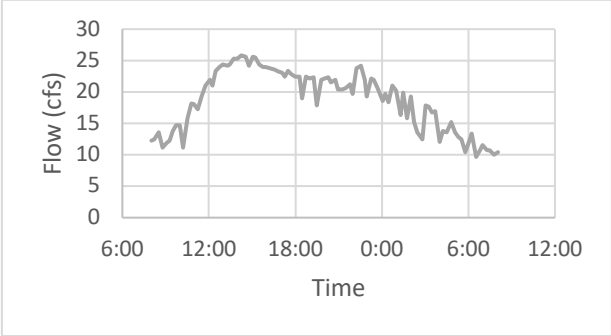

C: (Above) flow over time for control (November 14, 2020) day.

D: (Above) flow over time for the Oklahoma State (November 21, 2020) game.

E: (Above) flow over time for the Baylor (December 5, 2020) game.

Figure 4: Flow over time for all sampling days in the 2020 football season. Approximate games time are outlined in red. A represents the flow during Missouri State sampling period, B shows flow during the Kansas sampling period, C shows the flow during the control sampling period, D shows the flow over the duration of the Oklahoma State sampling period, and E shows the flow over the duration of the Baylor sampling period.

3.1.2 Population

The use of the SL data was used to give an estimate of the number of people present in the sewershed for each weekend that was sampled. Figure 5 contains the estimated population present in the Norman sewershed during each sampling period. Again, samples were collected from approximately 8:00 am Saturday to approximately 7:00 am the following Sunday. It should be noted that the population on campus was decreasing as the semester approached December for a couple of reasons. First, many classes had limited or no in-person meetings throughout the fall of 2020. The university policy was that classes of more than 30 people were to be held online. Second, after the Thanksgiving holiday, November 23 through November 27, students who traveled home were asked to stay there for the remainder of the semester, as all classes were moved online (OU Announces Calendar Updates to Fall, Spring Semesters , 2020, https://www.ou.edu/web/news_events/articles/news_2020/ou-announces-calendar-updates-to-fall-spring-semesters). This likely led to a gradual migration of students away from campus as the semester went on, however, there is no way to gather an accurate count of who left the sewershed across the entire semester. This means that our baseline population is likely incorrect for the football games that occurred later in the semester, however this error is less than the error of the SARS-CoV-2 concentration.

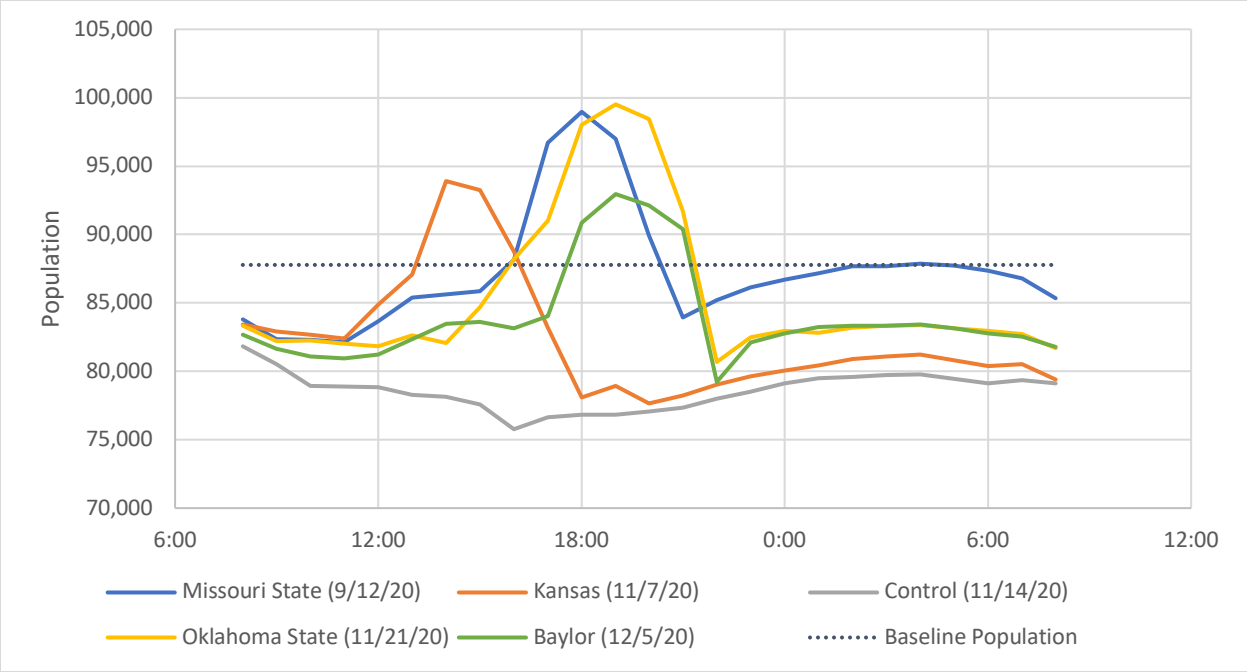

Figure 5: Population for each gameday during the 2020 football season

It should be noted that samples for Missouri State were only collected Saturday from approximately 9:30 am to 11:30 pm, but the population for the 24-hours corresponding with the other samples are included. Compared to the control weekend, the population for each gamedays was significantly greater using T-tests ($P < 0.01$, respectively). Table 5 shows the mean population for each time category for the 2020 football season.

Table 5: Mean population by time group for all games in the 2020 football season. In the 24-hour row, games with different superscript Greek letters are significantly different at the 95% confidence level.

	Missouri State (September 12, 2020)	**Kansas (November 7, 2020)**	**Control (November 14, 2020)**	**Oklahoma State (November 21, 2020)**	**Baylor (December 5. 2020)**
Before	89,079	82,855	N/A	90,476	85,413
During	92,458	87,066	N/A	92,587	88,688
After	N/A	85,829	N/A	N/A	N/A
Late-Night	87,075	80,424	79,288	82,967	82,946
24-hour	$87{,}258^{\alpha}$	$87{,}617^{\alpha}$	$87{,}619^{\alpha}$	$87{,}717^{\alpha}$	$87{,}722^{\alpha}$

Figure 6A displays the change in population over time for the Missouri State game. The population is greatest during the game. The population over time for the Kansas game is shown in Figure 6B. The population is greatest during the game. The population for the control day never was greater than the baseline population of 87,778. It is likely that many students returned home or traveled elsewhere for the weekend since the football team was off this weekend. The change in population over time for the control day is shown in Figure 6C. Figure 6D shows the change in population over time for the Oklahoma State sampling. Figure 6E shows the change in population over time for the Baylor game. The population is greatest during the game for this gameday.

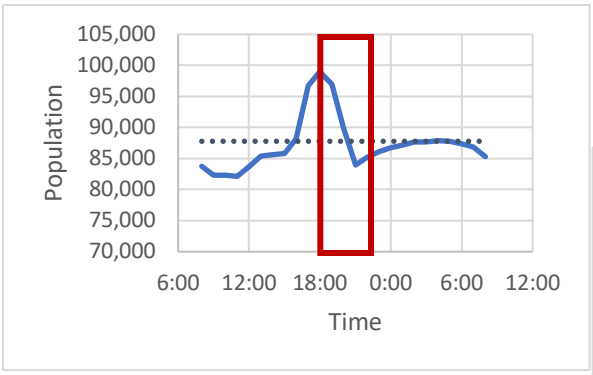

A: (Above) estimated population over time for Missouri State (September 12, 2020) game.

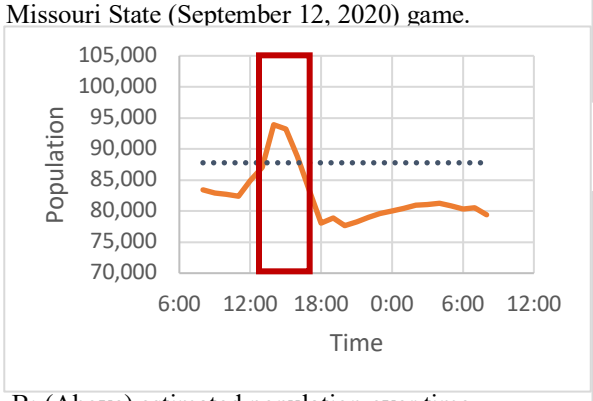

B: (Above) estimated population over time for Kansas (November 7, 2020) game.

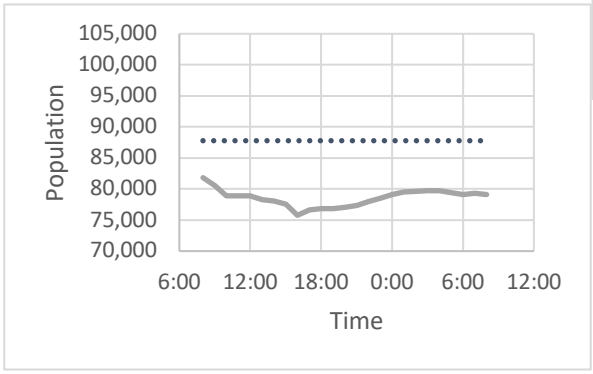

C: (Above) estimated population over time for control (November 14, 2020) day.

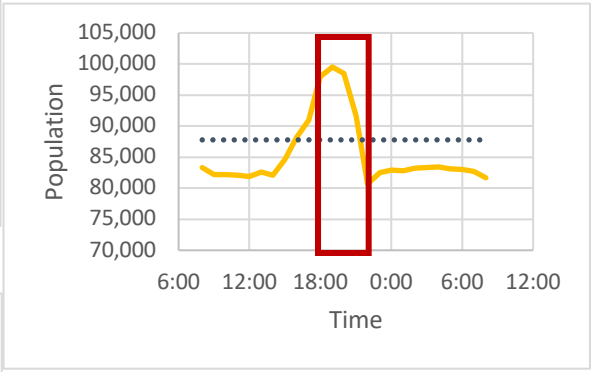

D: (Above) estimated population over time for the Oklahoma State (November 21, 2020)

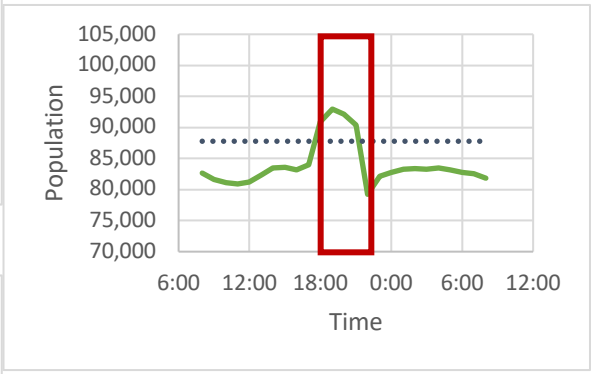

E: (Above) estimated population over time for the Baylor (December 5, 2020) game.

Figure 6: Estimated population over time for all games in the 2020 football season. Approximate game times are outlined in red. A represents the population during Missouri State sampling period, B shows population during the Kansas sampling period, C shows the population during the control sampling period, D shows the population over the duration of the Oklahoma State sampling period, and E shows the population over the duration of the Baylor sampling period.

For all days that were sampled, the before group is the same as the during group (P = 0.14). The difference between the before group and the late-night group is significant (P = 0.01).

The during group is also significantly different from the late-night group when all sampling days are analyzed together ($P < 0.01$).

The population was also analyzed was by dividing the day into time groups to determine if there was a relationship between the population and time at smaller scales. Figure 7A shows the population over time for the before group for all gamedays in 2020. The concentration was increasing over time for all gamedays, but the relationships between the variables were not significant at the 95% confidence level for any of the days. Figure 7B shows the population over time for the during game group for all games in the 2020 football season. The population was decreasing over time for all games except the Missouri State game, which increased very slightly. Oklahoma State had the strongest correlation between the two variables in the during game category and was significant at the 95% confidence level ($R^2 = 0.98$), the relationship for the Baylor game was significant at the 90% confidence level ($R^2 = 0.92$). Figure 7C shows the population over time for the late-night group. The population decreased over time for all games except the Missouri State game, which was increasing in the late-night hours.

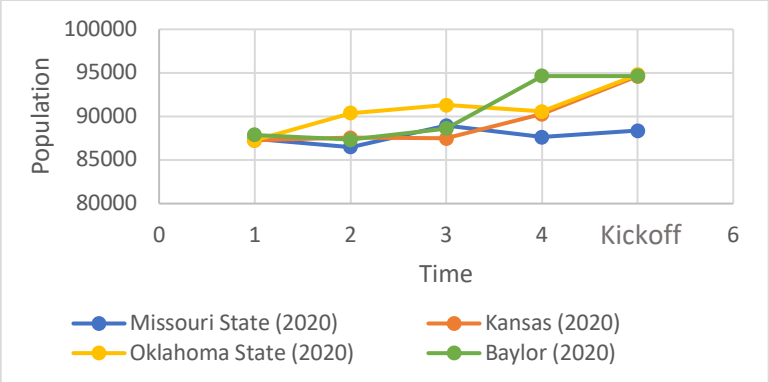

A (Above): SARS-CoV-2 population over time before the football game.

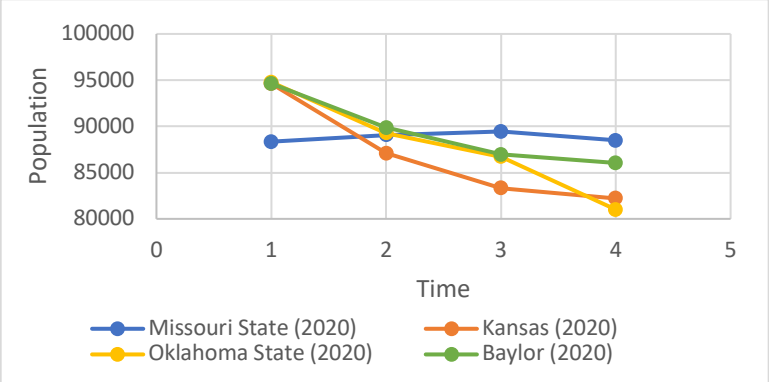

B (Above): SARS-CoV-2 population over time during the football game. 1 represents kickoff.

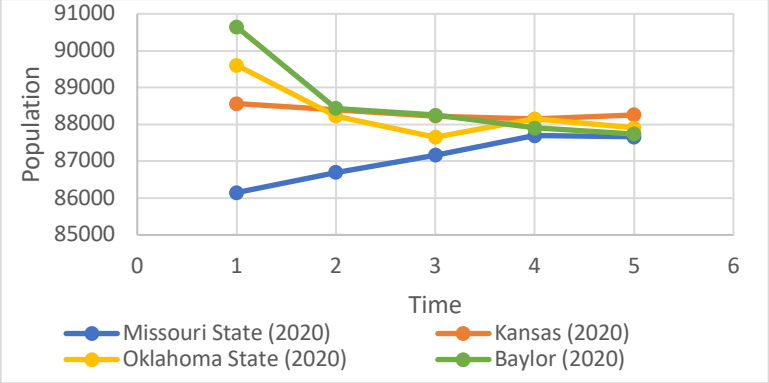

C (Above): SARS-CoV-2 population over time during the late-night category. 1 represents 11:00 pm.

Figure 7: Population over time, by time group, for all games in the 2020 football season.

3.1.3 Concentration of SARS-CoV-2 in Wastewater

The SARS-CoV-2 concentration for each sampling event were compared. Figure 8 displays the SARS-CoV-2 concentration over time for all the games in the 2020 season. When

compared to each other, the difference in concentration for each sampling day is significant ($P < 0.01$). Compared directly to the control day, the concentration from the Missouri State game is not significantly different ($P = 0.50$). The same is true of Kansas compared to the control ($P = 0.25$) and Oklahoma State compared to the control ($P = 0.95$). However, the concentration from the Baylor sampling compared to the control day was significantly different ($P < 0.01$).

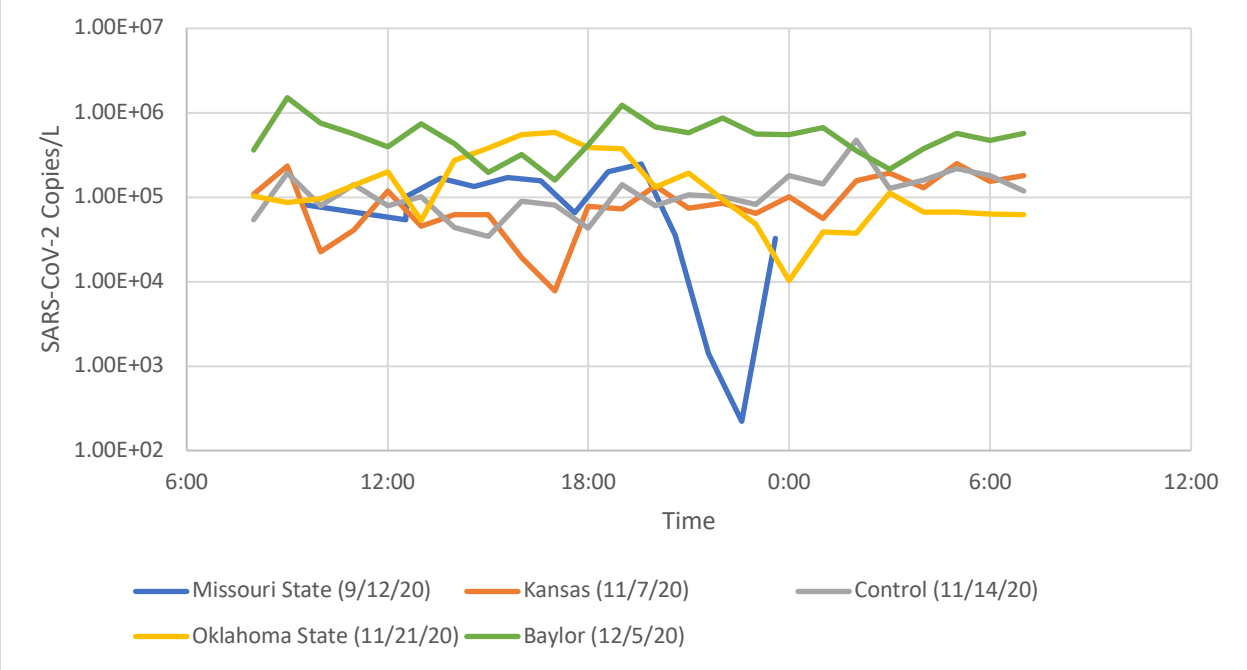

Figure 8: SARS-CoV-2 concentration over time for all games in the 2020 football season.

The average SARS-CoV-2 concentration by time group for all gamedays in 2020 can be found in Table 6.

Table 6: Mean SARS-CoV-2 concentration by time group for all games in the 2020 football season. Within the All row, games with different superscript Greek letters are significantly different at the 95% confidence level.

	Missouri State (September 12, 2020)	**Kansas (November 7, 2020)**	**Control (November 14, 2020)**	**Oklahoma State (November 21, 2020)**	**Baylor (December 5. 2020)**
Before	1.32×10^5	5.7×10^4	N/A	4.47×10^5	2.73×10^5
During	1.21×10^5	3.79×10^4	N/A	2.70×10^5	8.40×10^5
After	N/A	8.96×10^4	N/A	N/A	N/A
Late-Night	3.25×10^4	1.14×10^5	2.01×10^5	4.94×10^4	4.70×10^5
All	$1.03 \times 10^{5\,\alpha}$	$1.02 \times 10^{5\,\alpha}$	$1.27 \times 10^{5\,\alpha}$	$1.73 \times 10^{5\,\alpha}$	$5.64 \times 10^{5\,\beta}$

Figure 9A displays the concentration over time for the Missouri State game. The average concentration is greatest in the before game group. Figure 9B shows the SARS-CoV-2 concentration over time for the Kansas game. The concentration of SARS-CoV-2 in the wastewater is on average greatest in the late-night category for this game. Figure 9C shows the SARS-CoV-2 concentration over time for the control day. There is an evident peak in concentration in what would be the late-night category, occurring around 2:00 am. The concentration at that time was approximately 4.73×10^5 copies per liter of wastewater. Figure 9D displays the SARS-CoV-2 concentration over time for the Oklahoma State game. The concentration of SARS-CoV-2 is on average the greatest in the before game group. Figure 9E displays the SARS-CoV-2 concentration over time for the Baylor game. The greatest SARS-CoV-2 concentration occurs in the during game group.

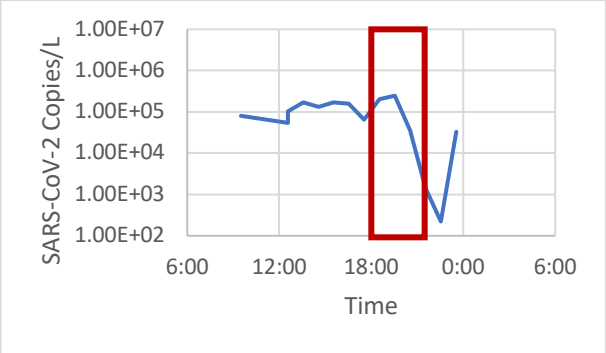

A: (Above) SARS-CoV-2 concentration over time for Missouri State (September 12, 2020) game.

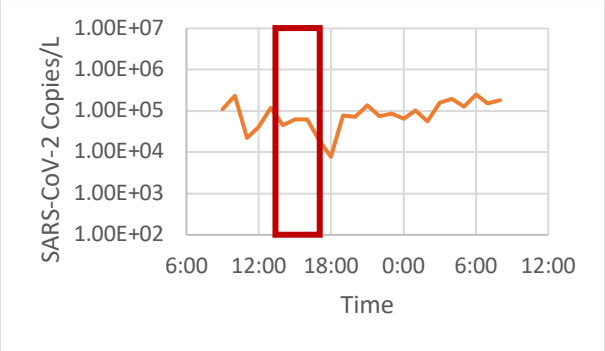

B: (Above) SARS-CoV-2 concentration over time for Kansas (November 7, 2020) game.

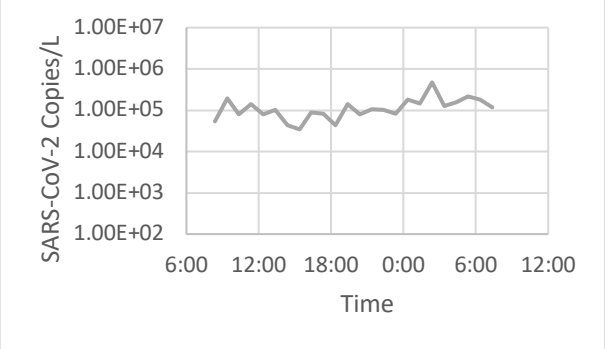

C: (Above) SARS-CoV-2 concentration over time for control (November 14, 2020) day.

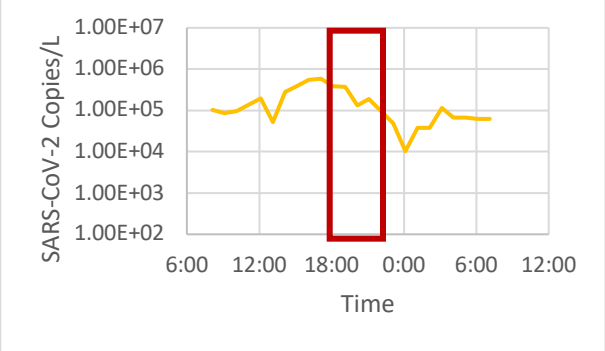

D: (Above) SARS-CoV-2 concentration over time for the Oklahoma State (November 21, 2020) game.

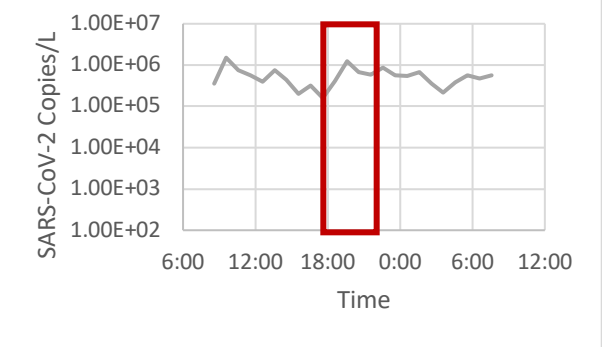

E: (Above) SARS-CoV-2 concentration over time for the Baylor (December 5, 2020) game.

Figure 9: SARS-CoV-2 concentration over time for all games in the 2020 football season. Approximate game times are outlined in red. A represents the concentration during Missouri State sampling period, B shows concentration during the Kansas sampling period, C shows the concentration during the control sampling period, D shows the concentration over the duration of the Oklahoma State sampling period, and E shows the concentration over the duration of the Baylor sampling period.

The SARS-CoV-2 before group is not significantly different from the during group across all games (P = 1.00), nor is it significantly different from the late-night group (P = 0.34). The

concentration of the during group is not significantly different from the late-night group across all games ($P = 0.52$).

To determine if there was an increase in SARS-CoV-2 in the wastewater because of football games, the gameday samples were compared to composite samples collected from the NWRF on days surrounding the football game. As part of regular monitoring for another project, members of the team collected samples from the NWRF on Tuesdays and Fridays, which represent the SARS-CoV-2 concentration from approximately Monday at 10:00 am through Tuesday at 8:00 am and Thursday starting at 10:00 am and ending Friday at 8:00 am. Along with this, additional samples were collected on Saturday and Sunday, representing the concentration from Friday to Saturday and Saturday to Sunday. Figure 10 shows the mean of the hourly gameday samples compared to the concentration of the composite samples from the NWRF. Both concentrations were increasing as the season progressed, which aligns with the trends in confirmed cases at the same time (refer to Figure 1). The difference in concentration between the NWRF time-weighted composite samples and the mean of the hourly Missouri State samples is not significant ($P = 0.33$). The same is true of the difference between the NWRF composite samples and the Kansas mean of the hourly samples ($P = 0.62$), the NWRF composite samples and Oklahoma State hourly samples average ($P = 0.681$), and the Baylor hourly average vs NWRF composite samples ($P = 0.38$). The difference between the control and NWRF samples is significant ($P < 0.01$).

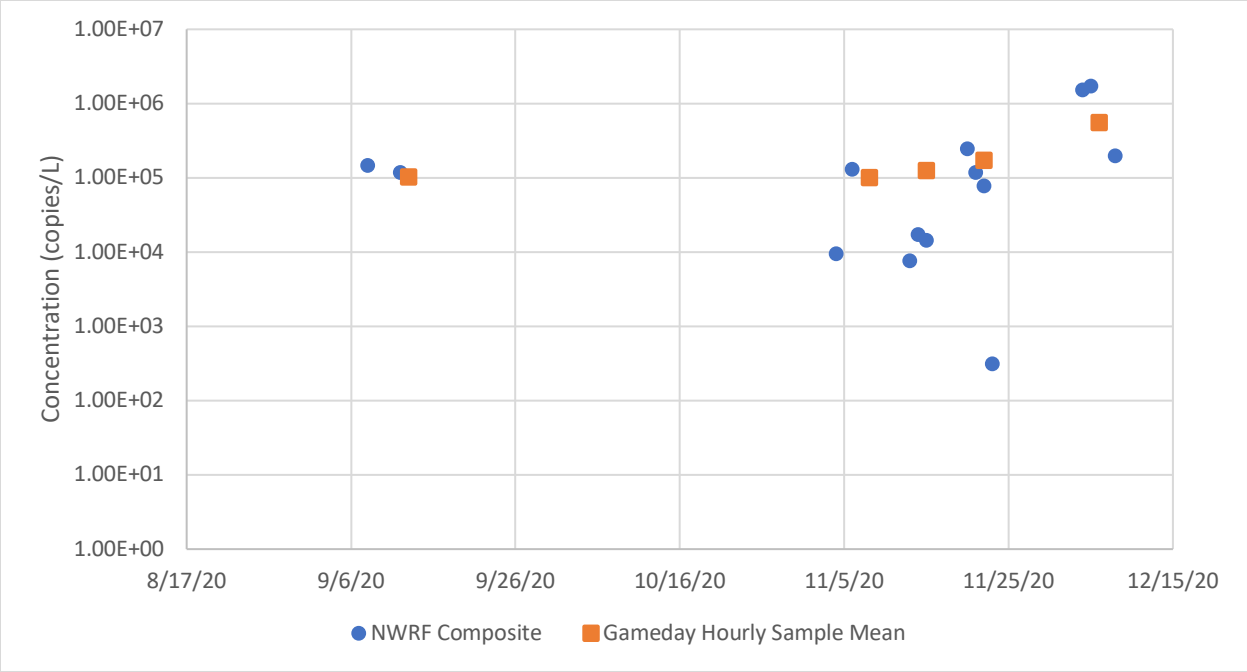

Figure 10: Gameday mean SARS-CoV-2 concentration compared to the concentration from the City of Norman, Oklahoma (NWRF) over the course of the 2020 football season.

Table 7 shows the mean concentration for the NWRF samples and the gameday samples per game for the 2020 football season.

Table 7: Average SARS-CoV-2 concentration (copies/L) for Norman Water Reclamation Facility (NWRF) and gameday samples for the 2020 football season.

	Missouri State (September 12, 2020)	**Kansas (November 7, 2020)**	**Control (November 14, 2020)**	**Oklahoma State (November 21, 2020)**	**Baylor (December 5. 2020)**
NWRF 24-Hour Composite	1.61×10^5	7.06×10^4	1.32×10^4	1.10×10^5	1.15×10^6
Gameday Hourly Sample Mean	1.06×10^5	1.08×10^5	1.39×10^5	2.08×10^5	5.76×10^5

Another way that the population was analyzed was to look at the relationships between the population and the SARS-CoV-2 concentration. This was done by running a linear regression between the two variables. Figure 11 shows the population compared to the concentration ($R^2 < 0.01$). This result indicates that there is no significant correlation between the two variables when

analyzing all the games together, though the concentration was greater when the population was greater, indicating a positive relationship between the two variables.

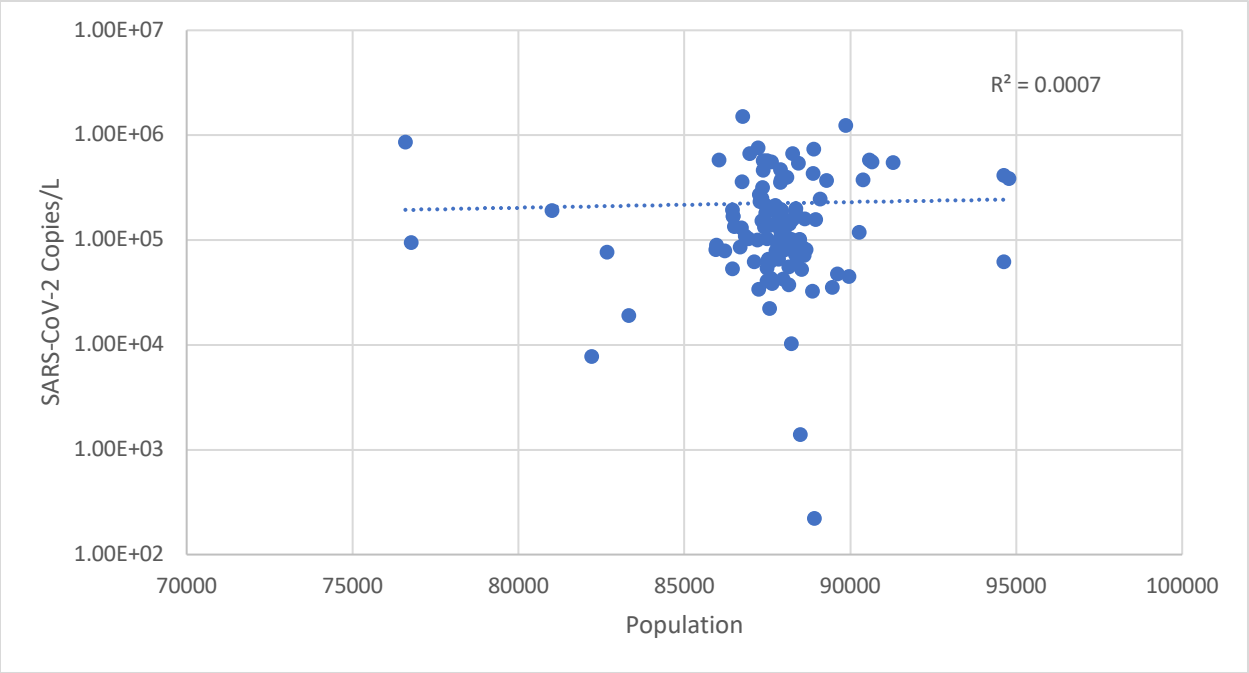

Figure 11: SARS-CoV-2 concentration versus population for all games in the 2020 football season.

Another analysis performed was to determine the strength of the relationship between the SARS-CoV-2 concentration and flow. Figure 12 shows the flow and the concentration for all games in the 2020 football season ($R^2 = 0.01$). The correlation between the two variables is negative, indicating that the concentration was greater when the flow was lesser, but this is not significant at the 95% confidence level.

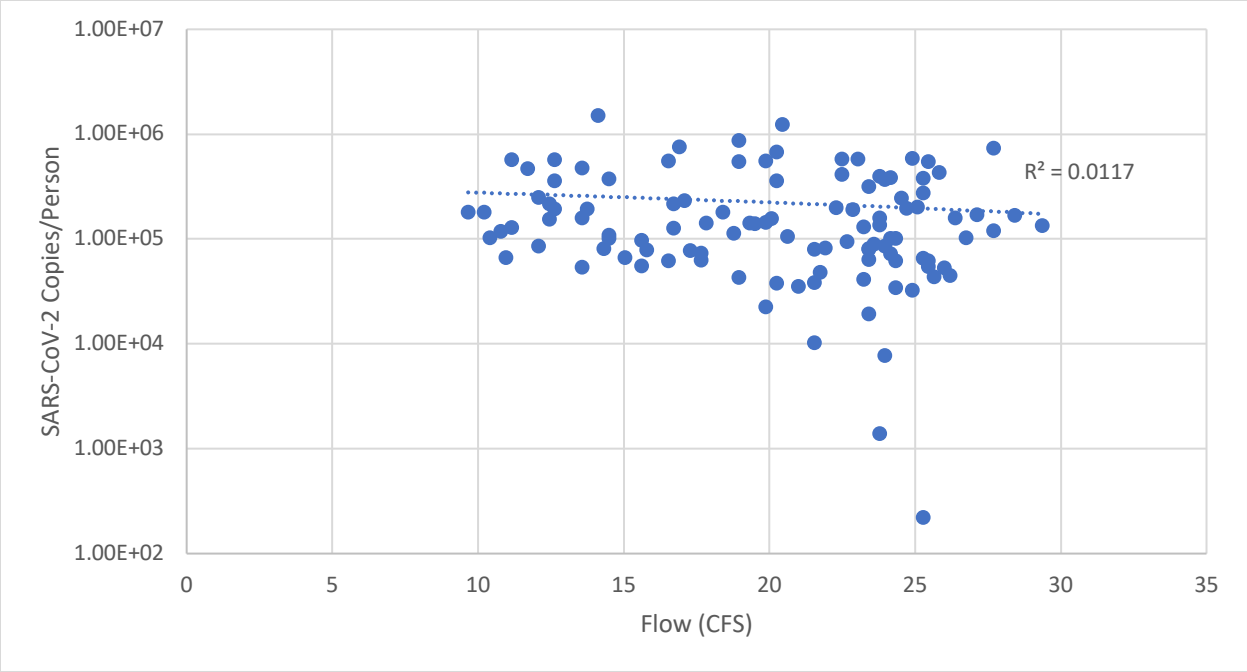

Figure 12: SARS-CoV-2 concentration versus flow for all games in the 2020 football season.

The correlations between flow, population, and SARS-CoV-2 concentration were also analyzed for each game individually. Table 8 shows the results of that analysis. None of the correlations were significant at the 95% confidence level.

Table 8: Results of correlation analysis (R^2 values) between the concentration and flow, and the concentration and population for the 2020 football season.

	Missouri State (September 12, 2020)	**Kansas (November 7, 2020)**	**Control (November 14, 2020)**	**Oklahoma State (November 21, 2020)**	**Baylor (December 5, 2020)**
Concentration vs. Flow	0.09	0.36	0.27	0.29	0.03
Concentration vs. Population	0.03	0.02	0.01	0.18	0.04

Figure 13A shows the SARS-CoV-2 concentration of the before game time group for the 2020 football season. The concentration was increasing over time for all games except the Missouri State game. Oklahoma State had the strongest correlation between the concentration and time over these four hours, which was significant at the 95% confidence level, increasing until the game started ($R^2 = 0.95$). Figure 13B shows the SARS-CoV-2 concentration over time

for the during game time group. The concentration was decreasing over time for all games, though none of the correlations were significant at the 95% confidence level. Figure 13C shows the SARS-CoV-2 concentration over time of the late-night group for all games in the 2020 football season. The concentration found in the late-night was decreasing for the Baylor gameday, although not significant.

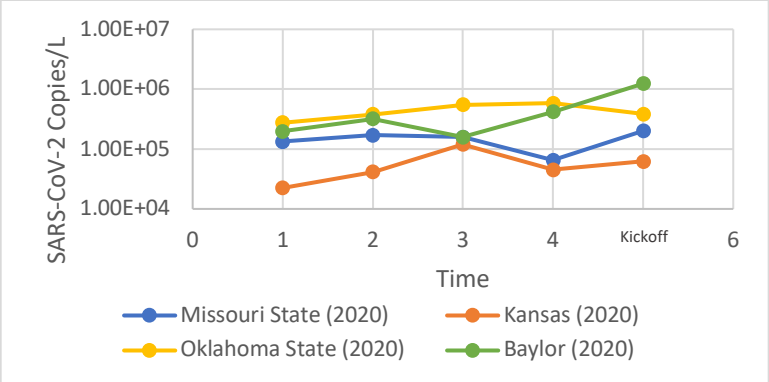

A (Above): SARS-CoV-2 concentration over time before the football game.

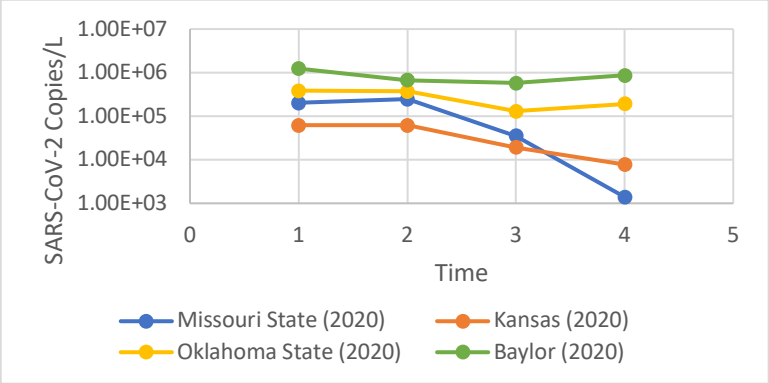

B (Above): SARS-CoV-2 concentration over time during the football game. 1 represents kickoff.

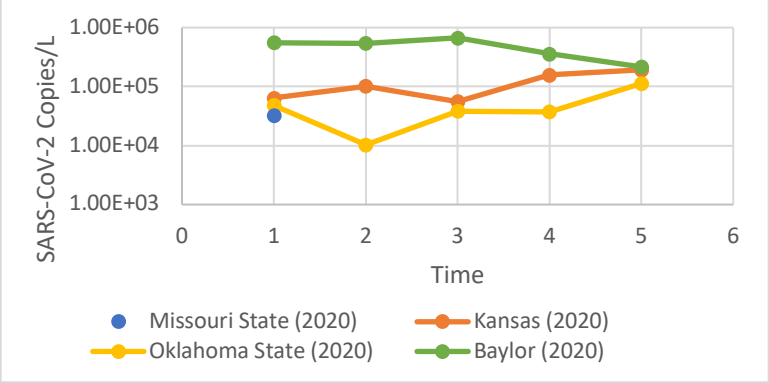

C (Above): SARS-CoV-2 concentration over time during the late-night category. 1 represents 11:00 pm.

Figure 13: SARS-CoV-2 concentration over time, by time category, for all games in the 2020 football season.

3.1.4 Viral Load per Person

The cell phone and flow data were used with the concentration data to calculate a viral load per person. Figure 14 displays the SARS-CoV-2 viral load per person over time for each

sampling day. By using a viral load per person, the differences between each day are more pronounced. Compared to each other, the difference in viral load per person for all games is significantly different ($P < 0.01$). Furthermore, when compared individually to the control day, the viral load per person of each gameday is significantly greater ($P < 0.01$ for all tests).

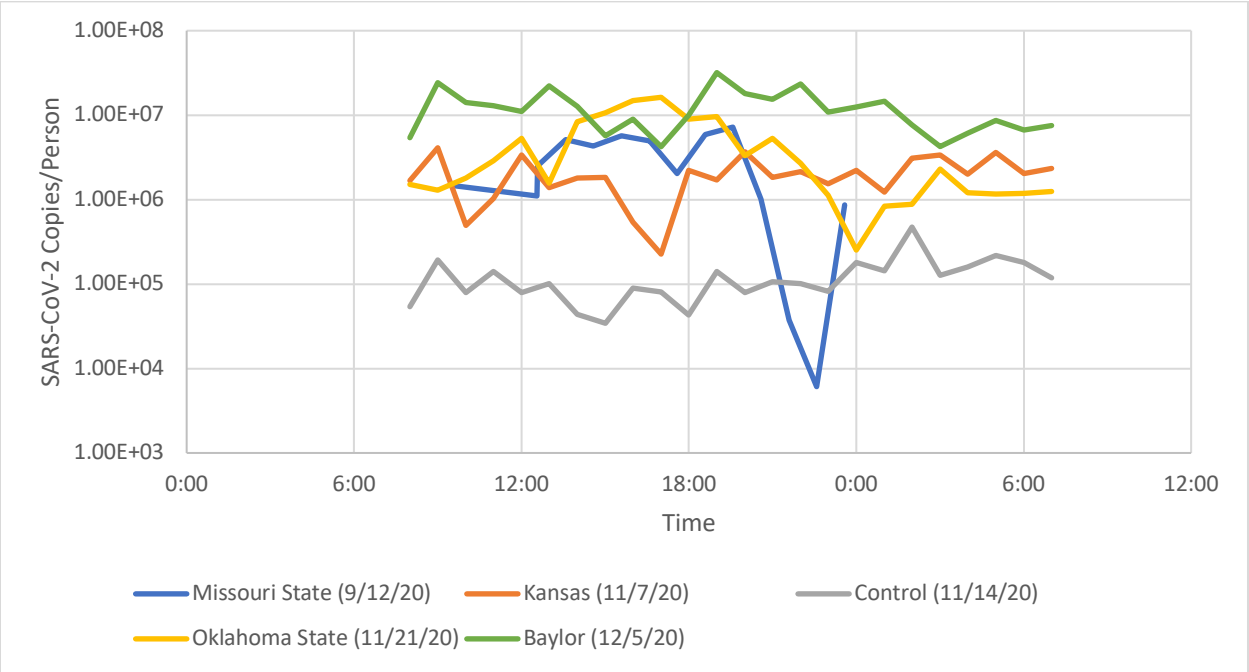

Figure 14: SARS-CoV-2 viral load per person over time for each sampling day.

Table 9 shows the average SARS-CoV-2 viral load per person per time group per day.

Table 9: Mean SARS-CoV-2 viral load per person by time group for all games in the 2020 football season. Within the All row, games with different Greek letters are significantly different at the 95% confidence level.

	Missouri State (September 12, 2020)	**Kansas (November 7, 2020)**	**Control (November 14, 2020)**	**Oklahoma State (November 21, 2020)**	**Baylor (December 5. 2020)**
Before	4.24×10^6	1.57×10^6	N/A	1.27×10^7	7.22×10^6
During	3.54×10^6	1.10×10^6	N/A	6.81×10^6	2.22×10^7
After	N/A	2.36×10^6	N/A	N/A	N/A
Late-Night	8.62×10^5	2.29×10^6	2.01×10^5	1.08×10^6	9.95×10^6
All	$3.09 \times 10^{6\ \alpha}$	$2.06 \times 10^{6\ \alpha,\chi}$	$1.27 \times 10^{5\ \beta,\delta,\phi,\gamma}$	$4.37 \times 10^{6\ \alpha,\delta,\varepsilon}$	$1.25 \times 10^{7\ \beta,\delta,\phi,\eta}$

Figure 15A shows the SARS-CoV-2 viral load per person over time for the Missouri State game. Figure 15B displays the SARS-CoV-2 viral load per person over time for the Kansas game. On average, the greatest viral load per person occurs in the after-game group. Figure 15C displays the SARS-CoV-2 viral load per person of the control weekend. The peak in the viral load per person occurs at 2:00 am with a viral load of 4.73×10^5 SARS-CoV-2 copies per person. Figure 15D shows the SARS-CoV-2 viral load per person for the Oklahoma State game. Figure 15E displays the SARS-CoV-2 viral load per person of the Baylor game The mean viral load per person is greatest in the during game group.

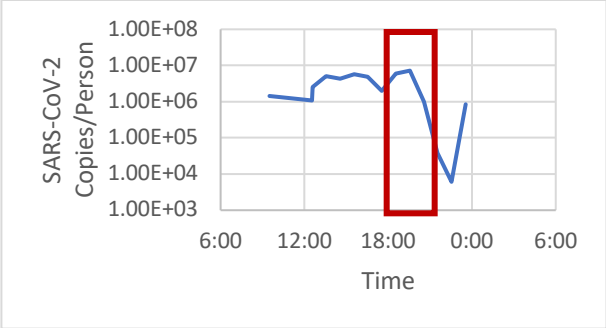

A: (Above) SARS-CoV-2 viral load per person over time for Missouri State (September 12, 2020) game.

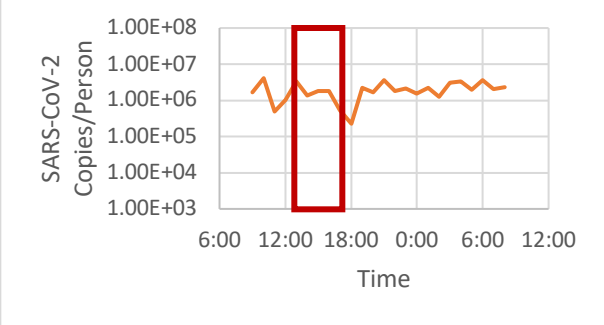

B: (Above) SARS-CoV-2 viral load per person over time for Kansas (November 7, 2020)

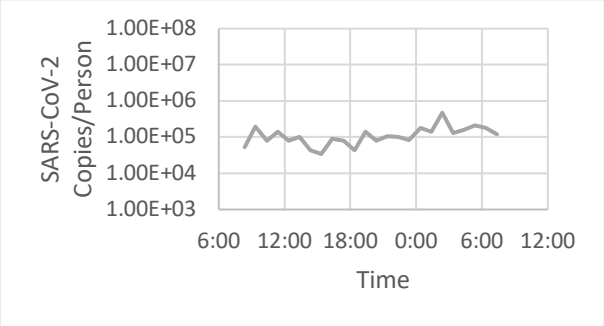

C: (Above) SARS-CoV-2 viral load per person over time for control (November 14, 2020) day.

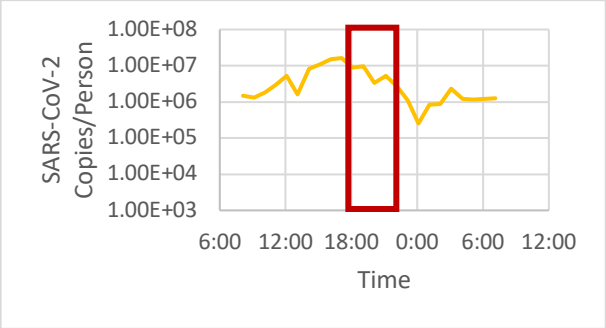

D: (Above) SARS-CoV-2 viral load per person over time for the Oklahoma State (November 21,

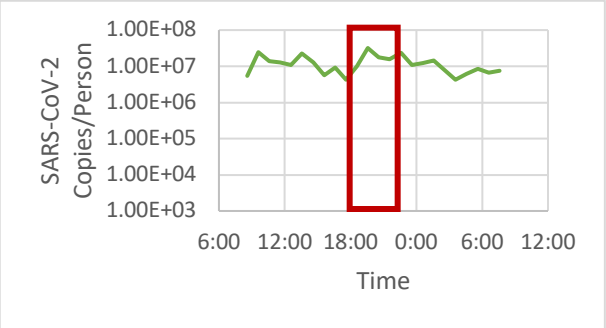

E: (Above) SARS-CoV-2 viral load per person over time for the Baylor (December 5, 2020)

Figure 15: SARS-CoV-2 viral load per person for all games in the 2020 football season. Approximate game times are outlined in red. A represents the viral load per person during Missouri State sampling period, B shows viral load per person during the Kansas sampling period, C shows the viral load per person during the control sampling period, D shows the viral load per person over the duration of the Oklahoma State sampling period, and E shows the viral load per person over the duration of the Baylor sampling period.

For all games together, the before group was not significantly different from the during group (P = 0.72) or the late-night group (P = 0.06). The during group of all games was not significantly different from the late-night group (P = 0.38).

Like the comparisons between the concentration and population, the viral load per person was compared against the population to determine the strength of the relationship between the two variables. Figure 16 shows the SARS-CoV-2 viral load per person over the population for all games in the 2020 football season ($R^2 < 0.01$). There is a weak positive correlation between the two variables.

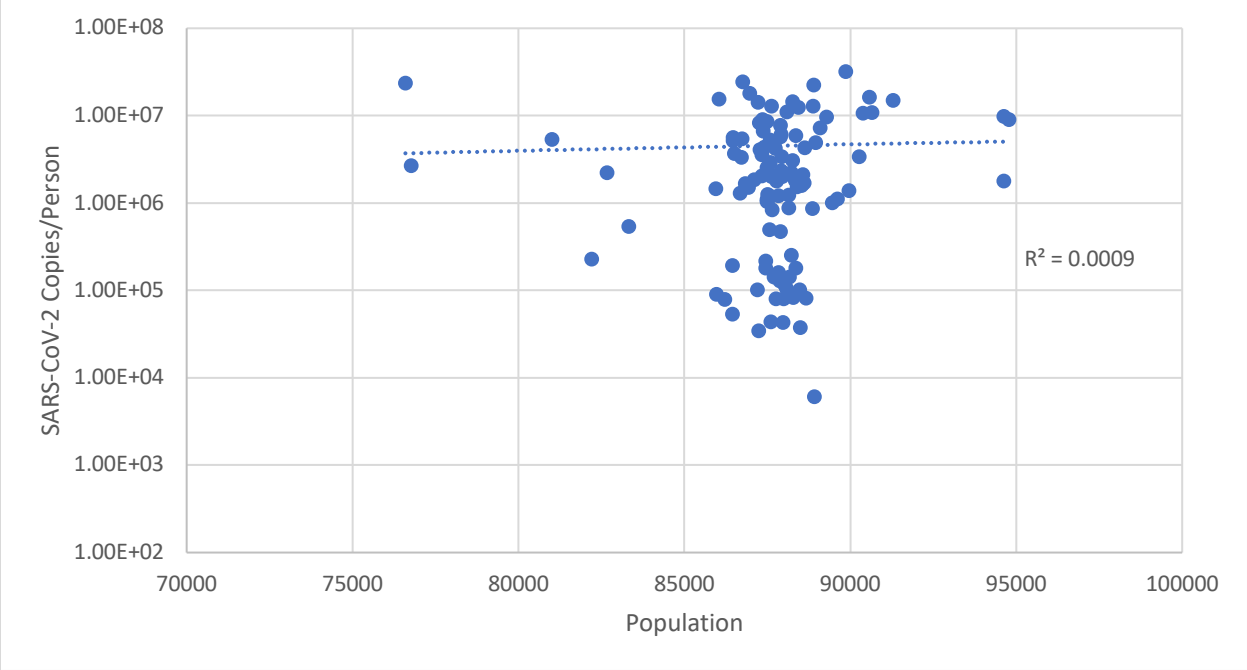

Figure 16: SARS-CoV-2 viral load per person versus the population for all games in the 2020 football season.

Figure 17 shows the SARS-CoV-2 viral load per person versus the flow. There is a weak positive correlation between the two variables ($R^2 = 0.02$).

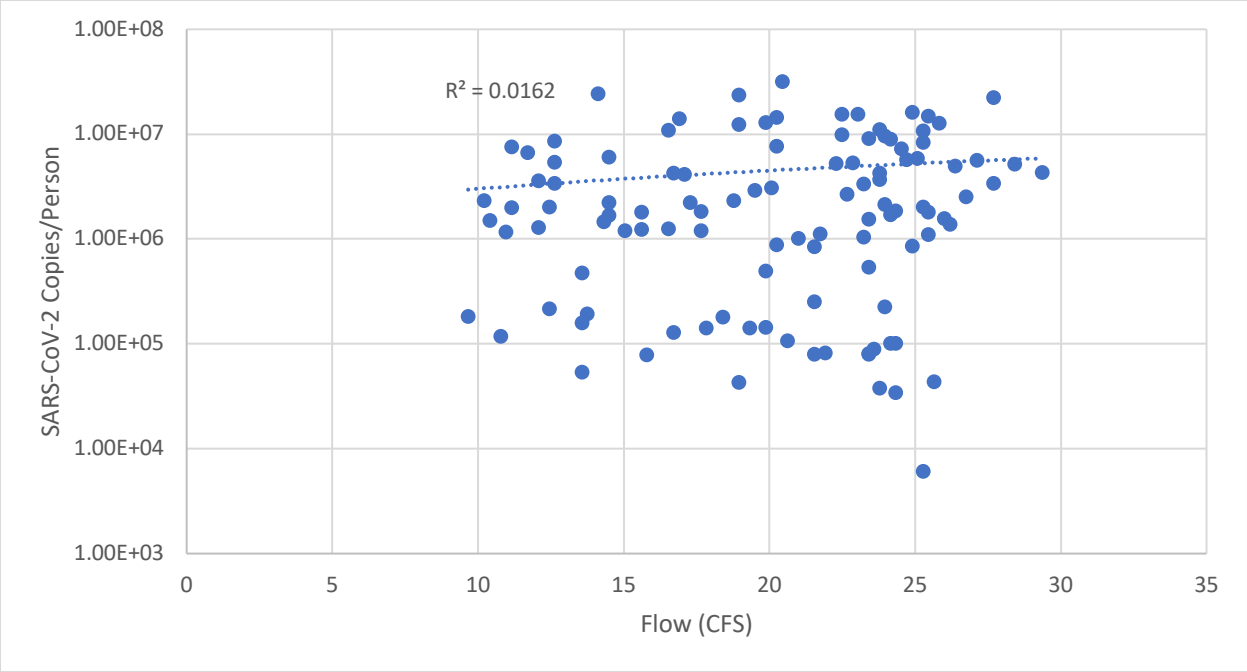

Figure 17: SARS-CoV-2 viral load per person versus the flow for all games in the 2020 football season.

A similar regression analysis was performed for each game individually. Table 10 shows the resulting R^2 values for each game for the viral load per person compared to the flow, as well as the viral load per person compared to the population. None of the correlations are significant at the 95% confidence level.

Table 10: Results of correlation analysis (R^2 values) between the viral load per person and flow, and the viral load per person and population for the 2020 football season.

	Missouri State (September 12, 2020)	**Kansas (November 7, 2020)**	**Control (November 14, 2020)**	**Oklahoma State (November 21, 2020)**	**Baylor (December 5, 2020)**
Concentration vs. Flow	0.16	0.07	0.27	0.36	0.05
Concentration vs. Population	0.02	0.05	0.01	0.15	0.05

Another way that the viral load per person was analyzed was by looking at specific time groups. Figure 18A shows the SARS-CoV-2 viral load per person of the before-game time category for all games in the 2020 football season. The viral load per person was increasing over time for all games except the Missouri State game, which was the first game of the season.

Figure 18B shows the SARS-CoV-2 viral load per person for all games in the 2020 football season for the during game category. The viral load per person was decreasing for all games in the 2020 football season. The Kansas game had the strongest correlation between the viral load per person and time at this time scale. Figure 18C shows the SARS-CoV-2 viral load per person for all these games during the late-night category. The viral load per person was increasing for the Oklahoma State and Kansas games but decreasing for the Baylor game and overall.

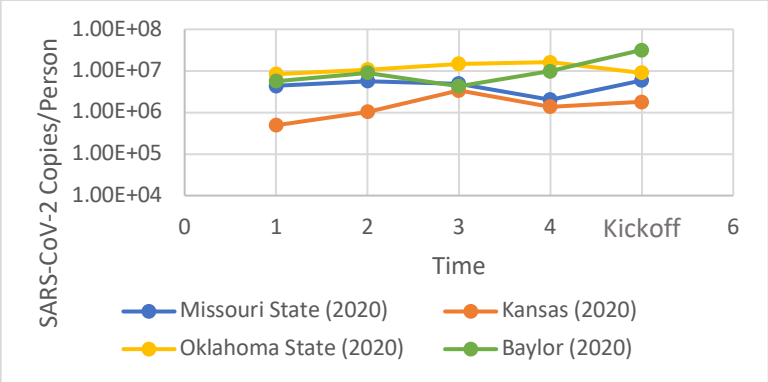

A (Above): SARS-CoV-2 viral load per person over time before the football game.

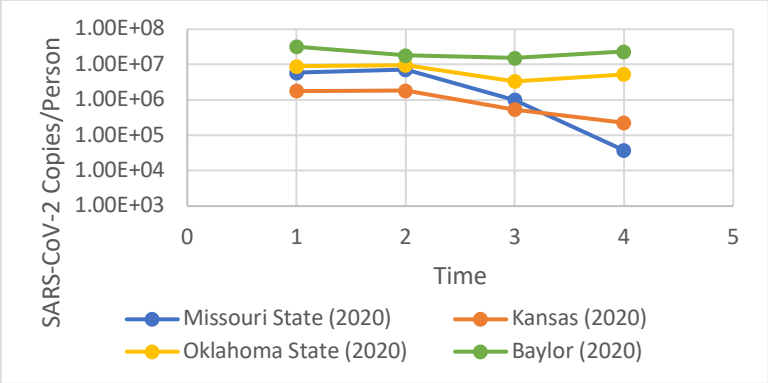

B (Above): SARS-CoV-2 viral load per person over time during the football game. 1 represents kickoff.

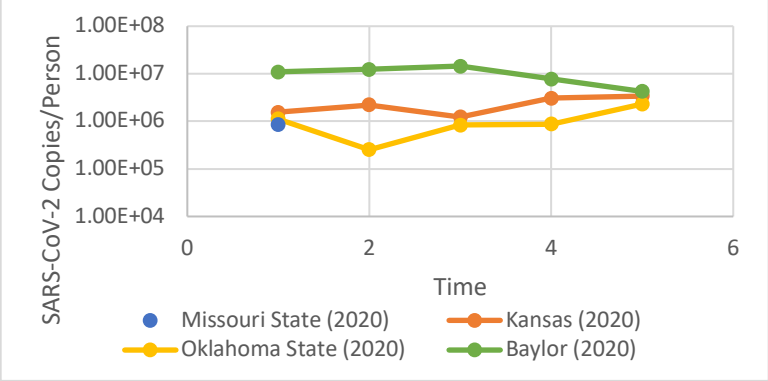

C (Above): SARS-CoV-2 viral load per person over time during the late-night category. 1 represents 11:00 pm.

Figure 18: SARS-CoV-2 viral load per person over time, by time category, for all games in the 2020 football season.

The variance of the concentration was compared to the variance of the population using a Levene Test for Equality of Variances to determine if including the population in the analysis

made a difference. If the variances were not significantly different, that means that using a viral load per person would not be significantly different from the concentration. For all sampling days in 2020 combined, the variances are significantly different at the 95% confidence level. This was true when all the games were looked at individually, with exception to the Missouri State game, which could be due to the small number of samples

3.1.5 Relative Viral Load per Person

The SARS-CoV-2 viral loads per person were corrected using the first sample of the day. This practice assumes that the first sample of the day is representative of the SARS-CoV-2 levels already in the sewershed and all changes in the viral load per person are due to travel into or out of the area. The resulting values from subtracting out the first sample concentration are referred to henceforth as the relative viral load per person. Therefore, a negative value would indicate that there is less virus present than the first sample of the day. Figure 19 shows the relative SARS-CoV-2 viral load per person for all sampling days in 2020. Compared to each other using an ANOVA, the relative viral load per person for each day is significantly different ($P < 0.01$). To determine if the amount of virus in the wastewater was related to the football game, each game was compared individually to the control day. The difference in relative viral load per person was not significant between the control and Missouri State ($P = 0.41$), Kansas ($P = 0.15$), or Oklahoma State ($P = 0.40$). The difference in relative viral load per person between the control and Baylor was significant ($P < 0.01$).

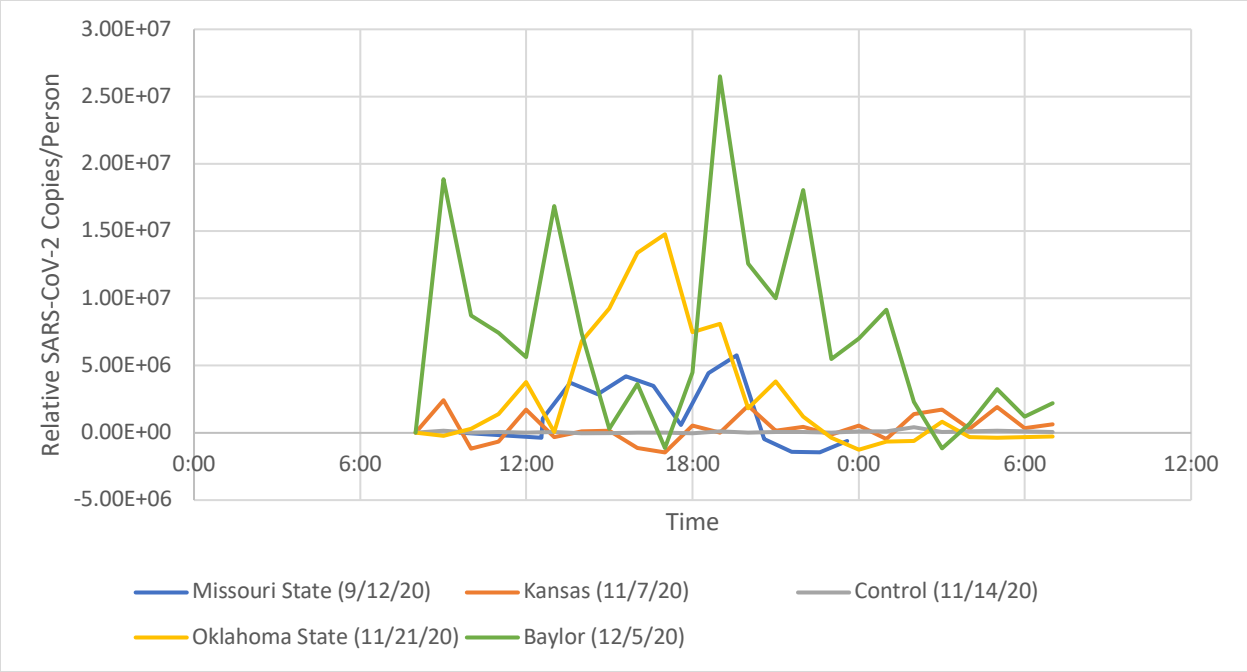

Figure 19: Relative SARS-CoV-2 viral load per person over time for the 2020 football season.

Table 11 shows the relative SARS-CoV-2 viral load per person by time group for all sampling days in the 2020 football season.

Table 11: Mean relative SARS-CoV-2 viral load per person by time group for all games in the 2020 football season. Within the All row, games with different superscript Greek letters are significantly different at the 95% confidence level.

	Missouri State (September 12, 2020)	**Kansas (November 7, 2020)**	**Control (November 14, 2020)**	**Oklahoma State (November 21, 2020)**	**Baylor (December 5. 2020)**
Before	2.79×10^{6}	-1.07×10^{5}	N/A	1.11×10^{7}	1.82×10^{6}
During	2.09×10^{6}	-5.80×10^{5}	N/A	5.31×10^{6}	1.68×10^{7}
After	N/A	6.80×10^{5}	N/A	N/A	N/A
Late-Night	-5.90×10^{5}	6.10×10^{5}	1.47×10^{5}	-4.23×10^{5}	4.55×10^{6}
All	$1.64 \times 10^{6\ \alpha}$	$3.08 \times 10^{5\ \beta,\chi}$	$7.34 \times 10^{4\ \beta,\chi,\phi,\eta}$	$2.86 \times 10^{6\ \alpha,\delta,\varepsilon}$	$7.06 \times 10^{6\ \beta,\delta,\phi,\gamma}$

Figure 20A displays the relative SARS-CoV-2 viral load per person over time. The greatest mean relative viral load per person is in the before game group. Figure 20B displays the relative SARS-CoV-2 viral load per person over time for the Kansas game. The greatest relative

viral load per person is on average during the after-game category. Figure 20C displays the relative SARS-CoV-2 viral load per person over time of the control day. There is a peak in relative viral load per person occurring in what would be the late-night category. The peak occurs around 2:00 am with a relative viral load per person of 4.19×10^5 relative SARS-CoV-2 copies per person. Figure 20D displays the relative SARS-CoV-2 viral load per person over time for the Oklahoma State game. The mean relative viral load per person is greatest in the before game category. Figure 20E shows the relative SARS-CoV-2 viral load per person over time for the Baylor game. The average relative viral load per person was greatest in the during game category.

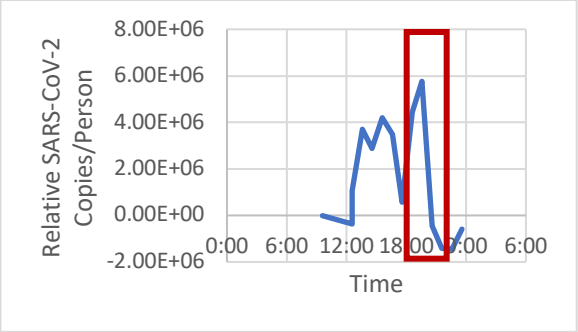

A: (Above) Relative SARS-CoV-2 viral load per person over time for Missouri State (September 12, 2020) game.

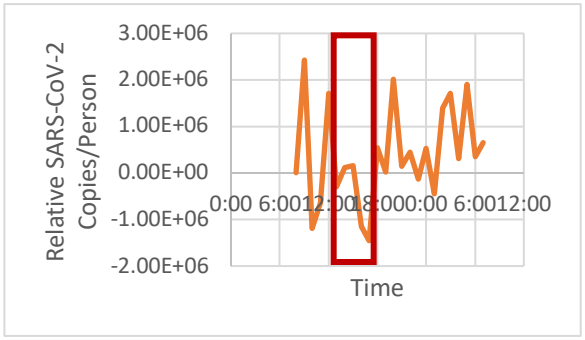

B: (Above) Relative SARS-CoV-2 viral load per person over time for Kansas (November 7, 2020) game.

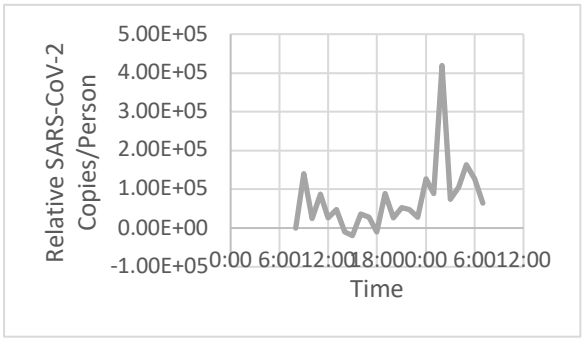

C: (Above) Relative SARS-CoV-2 viral load per person over time for control (November 14, 2020) day.

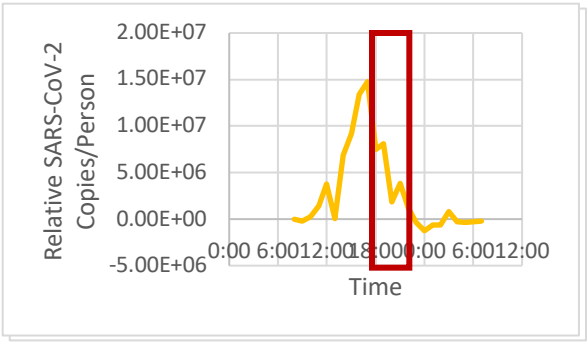

D: (Above) Relative SARS-CoV-2 viral load per person over time for the Oklahoma State (November 21, 2020) game.

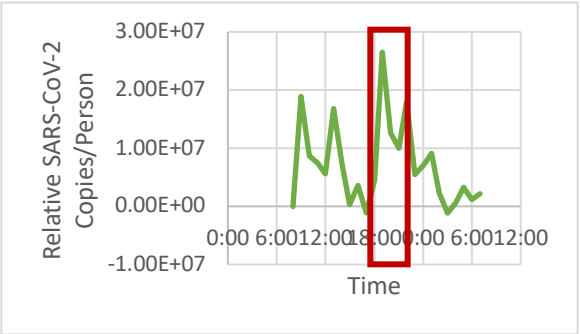

E: (Above) Relative SARS-CoV-2 viral load per person over time for the Baylor (December 5, 2020) game.

Figure 20: Relative SARS-CoV-2 viral load per person over time all games in the 2020 football season. Approximate game times are outlined in red. A represents the relative viral load per person during Missouri State sampling period, B shows the relative viral load per person during the Kansas sampling period, C shows the relative viral load per person during the control sampling period, D shows the relative viral load per person over the duration of the Oklahoma State sampling period, and E shows the relative viral load per person over the duration of the Baylor sampling period.

When compared together, the relative viral load person of the before category for all games is not significantly different from the during category (P = 0.87) or the late-night category (P = 0.073). The relative viral load per person for the during category for all games is not significantly different from the late-night category (P = 0.11).

Figure 21 shows the relative SARS-CoV-2 viral load per person compared to the population. There is a weak positive correlation between the population and the relative viral load per person, that is not significant at the 95% confidence level.

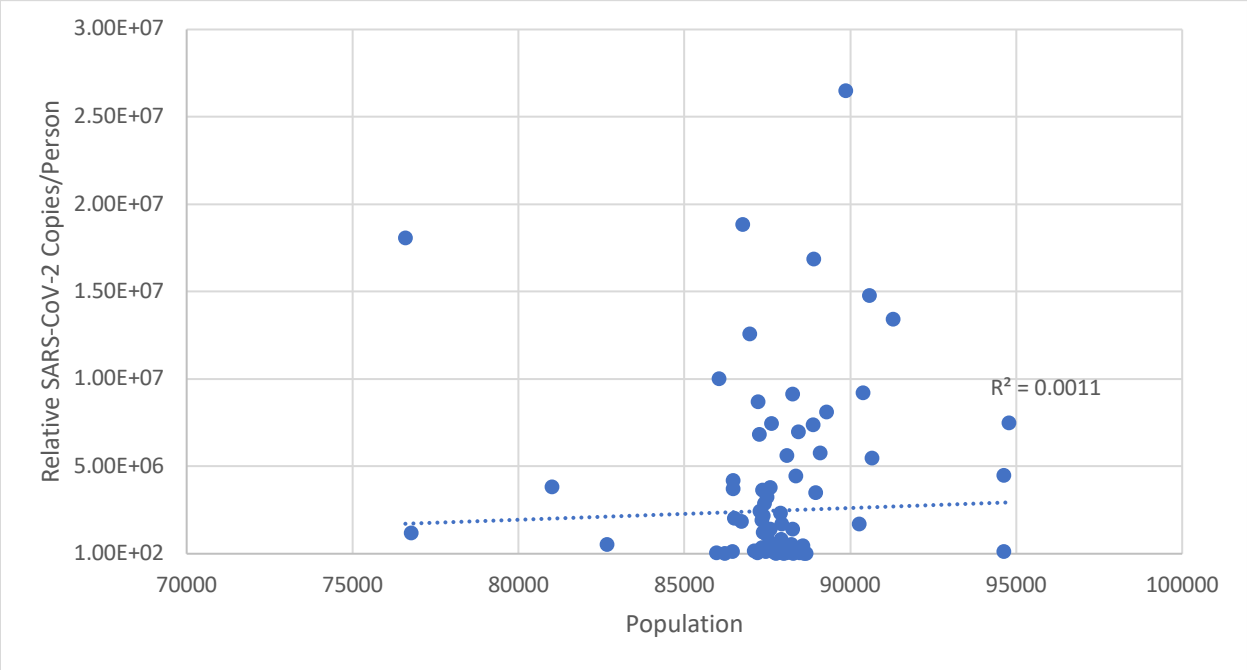

Figure 21: Relative SARS-CoV-2 viral load per person versus the population for all games in the 2020 football season.

Figure 22 shows the relative SARS-CoV-2 viral load per person versus the flow. Again, there is a weak positive correlation between the two variables ($R^2 = 0.03$).

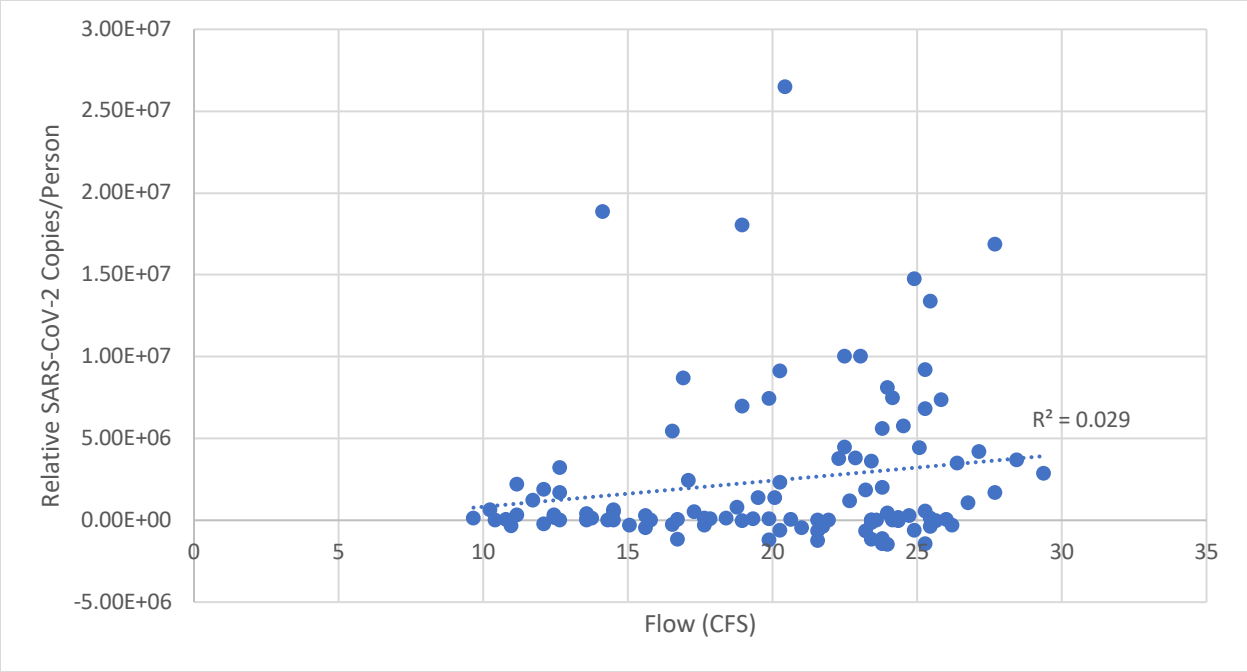

Figure 22: Relative SARS-CoV-2 viral load per person versus the flow for all games in the 2020 football season.

A similar regression analysis was performed at the individual game level as well as by seasons. Table 12 shows the resulting R^2 values when the relative viral load per person was compared to the flow as well as the population. There were no days that had significant relationships at the 95% confidence level.

Table 12: Results of correlation analysis (R^2 values) between the relative viral load per person and flow, and the relative viral load per person and population for the 2020 football season.

	Missouri State (September 12, 2020)	**Kansas (November 7, 2020)**	**Control (November 14, 2020)**	**Oklahoma State (November 21, 2020)**	**Baylor (December 5, 2020)**
Concentration vs. Flow	0.16	0.07	0.27	0.36	0.05
Concentration vs. Population	0.02	0.05	0.01	0.15	0.05

For these analyses, the relative viral load per person was calculated by subtracting out the first viral load per person of the time category, making all the first value zero. This was chosen because it further explains how the relative viral load per person changed at these time scales.

The correlation between the relative viral load per person and time was analyzed by time groups. Figure 23A shows the relative SARS-CoV-2 concentration over time for the before game group for all games in the 2020 football season. The relative viral load per person was increasing over time before kickoff for the Oklahoma State game. The relative viral load per person decreased over time for the Baylor game at this time category. The relative viral load per person was generally stable over time before the game for the Missouri State and Kansas games. Figure 23B shows the relative SARS-CoV-2 viral load per person over time for each game in the during game category. At this time scale, the relative viral load per person increased for the Baylor game, decreased for the Oklahoma State game, and remained mostly constant for the Missouri State and Kansas games. The relative SARS-CoV-2 viral load per person over time was analyzed for the late-night category. Figure 23C displays the results of this analysis. The relative viral load per person increased for the Kansas and Oklahoma State games at this time scale and decreased for the Baylor game.

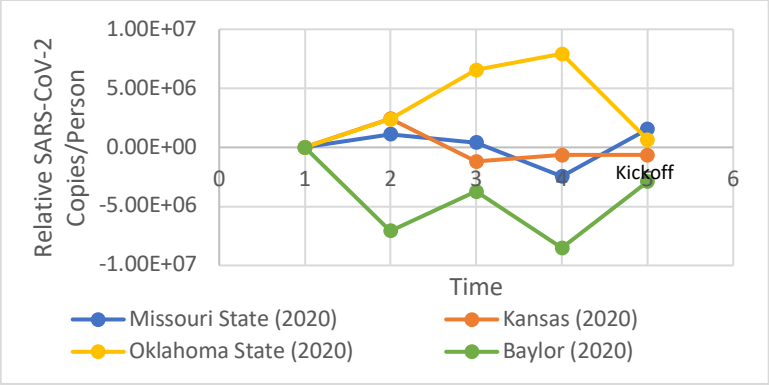

A (Above): Relative SARS-CoV-2 viral load per person over time before the football game. Time 1 represents the first of four hours before the game

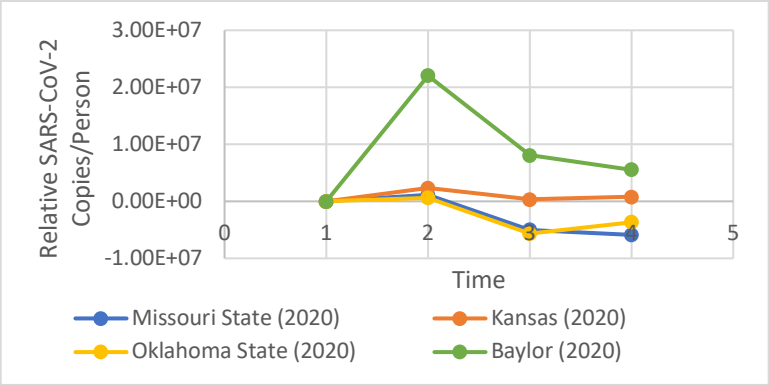

B (Above): Relative SARS-CoV-2 viral load per person over time during the football game. Time 1 represents kickoff

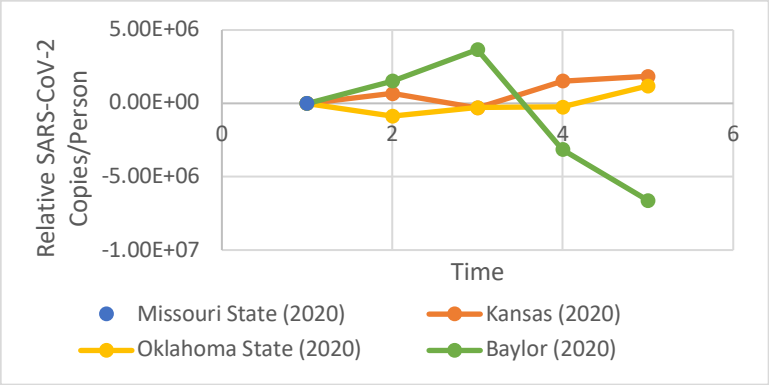

C (Above): Relative SARS-CoV-2 viral load per person over time during the late-night category. Time 1 represents 11:00 pm.

Figure 23: Relative SARS-CoV-2 viral load per person over time, by time category, for all games in the 2020 football season.

3.2 2021 Football Season

The results for the 2021 football season follow. Results are broken into five categories for each game: flow, population, concentration, viral load per person, and relative viral load per

person. The goal of these analyses is to determine if there was an increase in SARS-CoV-2 in the wastewater during home football games.

3.2.1 Flow

Flow data was collected from the NWRF at fifteen-minute time intervals and used to determine how the flow impacts the amount of SARS-CoV-2 in the wastewater. Figure 24 shows the flow over time for all games in the 2021 football season. When all games and the control were compared directly to each other using an ANOVA, the flow for each day was significantly different (P = 0.04). To determine if there was a difference in flow between days with a football game and the control, each game was compared to the control individually. The difference in flow for the Tulane game compared to the control was significant (P = 0.02). For the control compared to the Western Carolina (P = 0.20), Nebraska (P = 0.58), West Virginia (P = 0.42), Texas Christian (P = 0.05), and Iowa State (P = 0.47) games, the difference was not significant.

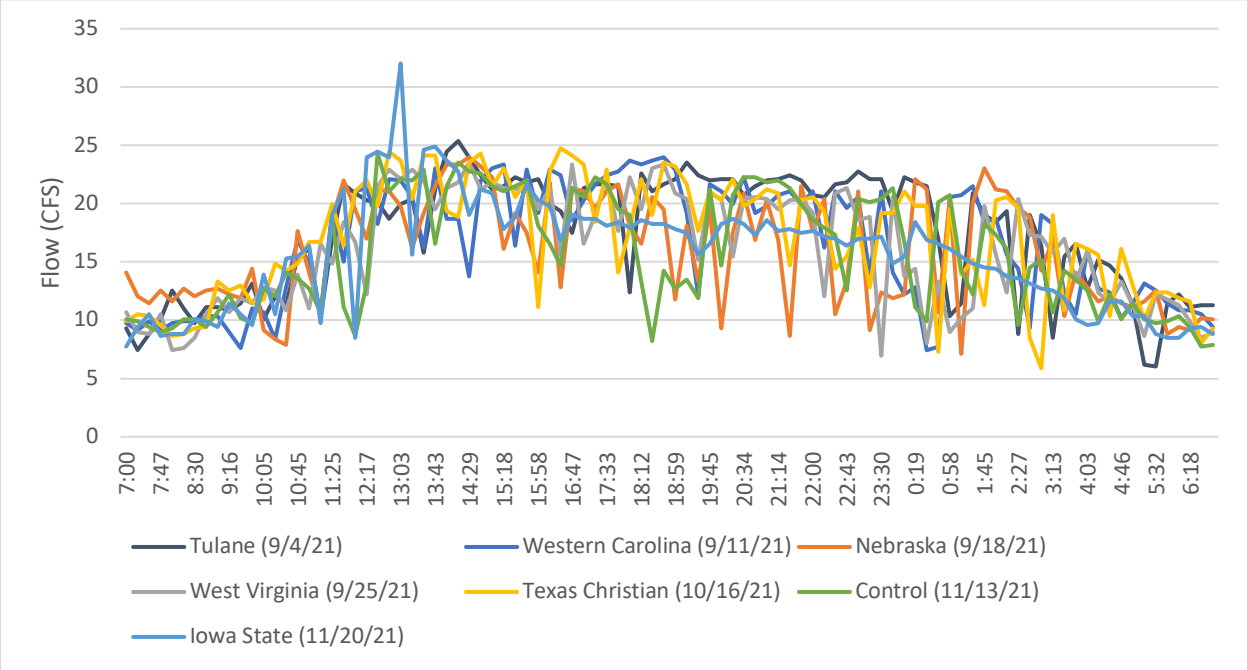

Figure 24: Flow over time for all sampling days in the 2021 football season.

Table 13 shows the mean flow per time group for all sampling days in the 2021 football season. In this table, the numbers with different superscript letters within the same column are significantly different from each other at the 95% confidence level.

Table 13: Mean flow (CFS) by time group for all games in the 2020 football season. For each game (within columns) time categories with different letter superscripts are significantly different as determined by Mann-Whitney tests at the 95% confidence level. Within the 24-hour row, games with different superscript Greek letters are significantly different at the 95% confidence level.

	Tulane (September 4, 2021)	**Western Carolina (September 11, 2021)**	**Nebraska (September 18, 2021)**	**West Virginia September 25, 2021)**	**Texas Christian (October 16, 2021)**	**Control (November 13, 2021)**	**Iowa State (November 20, 2021)**
Before	10.97^{A}	20.22^{D}	12.08^{E}	21.58^{G}	21.48^{I}	N/A	10.63^{K}
During	19.91^{B}	21.93^{D}	19.68^{F}	19.73^{G}	17.96^{J}	N/A	20.69^{L}
After	20.60^{B}	N/A	18.95^{F}	N/A	N/A	N/A	18.89^{M}
Late-Night	17.66^{C}	15.45^{E}	16.38^{F}	14.68^{H}	15.91^{J}	16.37	14.82^{N}
24-Hour	17.33^{α}	16.47^{α}	15.90^{α}	16.09^{α}	16.95^{α}	15.53^{β}	15.59^{β}

Figure 25A shows the flow over time for the Tulane game. When compared all at once using an ANOVA, the difference in flow for the before, during, and late-night categories is significantly different ($P < 0.01$). The average flow is greatest in the after-game category. Table 10 contains the results of the within game time group analysis. Figure 25B shows the flow over time for the Western Carolina game. Comparing the flow of the before, during, and late-night groups to one another using an ANOVA showed that the flow for each category was significantly different from one another ($P < 0.01$). The average flow was greatest in the during game group. Figure 25C displays the flow over time for the Nebraska game. When compared all at once, the difference in flow for the before, during, after, and late-night categories was significantly different, determined with an ANOVA ($P < 0.01$). The after-game category had the greatest average flow. Figure 25D shows the flow over time for the West Virginia sampling.

When compared to one another all at once using an ANOVA, the difference in flow for the before, during, and late-night categories was significant ($P < 0.01$). The category with the greatest average flow for this sampling day was the before game group. The flow over time for the Texas Christian game can be seen in Figure 25E. Compared to one another, the difference in flow for the before, during, and late-night categories was significant ($P < 0.01$). The average flow was greatest in before the game. Figure 25F shows the flow over time for the control sampling. Because there was no game, the day could not be split into time categories, however the greatest flow occurred around 12:30 pm. Figure 25G shows the flow over time for the Iowa State sampling. The difference in flow between the before, during, after, and late-night categories compared to one another at once is significant ($P < 0.01$). The average flow was greatest during the football game.

A: (Above) Flow over time for Tulane (September 4, 2021) game.

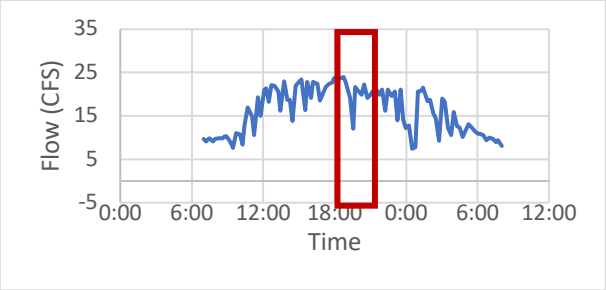

B: (Above) Flow over time for Western Carolina (September 11, 2021) game.

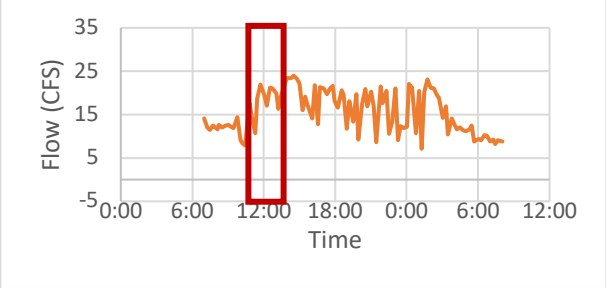

C: (Above) Flow over time for Nebraska (September 18, 2021) game.

D: (Above) Flow over time for the West Virginia (September 25, 2021) game.

E: (Above) Flow over time for the Texas Christian (October 16, 2021) game.

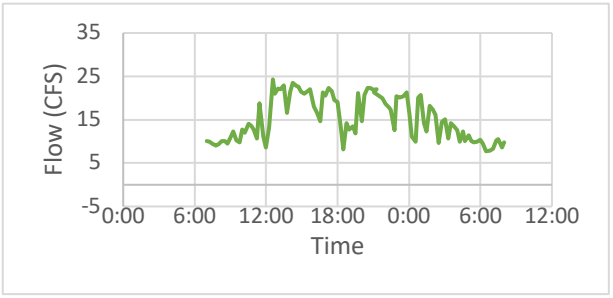

F: (Above) Flow over time for the control (October 13, 2021) day.

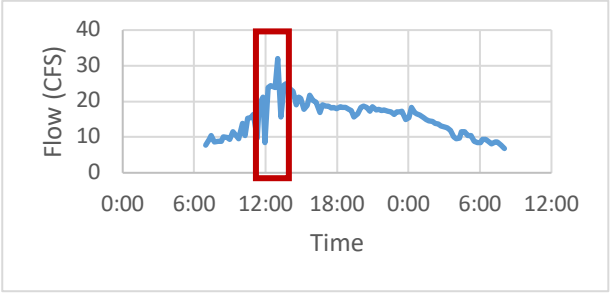

G: (Above) Flow over time for the Iowa State (November 20, 2021) game.

Figure 25: Flow over time for all games in the 2021 football season. Approximate game times are outlined in red. A represents the flow during the Tulane sampling period, B shows flow during the Western Carolina sampling period, C shows the flow during the Nebraska sampling period, D shows the flow over the duration of the West Virginia sampling period, E shows the flow over the duration of the Texas Christian sampling period, F shows the flow over the duration of the control sampling period, and G shows the flow over the duration of the Iowa State sampling period.

When the before, during, after, and late-night categories for all games are compared together, the difference between the before and during groups is significant ($P < 0.01$). The same is true of the before group compared to the after group ($P < 0.01$). However, the flow of the before group is not significantly different from the flow in the late-night group when all games are put together ($P = 0.83$). The flow in the during group compared to the after group is not significantly different ($P = 0.16$) but is significantly different from the late-night group ($P < 0.01$). Finally, the after group for all games is different from the late-night group ($P < 0.01$).

3.2.2 Population

SL data was used to estimate the population in the Norman sewershed during the 2021 football season. Figure 26 shows the population over time for all sampling days during the 2020 football season. The estimated population for each gameday in the 2021 season was significantly greater than the control ($P < 0.01$ for Tulane, Western Carolina, Nebraska, West Virginia, and Texas Christian; $P = 0.011$ for Iowa State). Compared to one another using an ANOVA analysis, the population for each day is significantly different ($P < 0.01$).

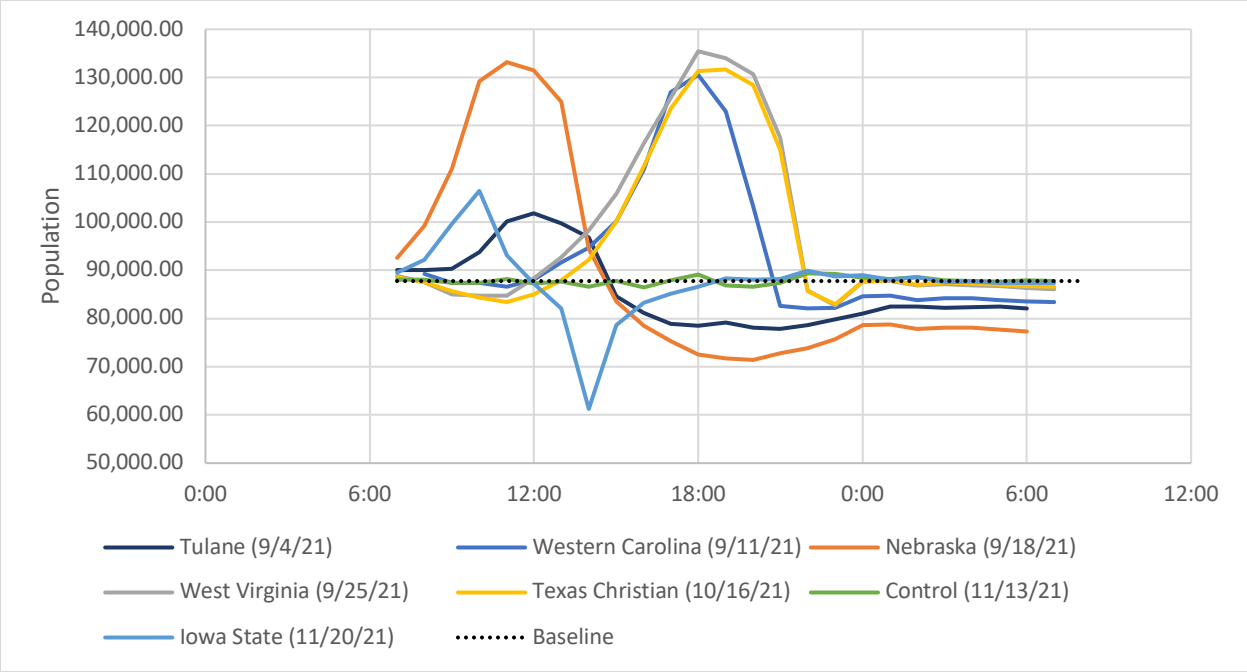

Figure 26: Estimated population over time for all games in the 2021 football season

Table 14 displays the population for each sampling day broken into time groups.

Table 14: Mean population by time group for all games in the 2021 football season. Within the 24-hour row, games with different Greek letter superscripts are significantly different at the 95% confidence level

	Tulane (September 4, 2021)	**Western Carolina (September 11, 2021)**	**Nebraska (September 18, 2021)**	**West Virginia September 25, 2021)**	**Texas Christian (October 16, 2021)**	**Control (November 13, 2021)**	**Iowa State (November 20, 2021)**
Before	91,084	108,185	107,992	120,876	116,650	N/A	96,948
During	99,648	109,840	121,040	116,993	115,213	N/A	80,932
After	80,814	N/A	77,471	N/A	N/A	N/A	83,424
Late-Night	81,600	83,911	77,788	86,436	86,597	87,841	87,627
24-Hour	$85{,}111^{\alpha}$	$93{,}133^{\beta,\chi}$	$88{,}582^{\alpha,\chi}$	$97{,}597^{\beta,\chi}$	$96{,}114^{\beta,\chi}$	$87{,}84^{\alpha,\chi}$	$87{,}660^{\alpha,\chi}$

The population was greatest just before or during the game for all days that had a football game. This affirms the hypothesis that people traveled into the city for the football games. Each game was presented individually. The first game is the Tulane game, this game was moved from New Orleans, Louisiana to Norman, Oklahoma due to a hurricane, with rather short notice. The

population was greatest during the football game. This data can be seen in Figure 27A. The population over time for the Western Carolina game is shown in Figure 27B. The population was greatest right at kickoff for this game. Figure 27C shows the population over time for the Nebraska game. Again, the population recorded was greatest at kickoff. Figure 27D shows the population over time for the West Virginia game. Again, the population was greatest just before kickoff for this game. Figure 27E shows the population over time for the Texas Christian game. The population reached its peak for this game just after kickoff. Figure 27F shows the population over time for the control day. The population for this day stayed consistently around the baseline population for the sewershed. Figure 27G shows the population over time for the Iowa State game.

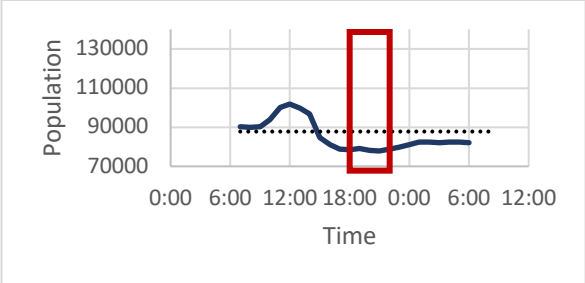

A: (Above) Estimated population over time for Tulane (September 4, 2021) game.

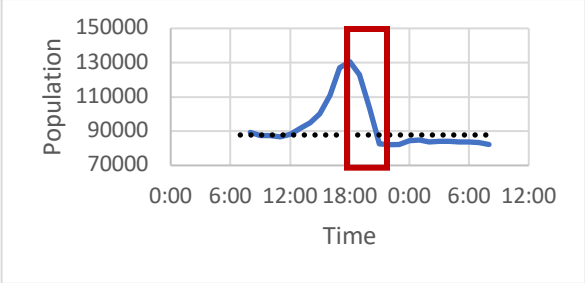

B: (Above) Estimated population over time for Western Carolina (September 11, 2021) game.

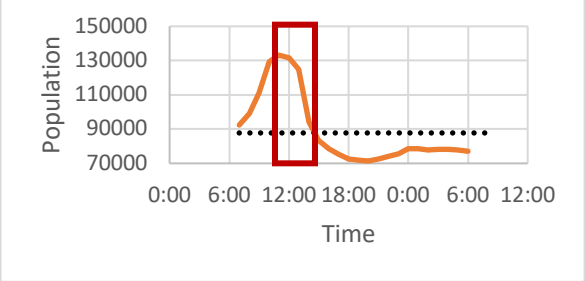

C: (Above) Estimated population over time for Nebraska (September 18, 2021) game.

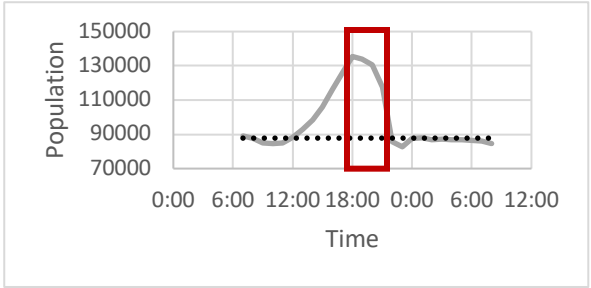

D: (Above) Estimated population over time for the West Virginia (September 25, 2021) game.

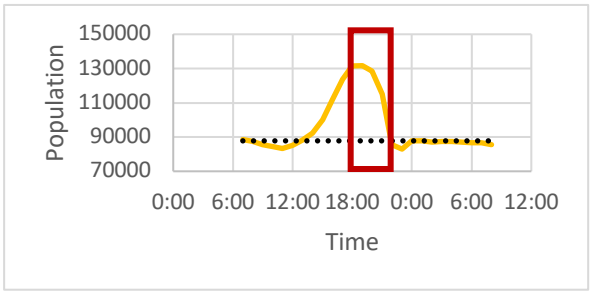

E: (Above) Estimated population over time for the Texas Christian (October 16, 2021) game.

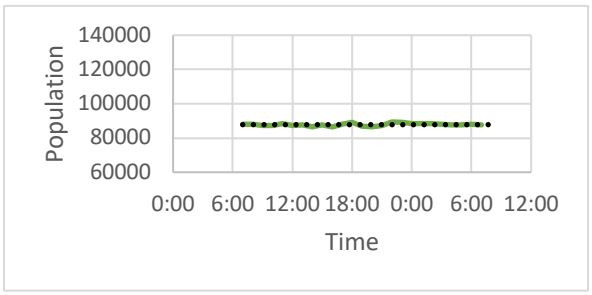

F: (Above) Estimated population over time for the control (October 13, 2021) day.

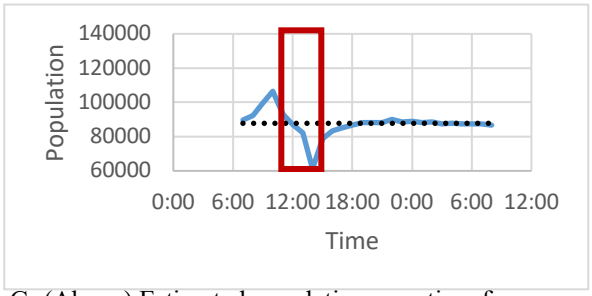

G: (Above) Estimated population over time for the Iowa State (November 20, 2021) game.

Figure 27: Population over time for all games in the 2021 football season. Approximate game times are outlined in red. A represents the population during the Tulane sampling period, B shows population during the Western Carolina sampling period, C shows the population during the Nebraska sampling period, D shows the population over the duration of the West Virginia sampling period, E shows the population over the duration of the Texas Christian sampling period, F shows the population over the duration of the control sampling period, and G shows the population over the duration of the Iowa State sampling period.

For all games in the 2021 season combined, the population in the before category was not significantly different from the during category ($P = 0.87$). The difference in population was also not significant when the after category was compared to the late-night category ($P = 0.40$). The population in the before group was significantly different from the after ($P < 0.01$) and late-night categories ($P < 0.01$). The population in the during group was significantly different from the after and late-night categories ($P < 0.01$ for both).

The population was also analyzed was by dividing the day into time groups to determine if there was a relationship between the population and time at smaller scales. Figure 28A shows the population over time for the before group for all gamedays in 2021. Figure 28B shows the population over time for the during game group for all games in the 2021 football season. Figure 28C shows the population over time for the after category for the Tulane, Nebraska, and Iowa State games, as they were the only games that had an after category. Figure 28D shows the population over time for the late-night group.

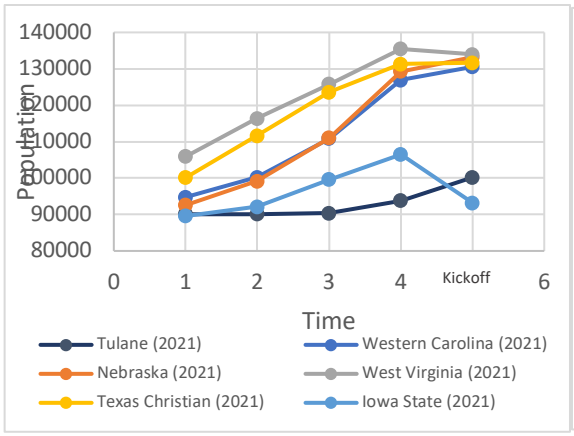

A (Above): Estimated population over time before the football game.

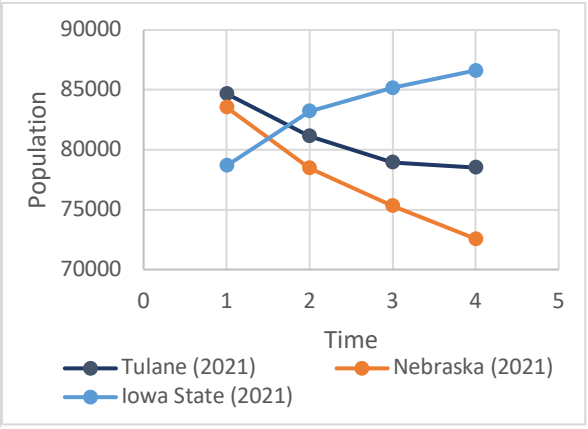

C (Above): Estimated population over time during the after category. 1 represents the first hour after the game.

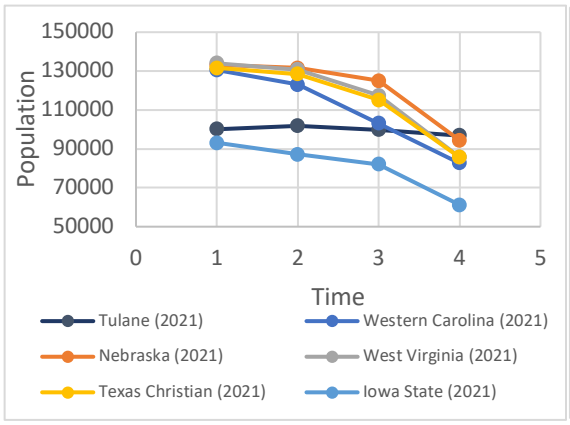

B (Above): Estimated population over time during the football game. 1 represents kickoff.

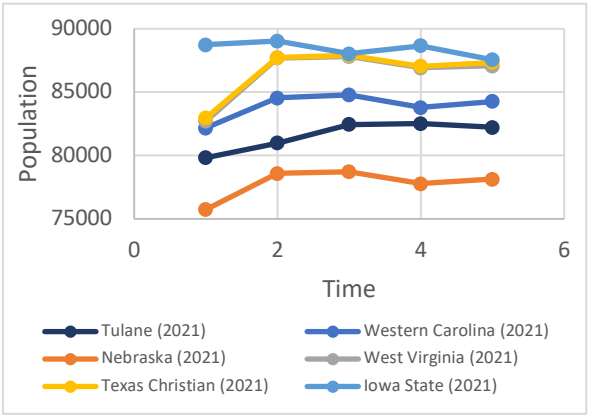

D (Above): Estimated population over time during the after category. 1 represents 11:00 pm.

Figure 28: Estimated population over time, by time category, for all games in the 2021 football season.

3.2.3 Concentration

To determine if there was an increase in SARS-CoV-2 due to the football games, statistical analysis was performed on the concentration data for the 2021 football season. The SARS-CoV-2 concentration of all days that were sampled in 2020 over time is shown in Figure 29. Each sampling day was compared to each other ($P < 0.01$). To further determine if the game played a role in the amount of SARS-CoV-2 in the wastewater, days with a game were compared to the control day. The difference in concentration from the control game was significant for the Tulane game ($P < 0.01$), the Western Carolina game ($P < 0.01$), the Nebraska game ($P = 0.04$),

and the Iowa State game (P = 0.02). The only game with a concentration that was not significantly different from the control was Texas Christian (P = 0.18). Furthermore, the time categories were compared to each other. The difference in concentration between the before and during groups (P = 0.19), the before and late-night (P = 0.15), during and after (P = 0.23), during and late-night (P = 0.86), and after and late-night (P = 0.23) categories is not significant. The only time groups with significantly different concentrations were the before and after categories, when all games were compared together (P = 0.03). When the time groups for all games were compared to one another at once, the difference in concentration between the time groups was not significant (P = 0.43).

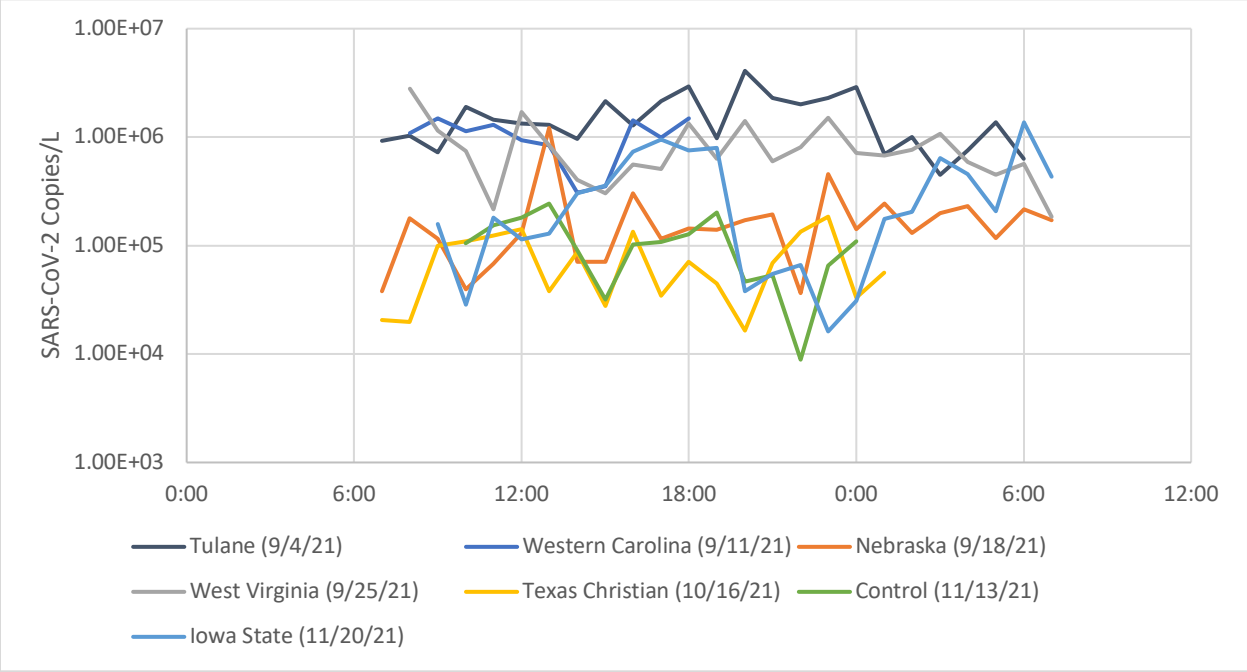

Figure 29: SARS-CoV-2 concentration over time for all days sampled in the 2021 football season.

The mean SARS-CoV-2 concentration per time group per sampling day can be found in Table 15.

Table 15: Mean SARS-CoV-2 concentration by time group for all games in the 2021 football season. Within the All row, games with different superscript Greek letters are significantly different at the 95% confidence level.

	Tulane (September 4, 2021)	**Western Carolina (September 11, 2021)**	**Nebraska (September 18, 2021)**	**West Virginia September 25, 2021)**	**Texas Christian (October 16, 2021)**	**Control (November 13, 2021)**	**Iowa State (November 20, 2021)**
Before	1.14×10^5	9.29×10^4	4.43×10^5	7.07×10^4	6.65×10^4	N/A	9.36×10^4
During	1.26×10^6	3.71×10^5	9.92×10^5	5.02×10^4	6.61×10^4	N/A	1.82×10^5
After	2.13×10^6	N/A	N/A	N/A	N/A	N/A	6.97×10^5
Late-Night	1.47×10^6	N/A	9.46×10^5	9.15×10^4	9.15×10^4	8.75×10^4	2.14×10^5
All	$1.57 \times 10^{6\,\alpha}$	$1.03 \times 10^{6\,\alpha,\chi}$	$1.97 \times 10^{5\,\beta,\delta}$	$8.54 \times 10^{5\,\beta,\chi}$	$7.60 \times 10^{4\,\beta,\delta}$	$1.09 \times 10^{5\,\beta,\delta}$	$3.56 \times 10^{5\,\beta,\delta}$

Figure 30A shows the SARS-Co-2 concentration over time for the Tulane game. The concentration in each time group was averaged and the time with the greatest concentration of SARS-CoV-2 was after the game. Figure 30B shows the SARS-CoV-2 concentration over time for the Western Carolina game. Due to mechanical errors, the autosampler discontinued sampling after 6:00 pm on Saturday. Because that was the time of kickoff, no comparisons between time groups can be made. Figure 30C shows the SARS-CoV-2 concentration over time for the Nebraska sampling. The late-night category had the greatest average concentration of 2.34×10^5 copies/L. The SARS-CoV-2 concentration over time for the West Virginia game can be seen in Figure 30D. The average concentration was greatest in the during category. Figure 36E shows the SARS-CoV-2 concentration over time for the Texas Christian game. The greatest average concentration occurred in the late-night group, despite the autosampler not collecting samples past 1:00 am on Sunday. Figure 30F shows the SARS-CoV-2 concentration over time for the control day. The autosampler had many technical problems throughout that day, starting at 10:00 am on Saturday and stopping at midnight on Sunday. Despite the problems, the greatest concentration was recorded at 1:00 pm on Saturday. Figure 30G shows the SARS-CoV-2

concentration over time for the Iowa State game. The concentration was greatest during the football game.

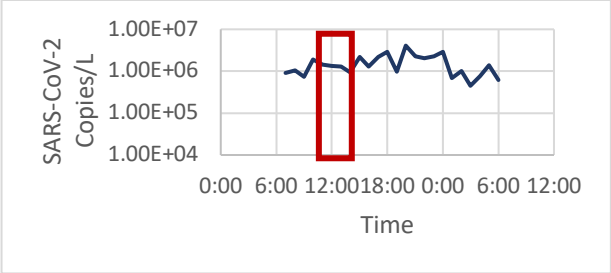

A: (Above) SARS-CoV-2 concentration over time for Tulane (September 4, 2021) game.

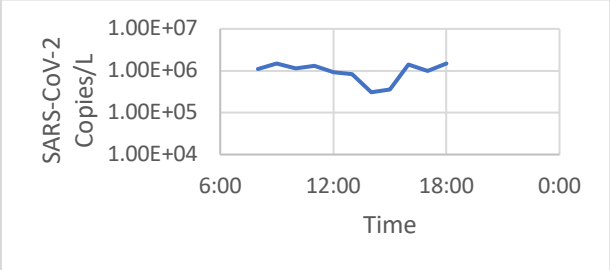

B: (Above) SARS-CoV-2 concentration over time for Western Carolina (September 11, 2021) game.

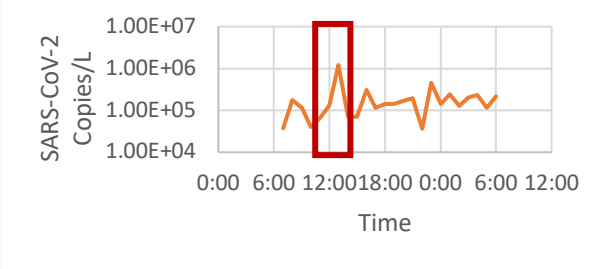

C: (Above) SARS-CoV-2 concentration over time for Nebraska (September 18, 2021) day.

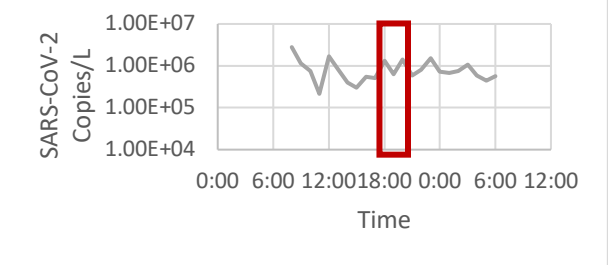

D: (Above) SARS-CoV-2 concentration over time for the West Virginia (September 25, 2021) game.

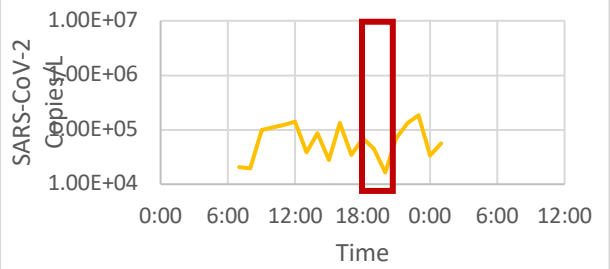

E: (Above) SARS-CoV-2 concentration over time for the Texas Christian (October 16, 2021) game.

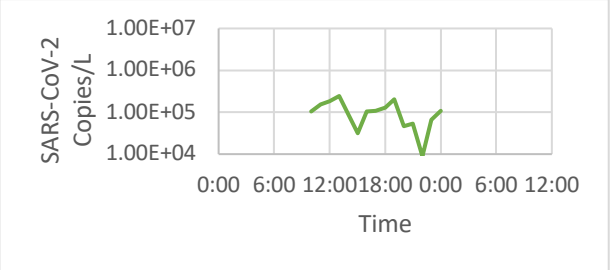

F: (Above) SARS-CoV-2 concentration over time for the control (October 13, 2021) day.

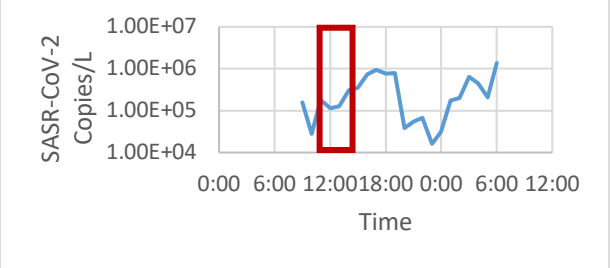

G: (Above) SARS-CoV-2 concentration over time for the Iowa State (November 20, 2021) game.

Figure 30: SARS-CoV-2 concentration over time for all games in the 2021 football season. Approximate game times are outlined in red. A represents the concentration during the Tulane sampling period, B shows concentration during the Western Carolina sampling period, C shows the concentration during the Nebraska sampling period, D shows the concentration over the duration of the West Virginia sampling period, E shows the concentration over the duration of the Texas Christian sampling period, F shows the concentration over the duration of the control sampling period, and G shows the concentration over the duration of the Iowa State sampling period.

The mean concentration of the gamedays was compared to the concentration of samples collected from the NWRF on nearby dates throughout the season. Figure 31 shows the mean concentration of the hourly gameday samples compared to the NWRF time-weighted composite samples over the course of the 2021 football season. The concentrations for each gameday were compared to the NWRF composite samples around the same time. The difference in the concentrations between the NWRF composite samples and Tulane was significant ($P < 0.01$). The concentration of the NWRF samples was not significantly different from the Western Carolina ($P = 0.23$), the West Virginia ($P = 0.07$), or the Iowa State samples ($P = 0.41$). The concentration of the NWRF samples was significantly different from the Nebraska ($P < 0.01$), the Texas Christian samples ($P = 0.01$), and the control samples ($P = 0.02$).

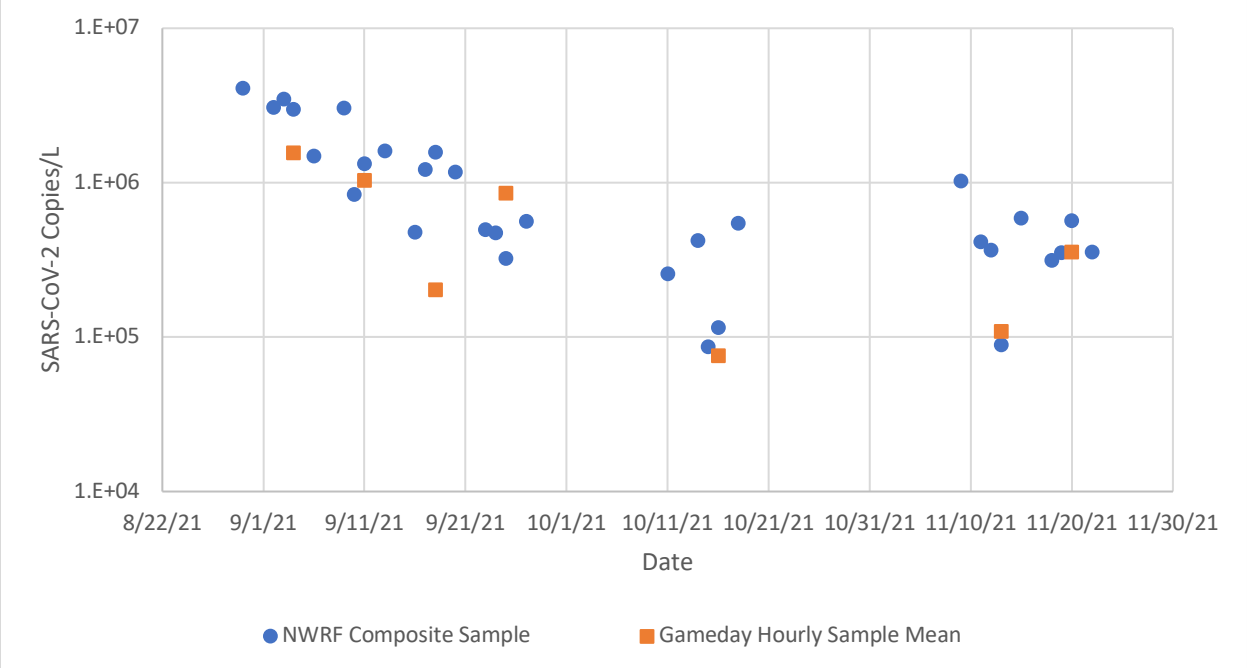

Figure 31: Gameday mean SARS-CoV-2 concentration compared to the concentration from the City of Norman, Oklahoma (NWRF) over the course of the 2021 football season.

Table 16 shows the mean SARS-CoV-2 concentration for both the gameday samples and samples collected from the NWRF on dates surrounding the football game.

Table 16: Average SARS-CoV-2 concentration (copies/L) for Norman Water Reclamation Facility (NWRF) and gameday samples for the 2021 football season.

	Tulane (September 4, 2021)	**Western Carolina (September 11, 2021)**	**Nebraska (September 18, 2021)**	**West Virginia September 25, 2021)**	**Texas Christian (October 16, 2021)**	**Control (November 13, 2021)**	**Iowa State (November 20, 2021)**
NWRF	3.02×10^6	1.70×10^6	1.11×10^6	4.63×10^5	2.85×10^5	4.97×10^5	3.97×10^5
Gameday	1.57×10^6	1.03×10^6	2.02×10^5	8.55×10^5	7.60×10^4	1.09×10^5	3.56×10^5

The SARS-CoV-2 concentration was compared to the flow to determine if there were any correlations between the two variables. Figure 32 displays the results of the analysis. There is a weak positive correlation between the two variables that is not significant at the 95% confidence level.

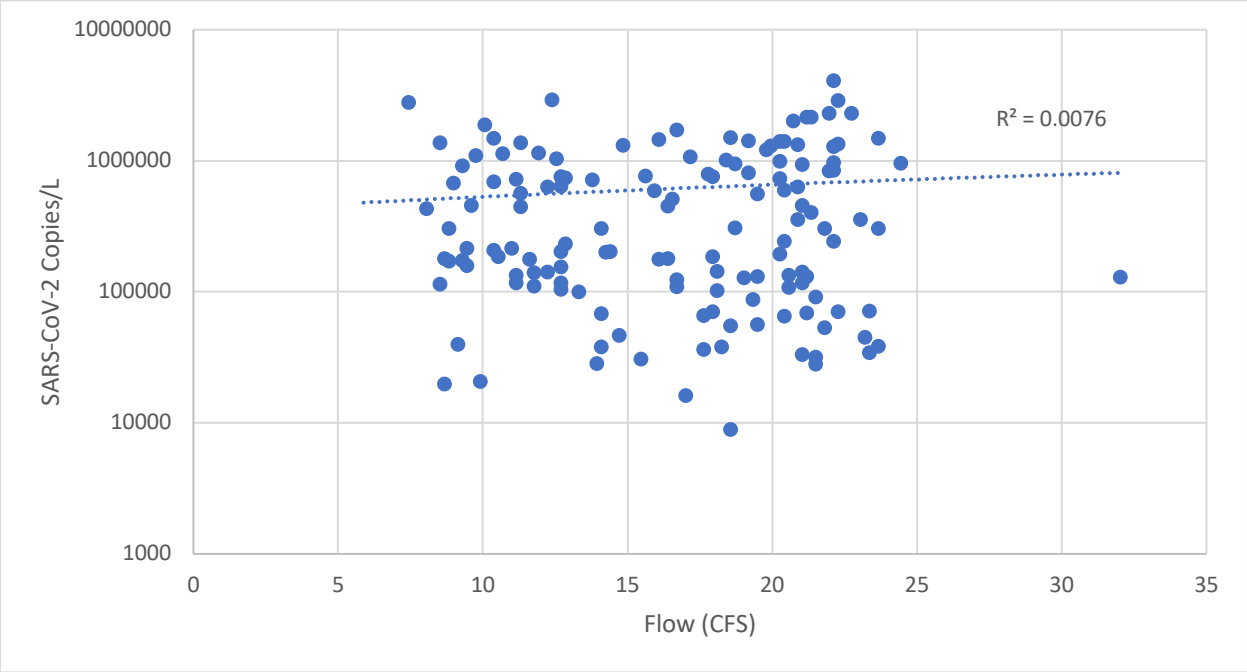

Figure 32: SARS-CoV-2 concentration versus the flow for all games in the 2021 football season.

Figure 33 shows the relationship between the concentration and the population. The correlation between the two variables is negative, but not significant at the 95% confidence level.

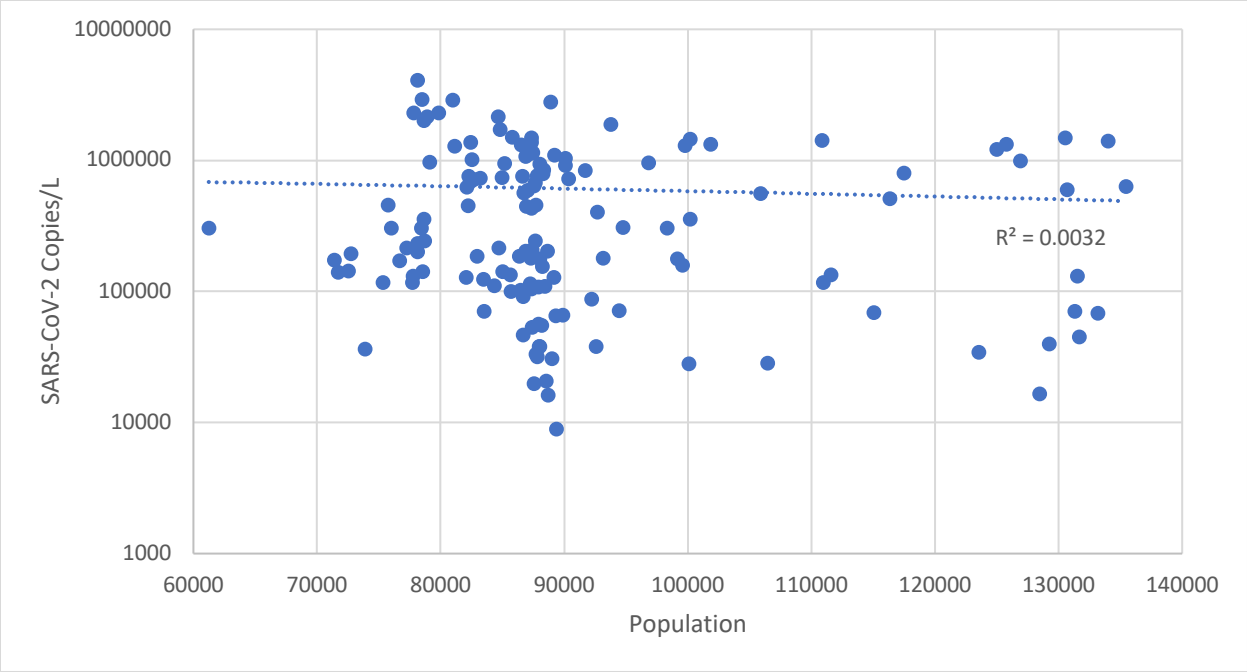

Figure 33: SARS-CoV-2 concentration versus population for all games in the 2021 football season

Table 17 shows the R^2 value resulting from the comparison of SARS-CoV-2 concentration versus the flow and the comparison of the concentration versus the population, as well as the direction of the correlation for all games in the 2021 football season. None of the results of this analysis were significant.

Table 17: Results of correlation analysis (R^2 values) between the concentration and flow, and the concentration and population for the 2021 football season.

	Tulane (September 4, 2021)	**Western Carolina (September 11, 2021)**	**Nebraska (September 18, 2021)**	**West Virginia (September 25, 2021)**	**Texas Christian (October 16, 2021)**	**Control (November 13, 2021)**	**Iowa State (November 20, 2021)**
Concentration vs. Flow	0.17	0.12	0.03	0.01	0.01	0.12	0.02
Concentration vs. Population	0.12	0.03	0.03	< 0.01	0.14	0.05	0.04

The SARS-CoV-2 concentration over time was analyzed by time group to determine if there were any significant correlations between the variables at a smaller time scale. Figure 34A shows the concentration over time for the before game group for all games in the 2021 football season. The concentration was increasing over time for some games in this time group and

decreasing for some. The game with the strongest relationship between the two variables was the Western Carolina game, which was increasing over time ($R^2 = 0.56$). Iowa State shows an R^2 of 1, which can be attributed to the fact that there were only two samples collected in this time group for that game. Figure 34B shows the SARS-CoV-2 concentration over time of all games in the 2021 football season for the during game category. Again, there was an almost even divide between the number of games that had a concentration that was decreasing over time and the number of games with a concentration increasing over time. The game with the strongest correlation between the two variables was the Tulane game ($R^2 = 0.86$). The concentration for the Tulane game was decreasing as the game went on. The SARS-CoV-2 concentration over time for the after category can be seen in Figure 34C. Only the Tulane, Nebraska, and Iowa State games had sufficient time after the game to be included in this category. While the concentration over time was increasing for both the Nebraska and Iowa State games at this time scale, the Tulane game had a much stronger negative relationship ($R^2 = 0.86$), thus making the relationship negative overall for this category, though very weak ($R^2 = 5.5 \times 10^{-6}$). Figure 34D shows the SARS-CoV-2 concentration over time for all games in the 2021 football season for the late-night group. Overall, the relationship between the variables is negative for all of the games in this season, despite the positive relationship for the Iowa State game. Iowa State had the strongest correlation between the two variables ($R^2 = 0.79$) followed by the Tulane game ($R^2 = 0.68$).

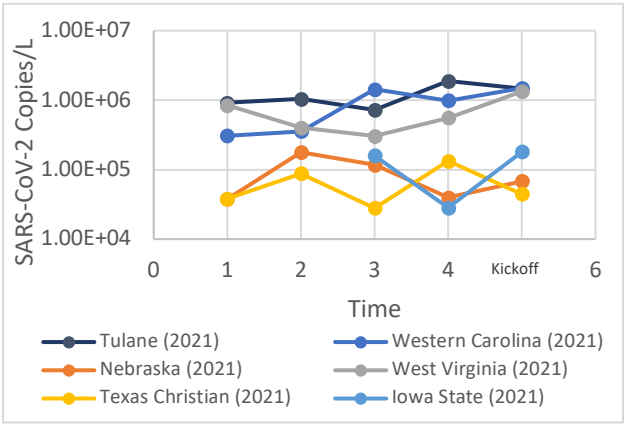

A (Above): SARS-CoV-2 concentration over time before the football game.

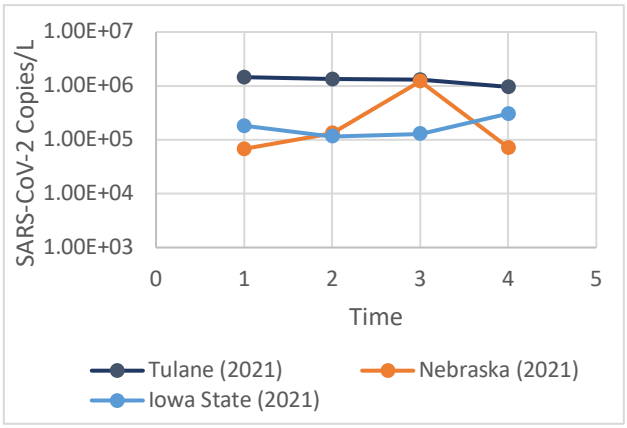

C (Above): SARS-CoV-2 concentration over time during the after category. 1 represents the first hour after the game.

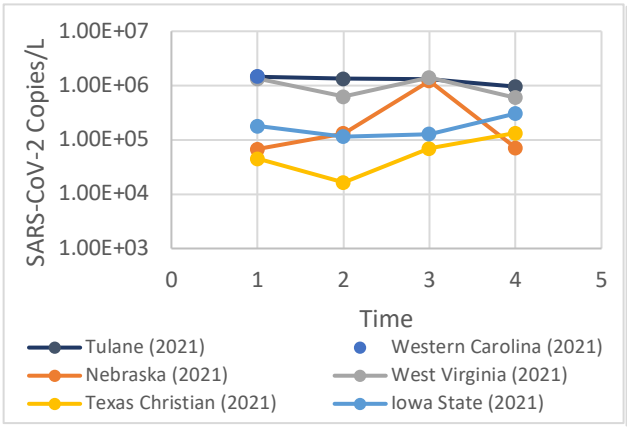

B (Above): SARS-CoV-2 concentration over time during the football game. 1 represents kickoff.

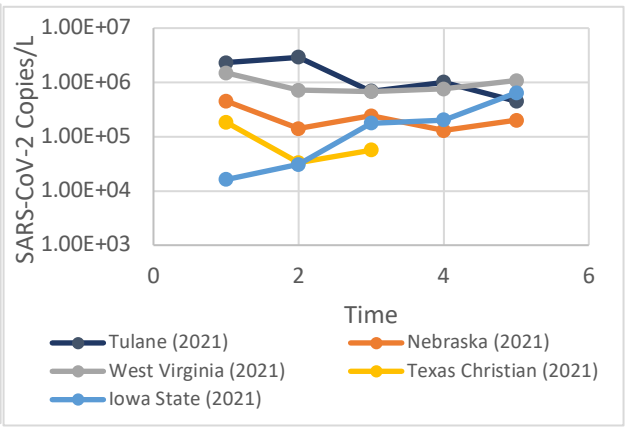

D (Above): SARS-CoV-2 concentration over time during the after category. 1 represents 11:00 pm.

Figure 34: SARS-CoV-2 concentration over time, by time category, for all games in the 2021 football season

3.2.4 Viral Load per Person

The viral load per person for the 2021 football season was analyzed. Figure 35 shows the SARS-CoV-2 viral load per person for all sampling days in the 2021 football season. Compared to the control day, the viral load per person was significantly different for the Tulane ($P < 0.01$), Western Carolina ($P < 0.01$), West Virginia ($P < 0.01$), and Iowa State ($P = 0.02$) games. The difference in viral load per person was not significant between the control and Nebraska ($P = 0.05$), and Texas Christian ($P = 0.73$).

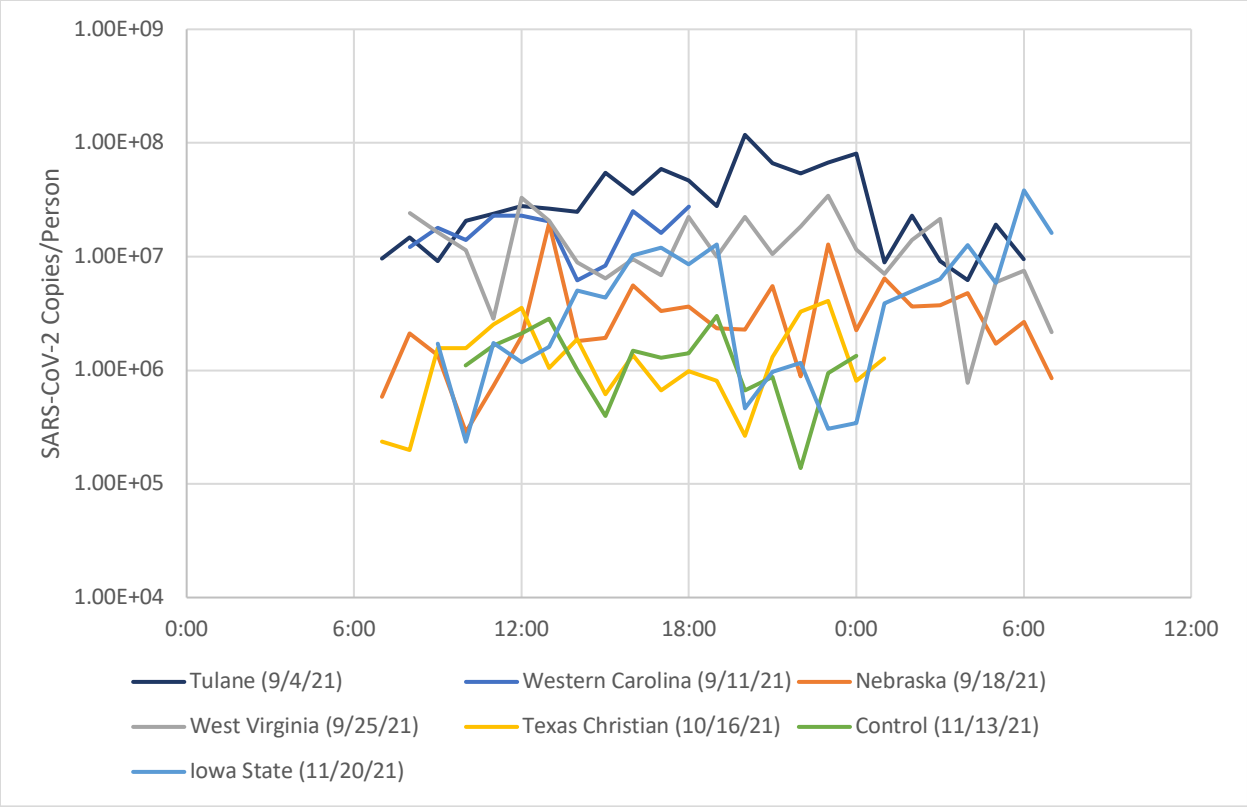

Figure 35: SARS-CoV-2 viral load per person over time for all games in the 2021 football season.

Table 18 shows the within game analysis for the 2021 football season.

Table 18: Mean SARS-CoV-2 viral load per person by time group for all games in the 2021 football season. Within the All row, games with different superscript Greek letters are significantly different at the 95% confidence level.

	Tulane (September 4, 2021)	**Western Carolina (September 11, 2021)**	**Nebraska (September 18, 2021)**	**West Virginia September 25, 2021)**	**Texas Christian (October 16, 2021)**	**Control (November 13, 2021)**	**Iowa State (November 20, 2021)**
Before	1.35×10^7	1.39 x 107	1.09×10^6	1.13×10^7	9.03×10^5	N/A	9.73×10^5
During	2.57×10^7	2.75×10^7	6.03×10^6	1.53×10^7	1.41×10^6	N/A	2.39×10^6
After	4.92×10^7	N/A	3.61×10^6	N/A	N/A	N/A	8.76×10^6
Late-Night	3.78×10^7	N/A	5.77×10^6	1.77×10^7	2.05×10^6	1.15×10^6	1.51×10^6
All	$3.51 \times 10^{7\,\alpha}$	$1.76 \times 10^{7\,\alpha,\chi}$	$3.71 \times 10^{6\,\beta,\delta,\varepsilon}$	$1.37 \times 10^{7\,\beta,\chi,\phi}$	$1.47 \times 10^{6\,\beta,\delta,\phi}$	$1.35 \times 10^{6\,\beta,\delta,\phi}$	$6.55 \times 10^{6\,\beta,\delta,\varepsilon}$

Figure 36A shows the SARS-CoV-2 viral load per person over time for the Tulane game.

The viral load per person was greatest around 8:00 pm on Saturday. Figure 36B shows the viral

load per person over time for the Western Carolina game. Because of an autosampler malfunction, there is no analysis performed on this game. The viral load per person was greatest at 6:00 pm, which was the time of kickoff. Figure 36C shows the SARS-CoV-2 viral load per person over time for the Nebraska game. The concentration was greatest 1:00 pm, during the game. The SARS-CoV-2 viral load per person for the West Virginia game is shown in Figure 36D. The concentration was greatest around 11:00 am or 11:00 pm. Figure 35E shows the SARS-CoV-2 viral load per person over time for the TCU (Texas Christian) game. The viral load per person reached its peak at 11:00 pm. Figure 36F shows the viral load per person over time for the control day, while Figure 36G shows the viral load per person over time for the Iowa State game.

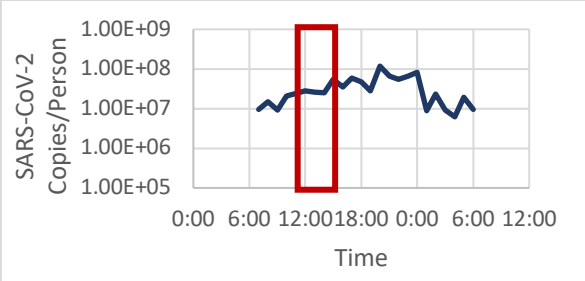

A: (Above) SARS-CoV-2 viral load per person over time for Tulane (September 4, 2021) game.

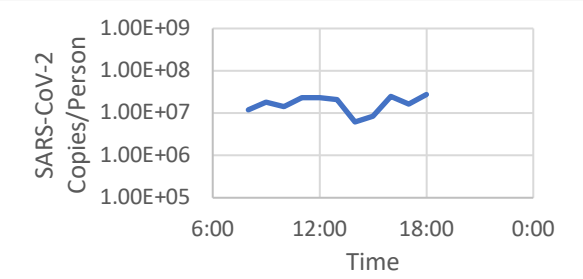

B: (Above) SARS-CoV-2 viral load per person over time for Western Carolina (September 11, 2021) game.

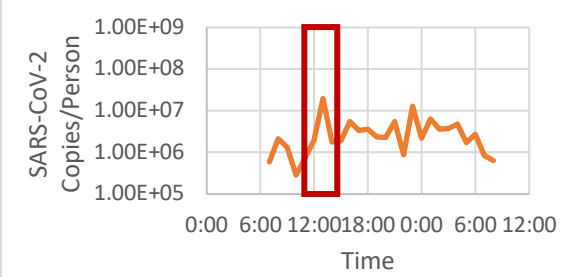

C: (Above) SARS-CoV-2 viral load per person over time for Nebraska (September 18, 2021) game.

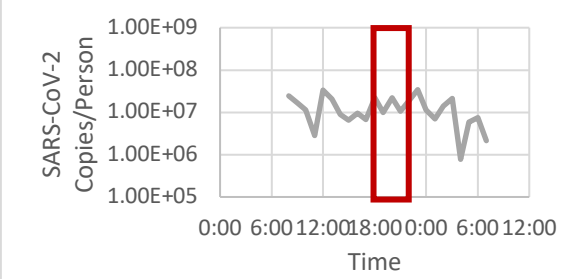

D: (Above) SARS-CoV-2 viral load per person over time for the West Virginia (September 25, 2021) game.

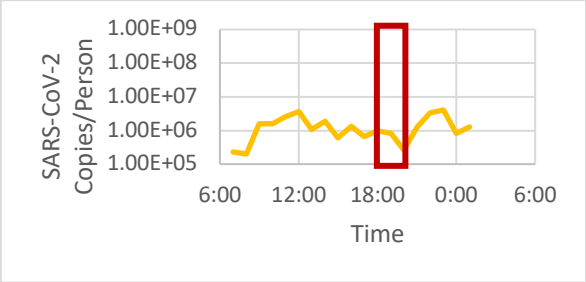

E: (Above) SARS-CoV-2 viral load per person over time for the Texas Christian (October 16, 2021) game.

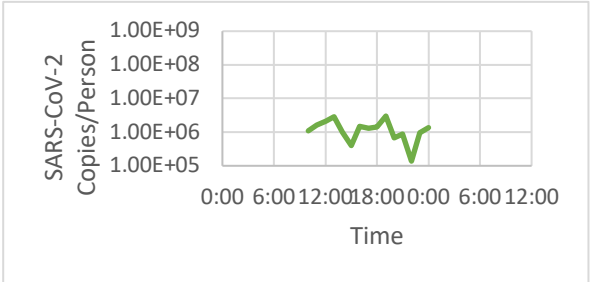

F: (Above) SARS-CoV-2 viral load per person over time for the control (October 13, 2021) day.

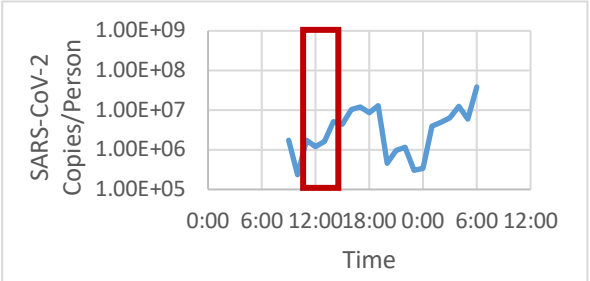

G: (Above) SARS-CoV-2 viral load per person over time for the Iowa State (November 20, 2021) game.

Figure 36: SARS-CoV-2 viral load per person over time for all games in the 2021 football season. Approximate game times are outlined in red. A represents the viral load per person during the Tulane sampling period, B shows the viral load per person during the Western Carolina sampling period, C shows the viral load per pe during the Nebraska sampling period, D shows the viral load per person over the duration of the West Virginia sampling period, E shows the viral load per person over the duration of the Texas Christian sampling period, F shows the viral load per person over the duration of the control sampling period, and G shows the viral load per person over the duration of the Iowa State sampling period.

The games were combined to analyze the viral load per person for time groups. The difference in viral load per person for the before group is not significant when compared to the during category (P = 0.06) or the late-night category (P = 0.70) but is the difference is significant when compared to the after category (P = 0.01). The viral load per person for the during group is not significantly different from the after (P = 0.11) or the late-night categories (P = 0.52). The after category is not significantly different from the late-night group (P = 0.41).

The viral load per person was analyzed over each time category to better understand how it is changing over shorter periods of time. Figure 37A shows the viral load per person before the game, which was increasing leading up to kickoff for the Tulane, Western Carolina, and West Virginia games and decreasing for the Nebraska, Texas Christian, and Iowa State games. Figure 37B shows the viral load per person over time for the during game category. The viral load per person at the during game time scale was increasing for the Nebraska, West Virginia, and Texas Christian games, but decreasing for the Tulane game. The viral load per person after the game can be seen in Figure 37C. The viral load per person was decreasing at this scale for the Tulane game and increasing for the Nebraska and Iowa State games. Figure 37D shows the viral load per person over time for the late-night category. The viral load per person was decreasing in the late-night hours for the Tulane, Nebraska, West Virginia, and Texas Christian games but was increasing for the Iowa State game. Across all time groups and games, the correlations between the viral load per person and time were not significant at the 95% confidence level.

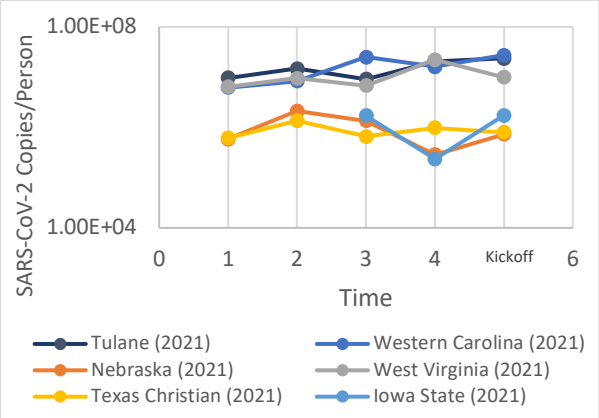

A (Above): SARS-CoV-2 viral load per person over time before the football game. 1 represents the first of four

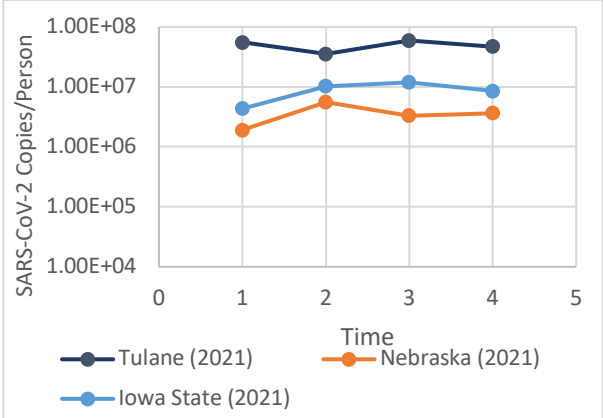

C (Above): SARS-CoV-2 viral load per person over time during the after category. 1 represents the first hour after the

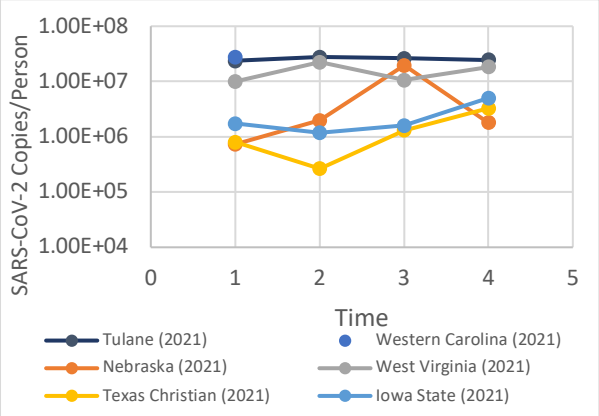

B (Above): SARS-CoV-2 viral load per person over time during the football game. 1 represents kickoff.

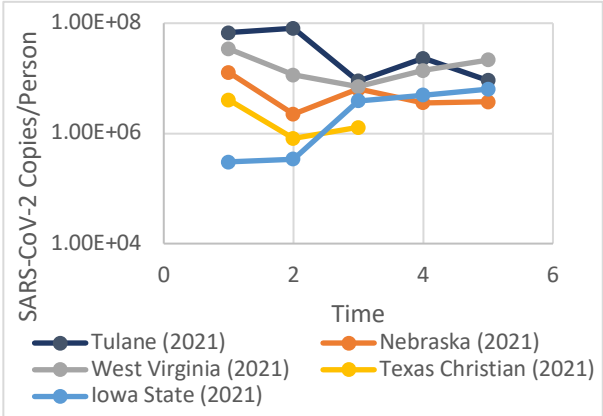

D (Above): SARS-CoV-2 viral load per person over time during the after category. 1 represents 11:00 pm.

Figure 37: SARS-CoV-2 viral load per person over time, by time category, for all games in the 2021 football season

Figure 38 shows the SARS-CoV-2 viral load per person (copies/person) versus the flow (CFS) for all games in the 2021 football season. The relationship between the two variables is positive, but not significant at the 95% confidence level.

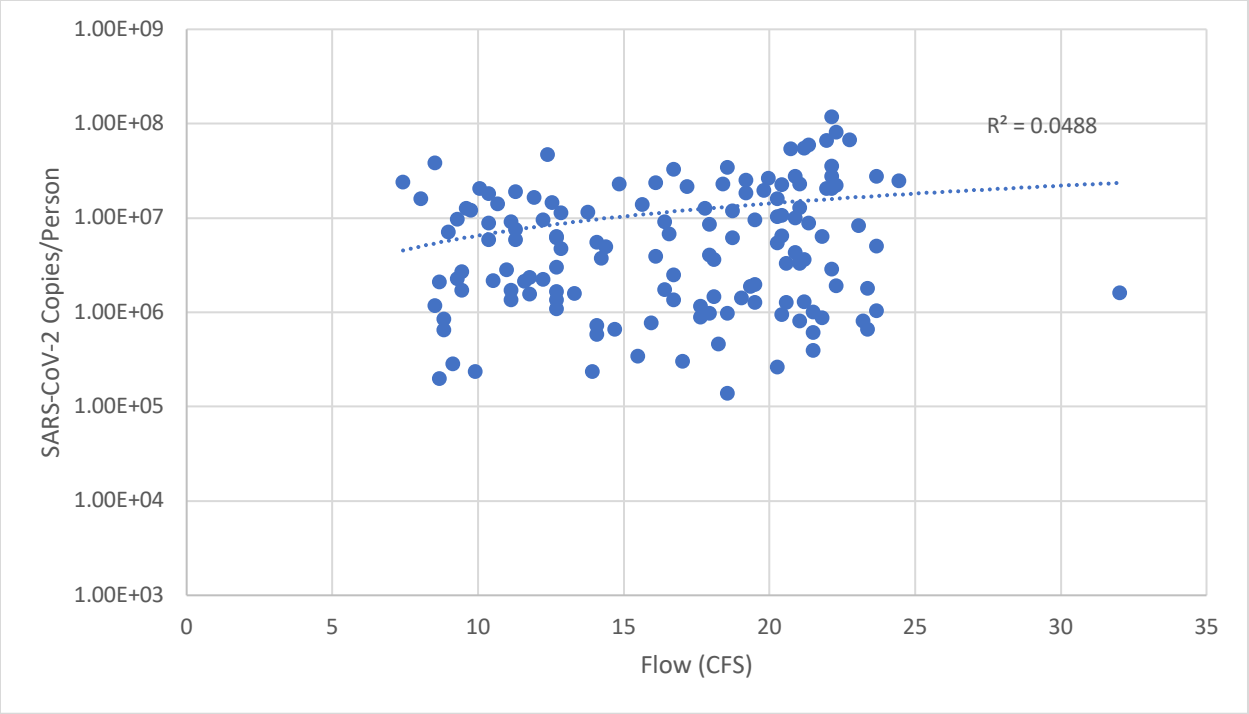

Figure 38: SARS-CoV-2 viral load per person versus the flow for all games in the 2021 football season.

Figure 39 shows the SARS-CoV-2 viral load per person (copies/person) over the population for all games in the 2021 football season. The relationship between these two variables is negative, however, the relationship is not significant.

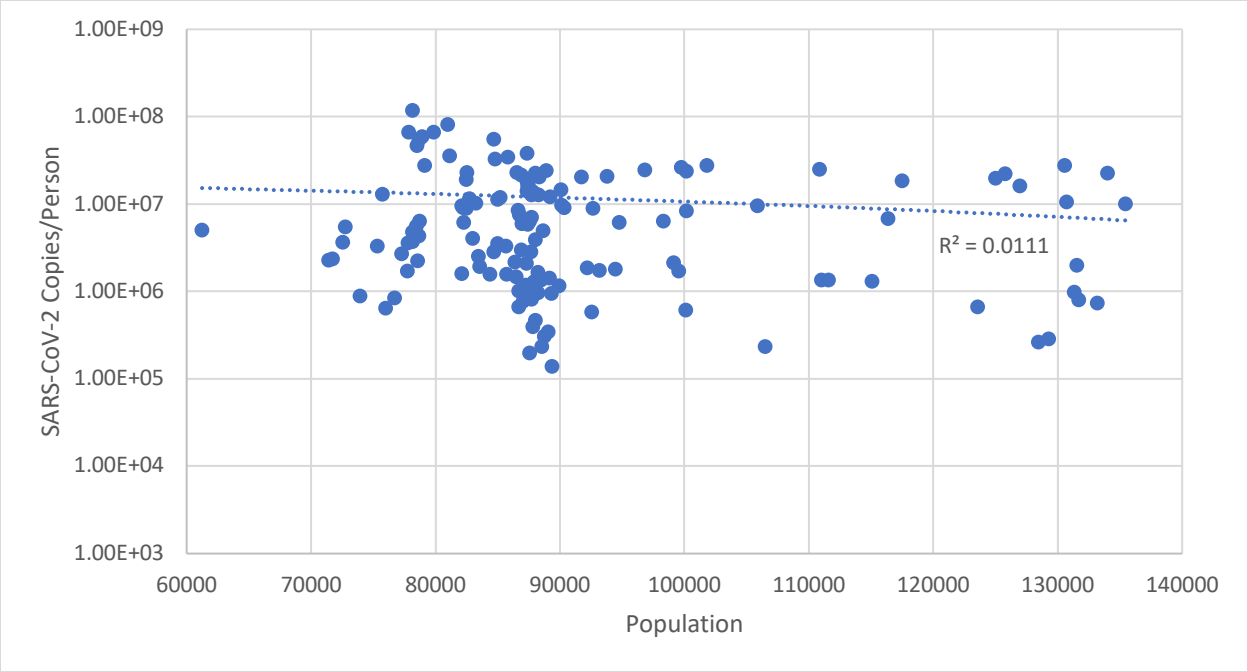

Figure 39: SARS-CoV-2 viral load per person versus population for all games in the 2021 football season.

Table 19 shows the R^2 value resulting from the comparison of SARS-CoV-2 concentration versus the flow and the comparison of the concentration versus the population, as well as the direction of the correlation for all games in the 2021 football season. None of the results of this analysis were significant.

Table 19: Results of correlation analysis (R^2 values) between the viral load per person and flow, and the viral load per person and population for the 2021 football season.

	Tulane (September 4, 2021)	**Western Carolina (September 11, 2021)**	**Nebraska (September 18, 2021)**	**West Virginia September 25, 2021)**	**Texas Christian (October 16, 2021)**	**Control (November 13, 2021)**	**Iowa State (Novembe r 20, 2021)**
Viral load per person vs. Flow	0.41	0.05	0.17	0.07	0.02	0.11	0.12
Viral load per person vs. Population	0.18	0.09	0.01	< 0.01	0.22	0.08	0.02

The variance of the concentration was compared to the variance of the population using a Levene Test for Equality of Variances to determine if including the population in the analysis made a difference. If the variances were not significantly different, that means that using a viral

load per person would not be significantly different from the concentration. For all sampling days in 2021 combined, the variances are significantly different at the 95% confidence level. This was true when all the games were looked at individually, with exception to the Western Carolina game, which was largely excluded from analysis due to the autosampler failing after 6:00 pm.

3.2.5 Relative Viral Load per Person

Figure 40 shows the relative SARS-Co-2 viral load per person over time for all games in the 2021 football season. The relative viral load per person is calculated with the viral load per person with the first sample of the day subtracted from the remainder of the samples. The relative viral load per person on the control day was significantly different from the relative viral load per person for every game ($P < 0.01$ for Tulane, Western Carolina, Nebraska, West Virginia, Texas Christian; $P = 0.04$ for Iowa State).

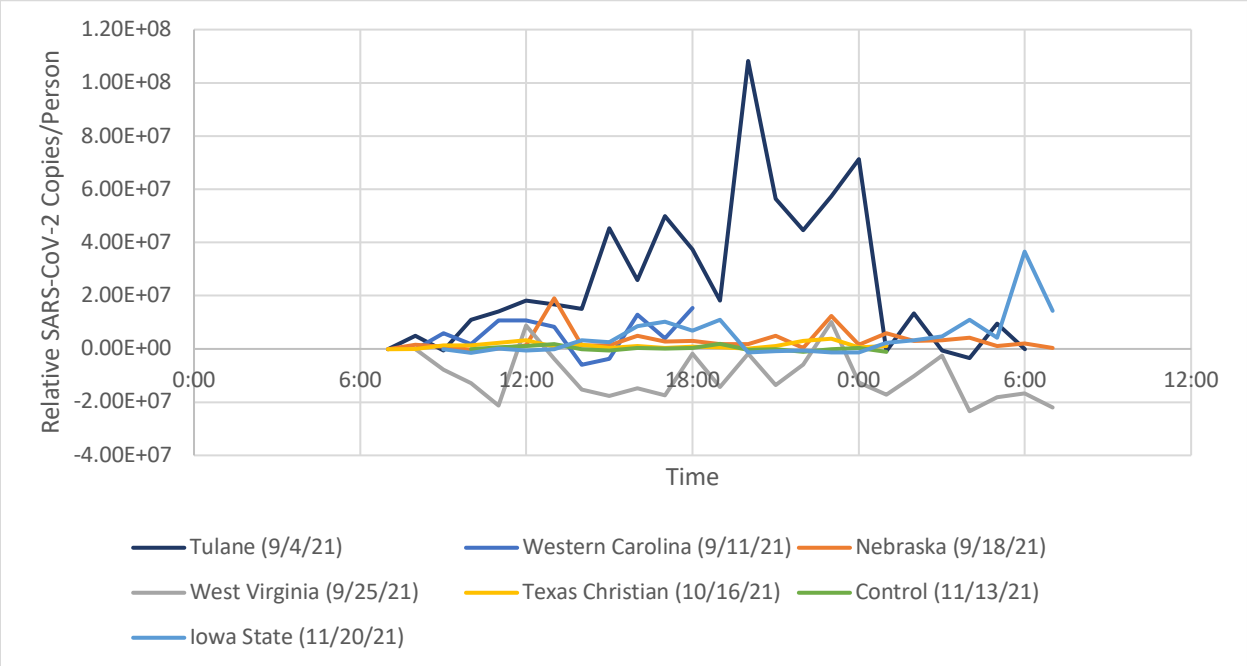

Figure 40: Relative SARS-CoV-2 viral load per person over time for all games in the 2021 football season.

Table 20 contains the mean relative viral load per person by time category for all games in the 2021 football season.

Table 20: Mean relative SARS-CoV-2 viral load per person by time group for all games in the 2021 football season. Within the All row, games with different superscript Greek letters are significantly different at the 95% confidence level.

	Tulane (September 4, 2021)	**Western Carolina (September 11, 2021)**	**Nebraska (September 18, 2021)**	**West Virginia September 25, 2021)**	**Texas Christian (October 16, 2021)**	**Control (November 13, 2021)**	**Iowa State (November 20, 2021)**
Before	3.86×10^6	1.78×10^6	5.00×10^5	-1.29×10^7	6.68×10^5	N/A	-7.38×10^5
During	1.60×10^7	1.54×10^7	5.45×10^6	-8.85×10^6	1.18×10^6	N/A	6.77×10^5
After	3.96×10^7	N/A	3.02×10^6	N/A	N/A	N/A	7.05×10^6
Late-Night	2.81×10^7	N/A	5.18×10^6	-6.51×10^6	1.82×10^6	-3.33×10^5	1.46×10^6
All	$2.55 \times 10^{7\,\alpha}$	$5.45 \times 10^{6\,\beta}$	$3.12 \times 10^{6\,\beta,\delta}$	$-1.05 \times 10^{7\,\chi}$	$1.24 \times 10^{6\,\chi,\delta}$	$1.69 \times 10^{5\,\chi}$	$4.84 \times 10^{6\,\beta,\delta}$

Figure 41A shows the relative SARS-CoV-2 viral load per person over time for the Tulane game. Using this method, the peak at 8:00 pm was more exaggerated. Figure 41B shows the relative viral load per person over time for the Western Carolina game, again the peak occurred at kickoff (6:00 pm). The relative SARS-CoV-2 viral load per person for the Nebraska game can be seen in Figure 41C. The peak again occurred around 1:00 pm. Figure 41D shows the relative viral load per person over time for the West Virginia game. Figure 41E shows the relative viral load per person over time for the TCU game. The data indicates a peak in the relative viral load per person at 11:00 pm. Figure 41F shows the relative viral load per person over time for the control day, the relative viral load per person was greatest at approximately 7:00 pm. Figure 41G shows the relative viral load per person over time for the Iowa State game, the relative viral load per person was greatest at 6:00 am on Sunday.

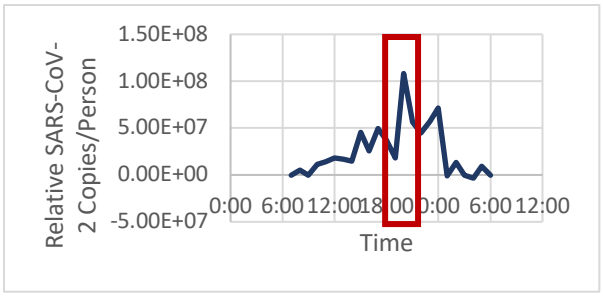

A: (Above) Relative SARS-CoV-2 viral load per person over time for Tulane (September 4, 2021) game.

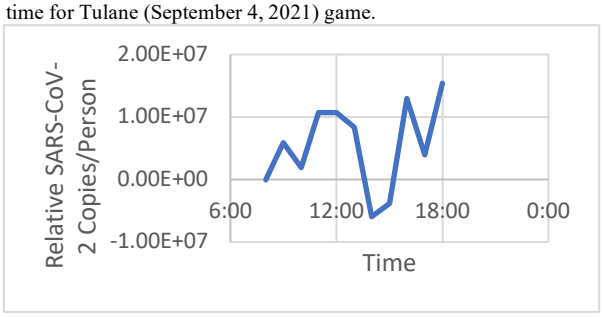

B: (Above) SARS-CoV-2 viral load per person over time for Western Carolina (September 11, 2021) game.

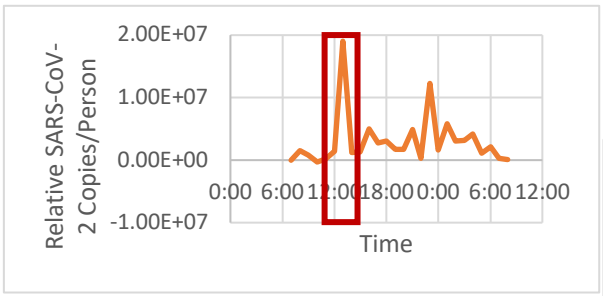

C: (Above) SARS-CoV-2 viral load per person over time for Nebraska (September 18, 2021) game.

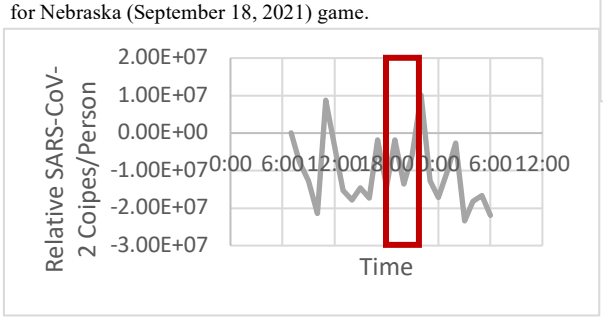

D: (Above) SARS-CoV-2 viral load per person over time for the West Virginia (September 25, 2021) game.

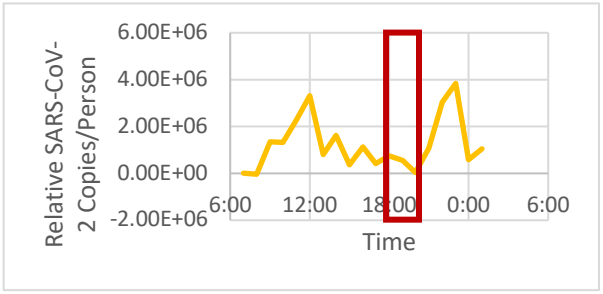

E: (Above) SARS-CoV-2 viral load per person over time for the Texas Christian (October 16, 2021) game.

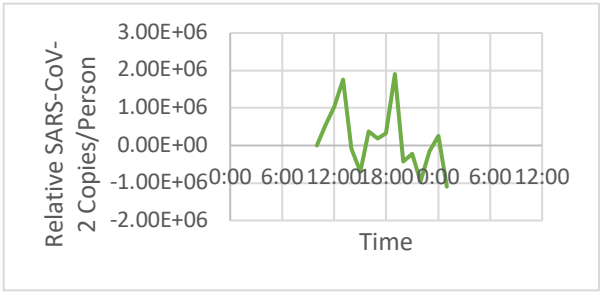

F: (Above) SARS-CoV-2 viral load per person over time for the control (October 13, 2021) day.

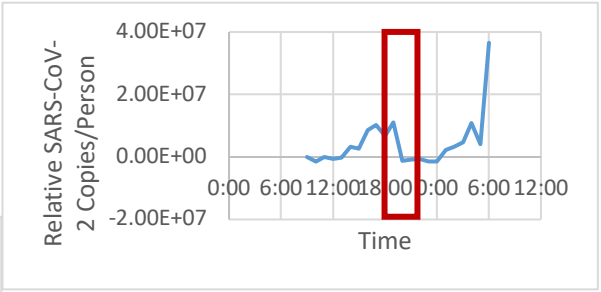

G: (Above) SARS-CoV-2 viral load per person over time for the Iowa State (November 20, 2021) game.

Figure 41: Relative SARS-CoV-2 viral load per person over time for the Tulane (9/4/21) game. Approximate game time is outlined in red. A represents the relative viral load per person during the Tulane sampling period, B shows the relative viral load per person during the Western Carolina sampling period, C shows the relative viral load per pe during the Nebraska sampling period, D shows the relative viral load per person over the duration of the West Virginia sampling period, E shows the relative viral load per person over the duration of the Texas Christian sampling period, F shows the relative viral load per person over the duration of the control sampling period, and G shows the relative viral load per person over the duration of the Iowa State sampling period.

All games in the 2020 season were combined to analyze the differences in relative viral load per person by time groups. The relative viral load per person in the before group is significantly different from the after group ($P < 0.01$) but not the during ($P = 0.32$) or late-night groups ($P = 0.48$). The difference in relative viral load per person for the during group is significant when compared to the after group ($P = 0.01$) but not the late-night ($P = 0.16$). The relative viral load per person for the after group is significantly different from the late-night category ($P < 0.01$).

For the next analyses, the first viral load per person of each time category was subtracted from the remaining viral loads in the time category, making the first sample zero. Figure 42A shows the relative viral load per person over time for the before game category. The relative viral load per person was increasing for the Tulane, Western Carolina, and West Virginia games. The relative viral load per person stayed nearly constant at the before game time scale for the Nebraska, Texas Christian, and Iowa State games. The relative viral load per person before the game was very slightly negative for the Nebraska game. Figure 42B shows the relative viral load per person over the duration of each game. The relative viral load per person increased for the Nebraska and Iowa State games, while it remained mostly constant for the remaining games at this time scale. Figure 42C shows the relative viral load per person for the after-game category. The relative viral load per person was very slightly increasing over these hours for the Nebraska and Iowa State games, while it varied, but ultimately decreased for the Tulane game. Figure 42D shows the relative viral load per person over the late-night hours. The relative viral load per person over this period was decreasing for all games expect the and Iowa State game, which was increasing.

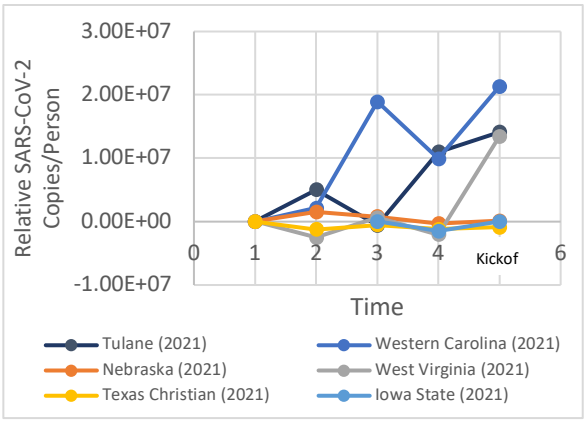

A (Above): SARS-CoV-2 viral load per person over time before the football game. Time 1 represents the first of hour hours before the game

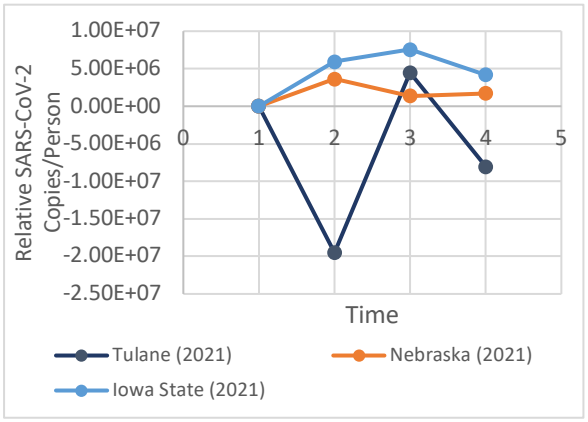

C (Above): SARS-CoV-2 viral load per person over time during the after category. 1 represents the first hour after the game

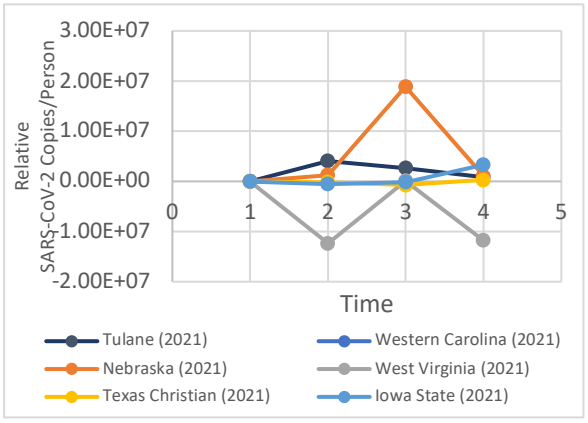

B (Above): SARS-CoV-2 viral load per person over time during the football game. Time 1 represents kickoff

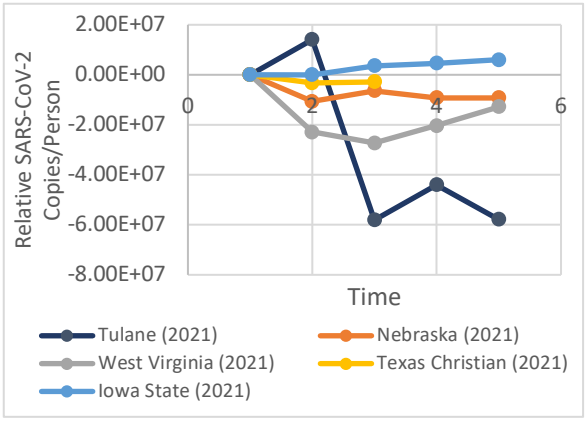

D (Above): SARS-CoV-2 viral load per person over time during the late-night category. Time 1 represents 11:00 pm.

Figure 42: Relative SARS-CoV-2 viral load per person over time, by time category, for all games in the 2021 football season

Figure 43 shows the correlation between the relative SARS-CoV-2 viral load per person versus the flow for all games in the 2021 football season. There is a weak positive correlation between the two variables ($R^2 = 0.05$).

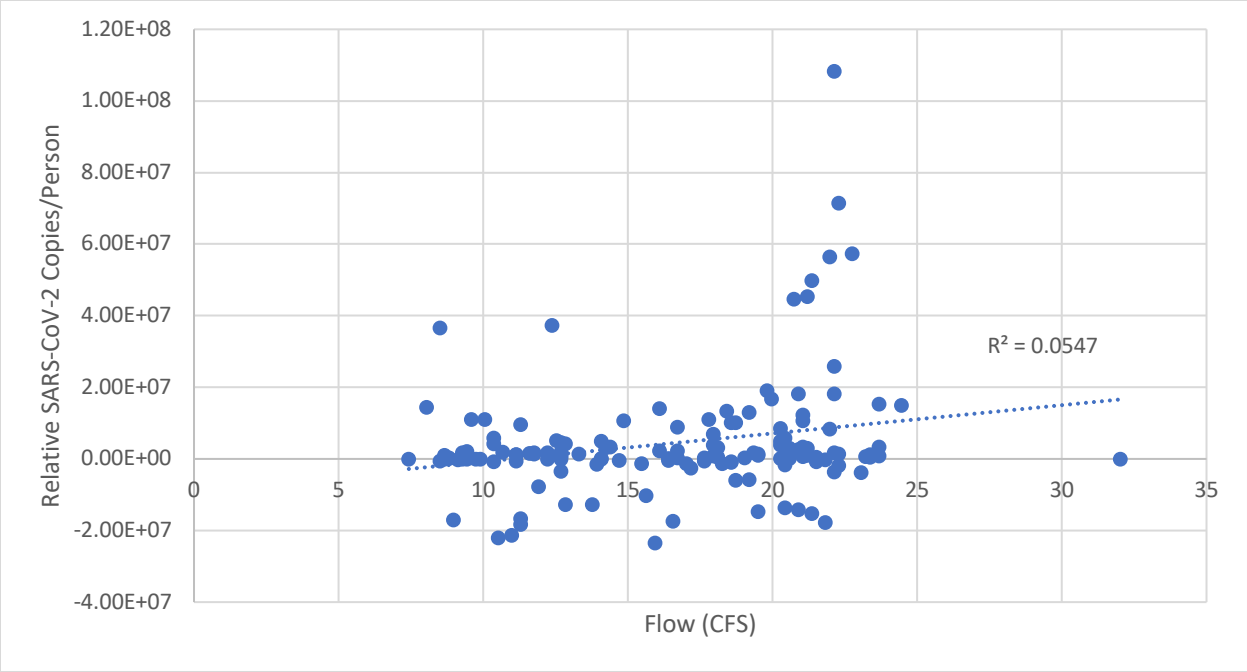

Figure 43: Relative SARS-CoV-2 viral load per person versus the flow for all games in the 2021 football season

Similar to Figure 43, Figure 44 shows the correlation between the relative viral load per person and the population. The relationship between the two variables is very weak ($R^2 = 0.04$) and negative.

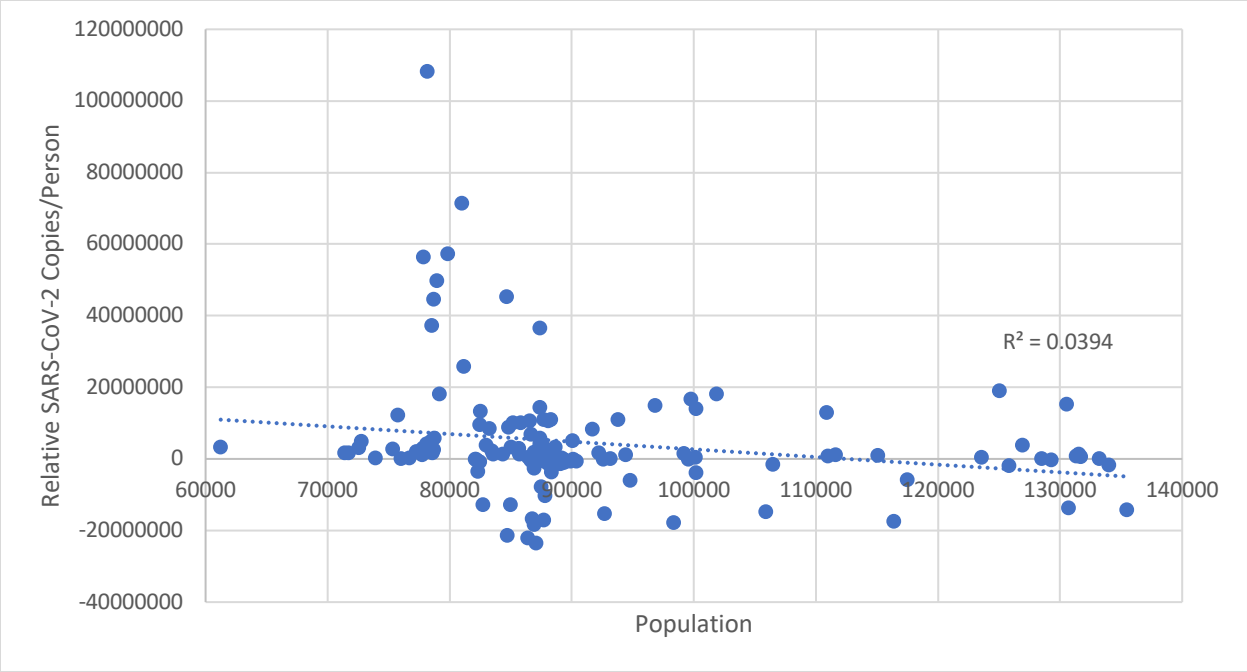

Figure 44: Relative SARS-CoV-2 viral load per person versus the population for all games in the 2021 football season

A correlation analysis between the relative viral load per person, flow, and population was completed for each day that was sampled in the 2021 football season. Table 21 shows the resulting R^2 values from this analysis. None of the relationships are significant at the 95% confidence level.

Table 21: Results of correlation analysis (R^2 values) between the viral load per person and flow, and the viral load per person and population for the 2021 football season.

	Tulane (September 4, 2021)	**Western Carolina (September 11, 2021)**	**Nebraska (September 18, 2021)**	**West Virginia September 25, 2021)**	**Texas Christian (October 16, 2021)**	**Control (November 13, 2021)**	**Iowa State (November 20, 2021)**
Concentration vs. Flow	0.41	0.05	0.17	0.07	0.02	0.11	0.12
Concentration vs. Population	0.18	0.09	0.01	< 0.01	0.22	0.08	0.02

3.3 Comparing Both Seasons

The flow for the 2020 football season was greater than the 2021 football season ($P < 0.01$). However, the concentration in the 2021 football season is significantly greater than the season prior ($P < 0.01$). Table 22 contains the mean flow (CFS), population, concentration

(Copies/L), viral load per person (Copies/Person), and relative viral load per person (Relative Copies/Person) for each football season.

Table 22: Mean flow (CFS), population, concentration (Copies/L), viral load per person (Copies/Person), and relative viral load per person (Relative Copies/Person) for the 2020 and 2021 football seasons.

	Flow (CFS)	**Population**	**Concentration (Copies/L)**	**Viral Load per Person (Copies/Person)**	**Relative Viral Load per Person (Relative Copies/Person)**
2020 Season	19.72	83,525	2.14×10^5	4.41×10^6	2.39×10^6
2021 Season	16.26	90,832	5.99×10^5	1.13×10^7	4.23×10^6

The flow for the 2020 season is greater than the 2021 ($P < 0.01$). The flow recorded for both seasons was also compared at the time category level. The difference in flow was significant when the before group was compared to the during ($P = 0.02$), after ($P < 0.01$), and late-night ($P < 0.01$) groups. The during group did not have significantly different flow compared to the after category ($P = 0.13$). The flow recorded in the late-night group was significantly different from the during ($P < 0.01$) and after categories ($P < 0.01$).

The estimated population of the 2021 football season is significantly greater than the 2020 season ($P < 0.01$). For both seasons together, the before group was not significantly different from the during group ($P = 0.27$), nor was the after category significantly different from the late-night group ($P = 0.32$). The differences in population were significant when the before group was compared to the after ($P = 0.04$) and late-night categories ($P < 0.01$) as well as when the during category was compared to the after ($P = 0.01$) and late-night categories ($P < 0.01$).

The concentration in the 2021 season was significantly greater than the 2020 season ($P < 0.01$). When both seasons are combined, the difference in concentration of the before category is not significantly different from the during ($P = 0.314$) or late-night groups ($P = 0.42$). The

concentration in the before category is significantly different from the after category ($P = 0.04$). The differences were not significant for the during category compared to the after ($P = 0.22$) or late-night category ($P = 0.74$). The concentration in the late-night category is not different from the late-night ($P = 0.50$).

The viral load per person of the 2021 season is significantly greater than the 2020 football season ($P < 0.01$). The two seasons were analyzed together for the time group analysis. The viral load per person of the before category is not significantly different from the during ($P = 0.06$) or late-night categories ($P = 0.16$) but is significantly different from the after category ($P = 0.02$). The viral load per person for the during group is not significantly different from the after ($P = 0.19$) or the late-night groups ($P = 0.90$). The viral load per person of the after category is not different from the late-night category ($P = 0.54$).

The relative viral load per person for the 2021 season is not significantly greater than the 2020 season ($P = 0.23$). When all gamedays in both seasons are combined, the relative viral load per person for the before category is not significantly different from the during ($P = 0.24$) or late-night categories ($P = 0.06$) but is significantly different from the after category ($P < 0.01$). The difference in relative viral load per person is significant when comparing the during group to the after group ($P = 0.02$), the during group to the late-night group ($P = 0.02$), and the after group to the late-night group ($P < 0.01$).

Determining if there were strong relationships between variables such as flow and concentration, population and concentration, flow and viral load per person, population and viral load per person, flow and relative viral load per person, and population and relative viral load per person was of great importance. Figure 45 shows the correlations between the flow and concentration for the 2020 and 2021 football seasons. Though the correlation was positive for the

2021 football season, overall, the relationship between these two variables is very slightly negative.

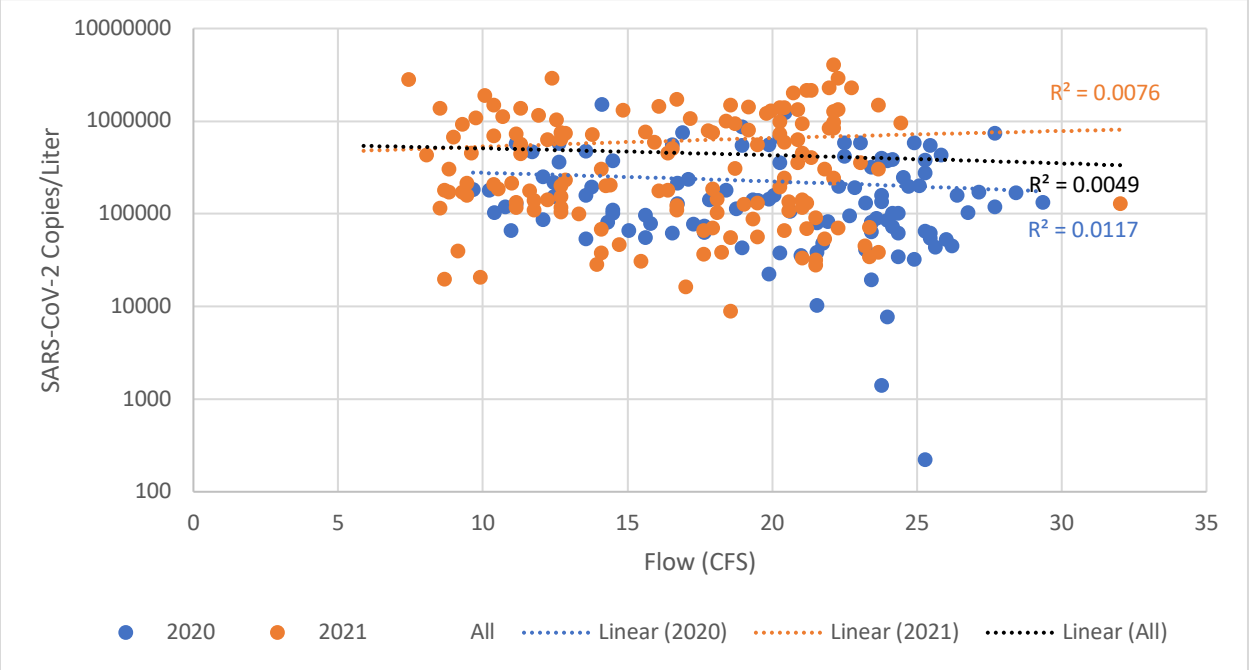

Figure 45: SARS-CoV-2 concentration versus the flow (CFS) for the 2020 and 2021 football seasons.

Figure 46 shows the overall correlation between the viral load per person and flow, as well as the correlation between the two variables for the 2020 and 2021 football seasons. There is almost no relationship between the two variables when both seasons are analyzed together. The 2021 football season has a stronger correlation between the two variables than the 2020 season.

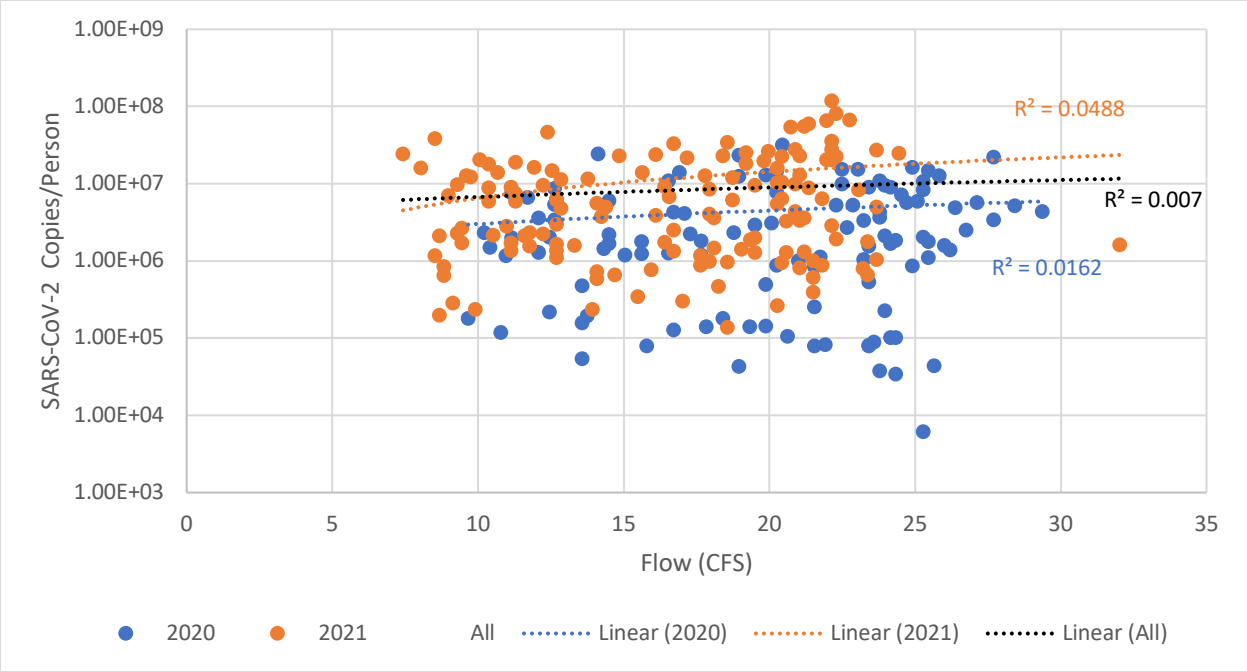

Figure 46: SARS-CoV-2 viral load per person versus the flow (CFS) for the 2020 and 2021 football seasons.

Figure 47 shows the correlations between the relative viral load per person and flow for all of the sampling days analyzed. Using the relative viral load per person results in the strongest correlations for both seasons, as well as the seasons combined.

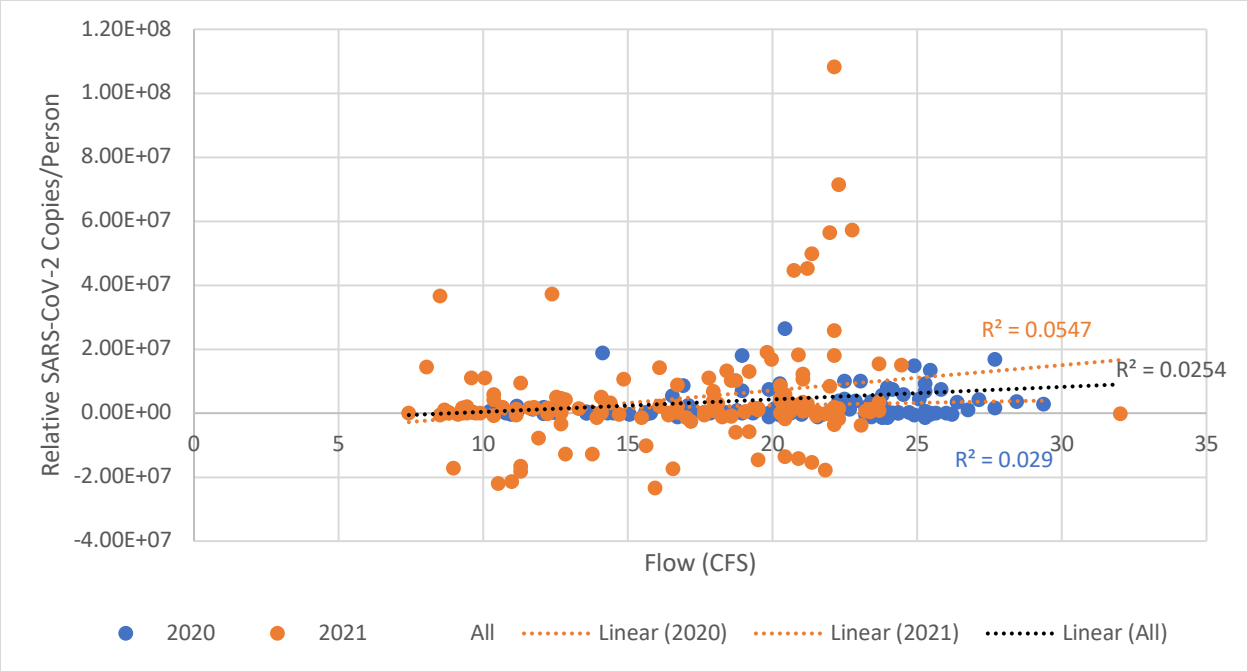

Figure 47: Relative SARS-CoV-2 viral load per person versus the flow (CFS) for the 2020 and 2021 football seasons.

Figure 48 shows the SARS-CoV-2 concentration versus the population for all games in the 2020 and 2021 seasons, as well as both seasons combined. The correlation between these variables is very weak for both seasons, and especially when the seasons are combined. There is essentially no correlation between the two variables when the seasons are combined, as evidenced by the very small R^2 value shown on the figure, as well as the nearly perfectly horizontal trendline.

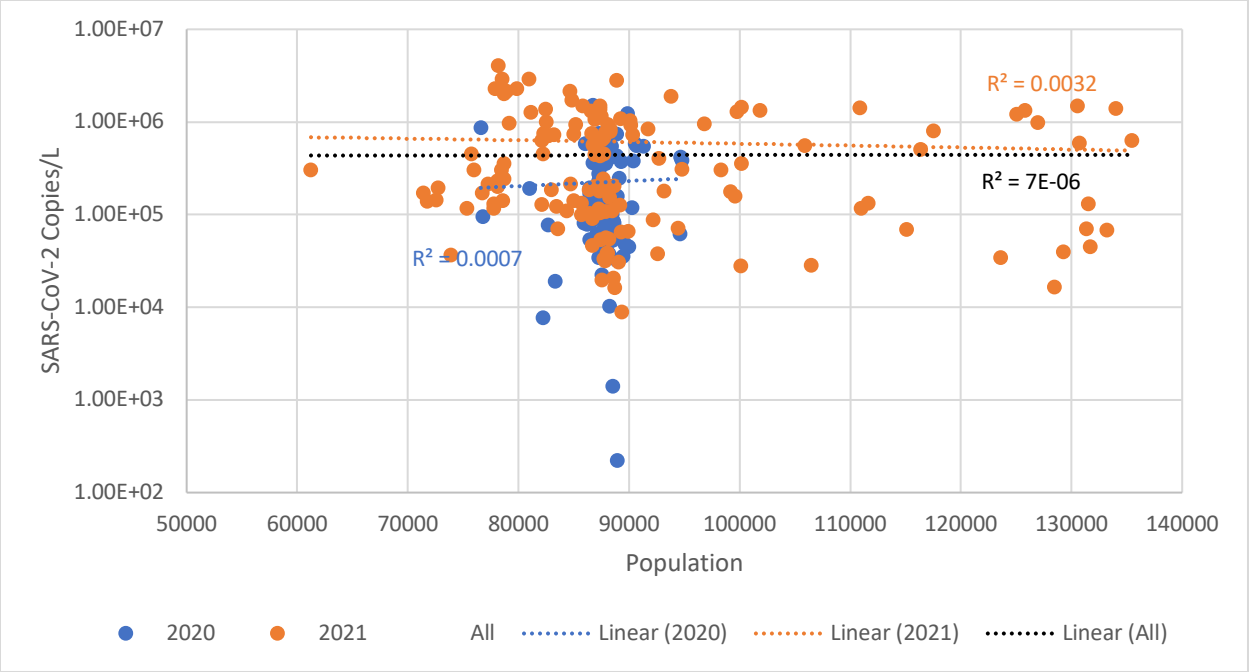

Figure 48: SARS-CoV-2 concentration versus the population for the 2020 and 2021 football seasons.

Figure 49 shows the correlations between the viral load per person and the population. The viral load per person has a slightly stronger relationship than the concentration did when compared to the population. The 2020 football season had the weakest correlation between the two variables, though it is positive. While the correlations for the 2021 season and both seasons combined is stronger, they are negative.

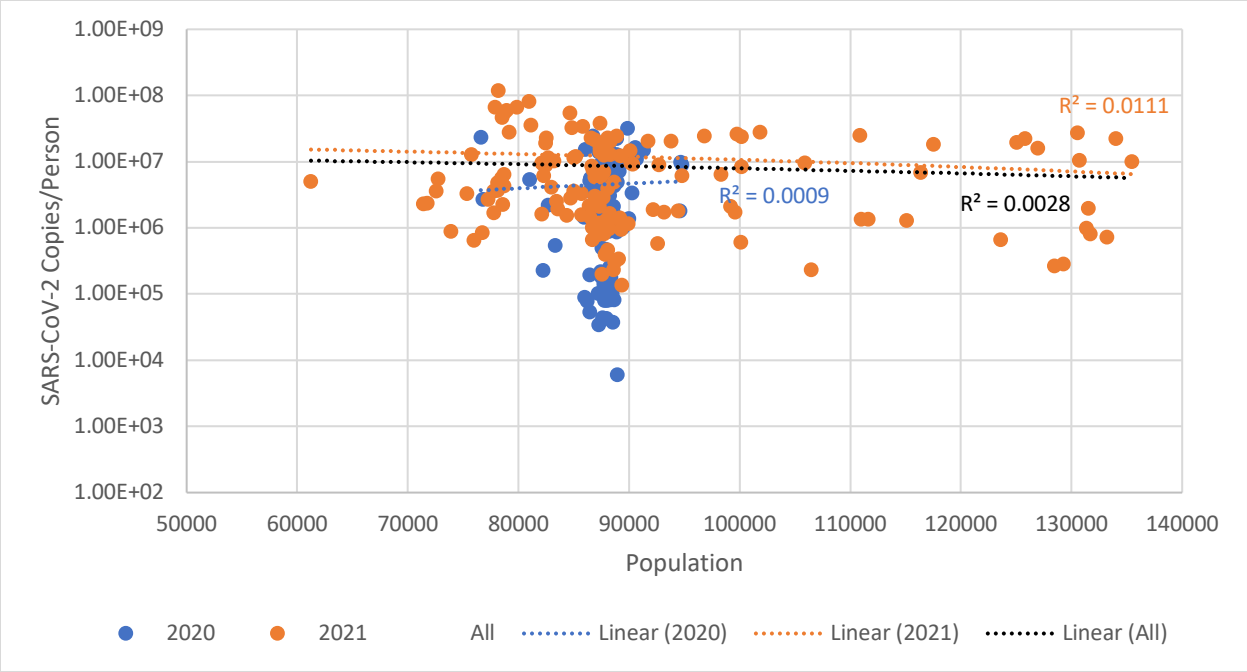

Figure 49: SARS-CoV-2 viral load per person versus the population for the 2020 and 2021 football seasons.

Figure 50 shows the relative viral load per person versus the population for the 2020 and 2021 football seasons, as well as both seasons combined. The correlation between the two variables when the seasons are combined is not statistically significant at the 95% confidence level, but it is stronger than when the concentration and viral load per person are compared to the population.

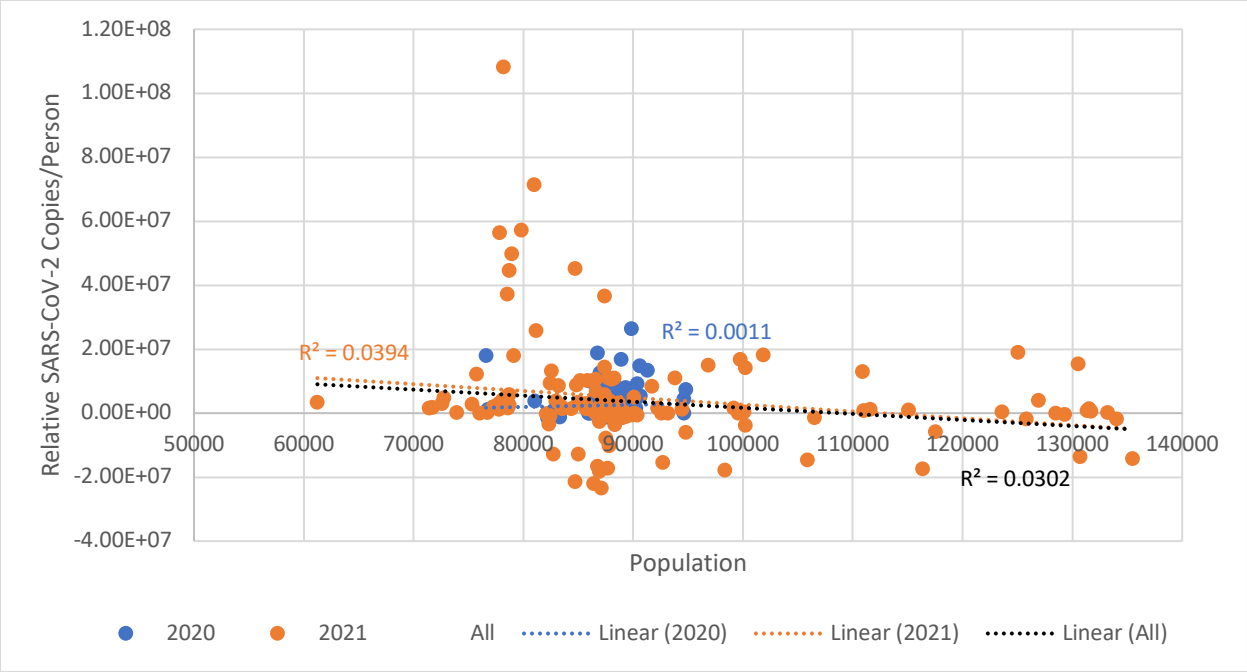

Figure 50: Relative SARS-CoV-2 viral load per person versus the population for the 2020 and 2021 football seasons.

CHAPTER 4

DISCUSSION

The population estimated by StreetLight likely did not match the number of people in the sewershed, but still provided a good estimate. Further, the SARS-CoV-2 concentrations and viral loads per person were so great that the error resulting from the population estimation was small enough that the population data was still used. The first part in determining this was to calculate the relative standard deviation of the concentration, population, and viral load per person. The relative standard deviation is a percentage calculated by dividing the standard deviation of a group by the mean of that group, then multiplying by 100 to get it in percent form. This tells how far away the standard deviation is away from the mean. Table 23 shows the mean concentration, population, and viral load per person for each game, as well as the relative standard deviation of the concentration, population, and viral load per person. The concentration for each sample was the geometric mean of the triplicates, and similarly, the relative standard deviation for each sample was calculated from the triplicates for both the concentration and viral load per person. For all the games except the Missouri State game, the mean relative standard deviation for the concentration and the mean relative standard deviation for the viral load per person were the same. This means that when the flow and population were used to calculate the viral load per person for the Missouri State game, it made the standard deviation further away from the mean. However, for all the remaining games for both seasons, using the flow and population did not change the distance of the standard deviation away from the mean. Missouri State also had the largest relative standard deviation, indicating that there was a large range of values for the triplicates. The games in the 2021 football season saw a greater relative standard deviation for

the population, which makes sense because there was a greater difference between the smallest and largest values for this season compared to the 2020 season.

Table 23: The mean concentration, population, and viral load per person for each game as well as the mean relative standard deviation of the sample triplicates, and the relative standard deviation of the concentration and viral load per person, and the relative standard deviation of the population for each game.

Game	Mean Concentration (copies/L)	Mean Concentration Relative Standard Deviation (%)	Mean Population	Population Relative Standard Deviation (%)	Mean VLPP (copies/person)	Mean VLPP Relative Standard Deviation (%)
Missouri State (September 12, 2020)	1.76×10^5	74.59	87,930	1.26	3.32×10^6	78.48
Kansas (November 7, 2020)	1.02×10^5	37.66	87,620	2.82	2.06×10^6	37.66
Control (November 14, 2020)	1.27×10^5	44.57	87,620	0.82	2.97×10^6	44.57
Oklahoma State (November 21, 2020)	1.73×10^5	49.74	87,720	3.78	4.37×10^6	49.74
Baylor (December 5, 2020)	5.64×10^5	28.78	87,720	3.32	1.25×10^7	28.78
Tulane (September 4, 2021)	1.51×10^6	24.31	85,620	9.02	3.37×10^7	24.31
Western Carolina (September 11, 2021)	1.03×10^6	30.28	99,410	16.31	1.56×10^7	30.28
Nebraska (September 18, 2021)	2.25×10^5	42.26	88,100	23.07	4.03×10^6	42.26
West Virginia (September 25, 2021)	8.55×10^5	22.41	97,100	18.05	1.38×10^7	22.41
Texas Christian (October 17, 2021)	7.60×10^4	42.07	98,990	18.33	1.47×10^6	42.07
Control (November 13, 2021)	9.31×10^4	42.07	87,810	1.07	1.75×10^6	30.24
Iowa State (November 20, 2021)	3.55×10^5	37.24	87,380	9.04	6.52×10^6	37.24

The percent of the overall uncertainty for the viral load per person that comes from the population was analyzed. This was accomplished by assuming certain relative standard deviations for the population. These assumed standard deviations were 1%, 5%, 10%, and 25%. The relative standard deviations for the concentration were calculated and added to the assumed standard deviation from the population, which resulted in the relative standard deviation for the viral load per person. For this analysis, the uncertainty coming from the flow was assumed to be negligible. Finally, the percent uncertainty resulting from the population in the viral load per person was calculated by dividing the assumed population relative standard deviation by the relative standard deviation for the viral load per person. Figure 51 shows the percent uncertainty from the population over the assumed population relative standard deviation for the 2020 football season. The greatest percent uncertainty resulting from the population was assuming a 25% relative standard deviation for the Baylor game, which correlates to about 50% of the uncertainty coming from the population and not the concentration or flow. It is most likely that the Baylor game had a greater relative standard deviation for the population due to students leaving campus as the semester progressed, so it is believable that the uncertainty resulting from the population would be greater for this game. This likely was true to a lesser extent for the Oklahoma State game as well, as it occurred later in the season. However, for games earlier in the season (Missouri State, Kansas, and the control), when the population estimates were likely closer to the 1%, 5%, and 10% relative standard deviation values, the uncertainty resulting from the population was under 25%, this means that the majority of that uncertainty came from the concentration, rather than the population.

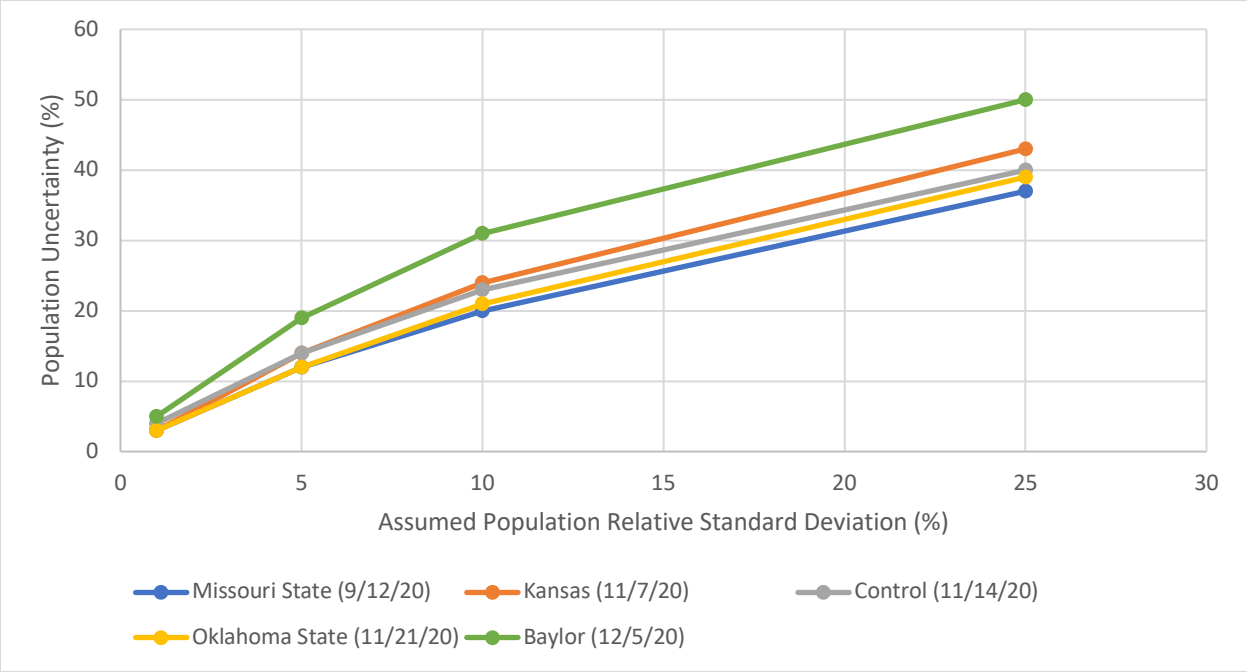

Figure 51: Percent uncertainty from the population over the assumed relative standard deviation for the population for all games in the 2020 football season.

The relative standard deviations were used to calculate the percent uncertainty from the population in the viral load per person for the 2021 season as well. Figure 52 shows the percent of the uncertainty in the viral load per person that comes from the population over the assumed relative standard deviation for the population for the 2021 season. Because there were more people in town for the 2021 season, there was greater uncertainty in the viral load per person compared to the 2020 season, with the greatest percentage coming from the population is 57%, which was associated with the 25% assumed relative standard deviation for the Tulane and West Virginia games. However, for this season, there was not a gradual exodus from campus, like there was the season prior, meaning that the population relative standard deviation for each game was likely closer to 1% or 5%, for which the greatest population uncertainty was 24%, which occurred on the West Virginia game. Ultimately, for both seasons, the majority of the uncertainty in the viral load per person measure comes from the concentration itself, thus using StreetLight to estimate the population in the sewershed in this manner is effective.

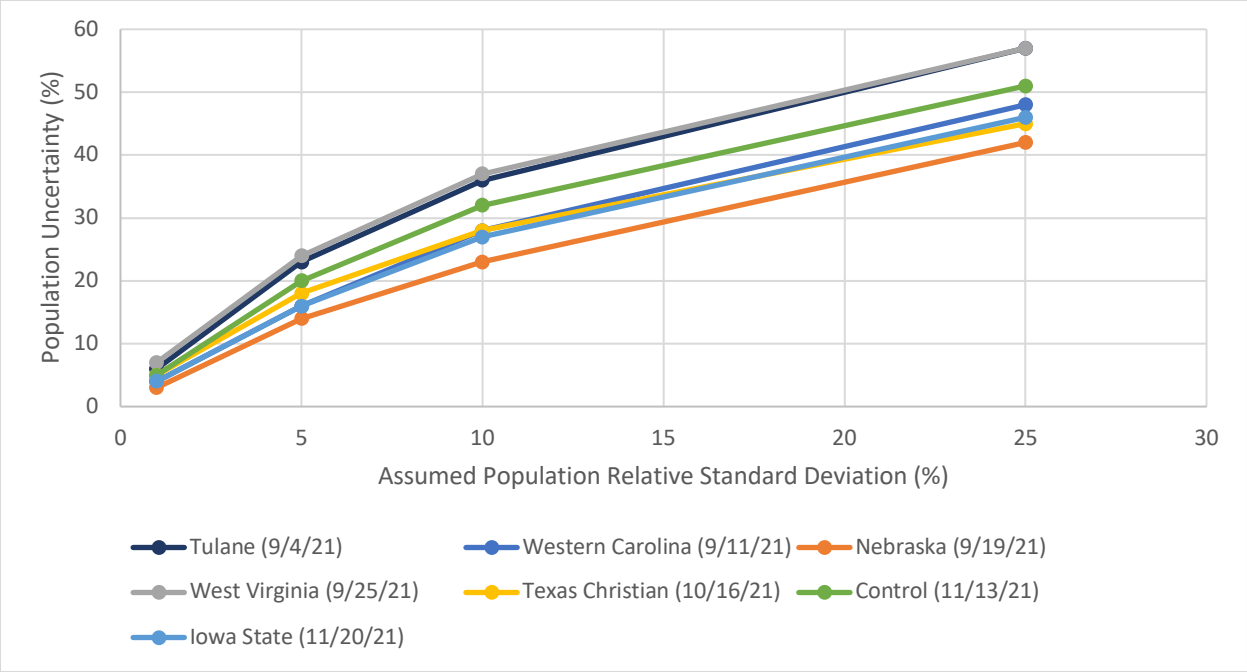

Figure 52: Percent uncertainty from the population over the assumed relative standard deviation for the population for all games in the 2021 football season.

There is some unaccounted-for delay from when a toilet is flushed within the sewershed to the time that same water reaches the wastewater treatment facility. This means that there is some discrepancy between when the water was sampled versus when it was flushed. So, if a person who is shedding SARS-CoV-2 were to use the restroom in the latter part of the game, it might get counted in the after-game group for the purposes of our analysis, rather than the during game group. There are also more "mobile restrooms" including port-a-potties and RV restrooms in the sewershed on gamedays than there are on other days of the week. This is because the University allows people to park their RV or camper at the University to attend football games. The University also sets out port-a-potties for tailgaters to use during gameday festivities. To that end, there is an unknown amount of wastewater that does not reach the wastewater treatment facility and is not included in this analysis.

Notably, much of the variation in the amount of SARS-CoV-2 in the wastewater can be attributed to the trends in cases throughout the seasons (refer to Figure 1), rather than the football

games themselves. For instance, the Delta Variant was at a peak at the start of the 2021 football season, as reflected by the case data at the time, and matches with the greatest amount of SARS-CoV-2 in the wastewater at the time. A similar phenomenon was occurring at the end of the 2020 football season, where confirmed cases were increasing after Thanksgiving and going into the December holidays. To confirm this, the mean of the hourly viral load per person for each game was compared to the number of new cases in Oklahoma during the week leading up to the corresponding game, seen in Figure 51, to determine if there was a correlation. There is a positive relationship between the variables, indicating that there typically is more SARS-CoV-2 in the wastewater when the weekly cases were greater, however this relationship was not significant at the 95% confidence level. The NWRF composite samples taken on days surrounding the gameday from the wastewater treatment plant also indicate that the SARS-CoV-2 concentration in wastewater followed the trends of the confirmed cases. The concentration of SARS-CoV-2 in the wastewater was increasing over time for both gameday and NWRF composite samples in 2020. For the 2021 football season the concentration was decreasing over time for both the NWRF and gameday samples. Again, the correlation was slightly stronger for the gameday samples ($R^2 = 0.48$) compared to the NWRF ($R^2 = 0.44$). An interesting result from the comparison of the gameday concentration to the NWRF concentration is that for the 2021 football season, only the West Virginia game was greater than the NWRF, though the difference was not significant.

Despite these trends aligning with the confirmed cases, the amount of SARS-CoV-2 found in the wastewater was greater in 2021, when there were no regulations about tailgating or attendance. In fact, the population, concentration, viral load per person, and relative viral load per person were all greater in the 2021 football season than they were in the 2020 football season

(the difference was significant for all metrics except relative viral load per person). This does indicate that at least some of the variability in SARS-CoV-2 was due to football game attendance. Figure 53 shows the confirmed COVID-19 cases in the state compared to the average viral load per person of the hourly gameday samples.

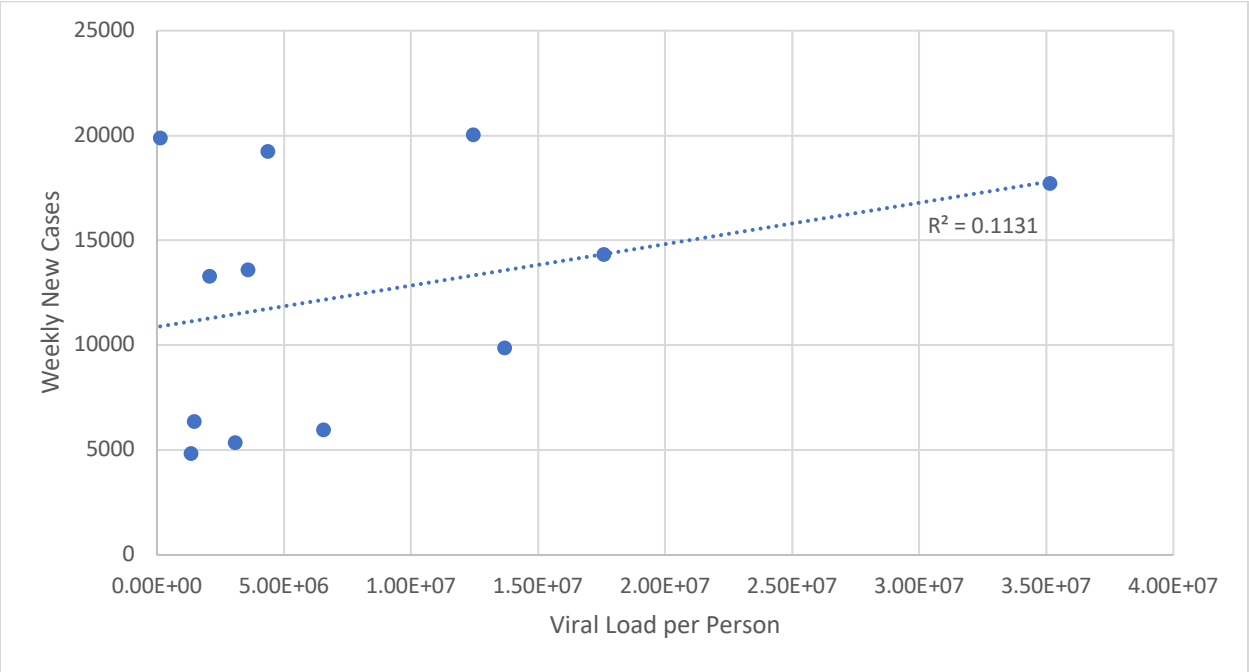

Figure 53: Average of the hourly SARS-CoV-2 viral load per person for each game versus the number of confirmed COVID-19 cases for the week prior to the game.

Table 24 shows the gameday compared to the control for that season for the concentration, viral load per person, relative viral load per person, population, and flow for every game. Red boxes with an upwards facing arrow indicate that the gameday was significantly greater than the control. Yellow boxes with side-to-side arrows indicate that the difference between the gameday and the control was not significant. Green boxes with downward facing arrows indicate that the gameday was significantly less than the control. There were more games that were significantly greater than the control with any metric of measuring SARS-CoV-2 However, this was more of the case for the 2021 season. When the concentration and relative viral load per person were used as the SARS-CoV-2 metric for the 2020 season most of the

games did not have a significant difference. The relative viral load per person for the West Virginia game was less than the control. This was because the first sample of the day for this game was greater than the remaining samples for the day, making the relative viral load per person negative.

Table 24: Comparison of the SARS-CoV-2 concentration, viral load per person, relative viral load per person, population, and flow for each game compared to the control for that season. Red boxes with upward arrows indicate that the game was significantly greater than the control. Yellow boxes with side-to-side arrows indicate that the game was not significantly different from the control. Green boxes with downward arrows indicate that the game was significantly less than the control.

Compared to Control	Missouri State 2020	Kansas 2020	Oklahoma State 2020	Baylor 2020	Tulane 2021	Western Carolina 2021	Nebraska 2021	West Virginia 2021	Texas Christian 2021	Iowa State 2021
Concentration	↔	↔	↔	↑	↑	↑	↑	↑	↔	↑
Viral Load/person	↑	↑	↑	↑	↑	↑	↔	↑	↔	↑
Relative Viral Load per person	↔	↔	↔	↑	↑	↑	↑	↓	↑	↑
Population	↑	↑	↑	↑	↑	↑	↑	↑	↑	↑
Flow	↑	↔	↑	↔	↑	↔	↔	↔	↔	↔

Across seasons, analysis was improved when a version of the viral load per person (relative viral load per person) was used as the SARS-CoV-2 metric. Using the relative viral load per person as the metric for SARS-CoV-2 resulted in the best correlations between flow versus SARS-CoV-2 and population versus SARS-CoV-2 for both seasons. Also, when the viral load per person and the relative viral load per person were used as the SARS-CoV-2 metric, there were more games in the 2021 football season that had within day variability. This is because the viral load per person is a unique metric that has not often been used in this type of work. The benefit to this metric is that it is not dependent on the population or size of a drainage and could be compared to anywhere in the world that can also calculate the number of copies per person. To date, there is not another SARS-CoV-2 WBE study that uses a viral load per person metric.

This is likely due to the difficulty of gathering a proper estimate of the population in the sewershed. Other similar estimations of viral loads were calculated based on the known number of cases in the sewershed at the time which misses those who are asymptomatic, pre-symptomatic, or mildly symptomatic and did not or have not yet been tested. To compare how the viral load per person impacted the temporal variability of SARS-CoV-2 in the wastewater, it was compared to the concentration for the Baylor (December 5, 2020) and Tulane (September 4, 2021) games. These games were selected for their relatively great variability. The viral load per person exaggerated the peaks around game time for the Baylor game, however, when the population and flow were smaller compared to the game time, the peaks are less apparent using the viral load per person. The SARS-CoV-2 concentration and viral load per person for the Baylor game are shown in Figure 54.

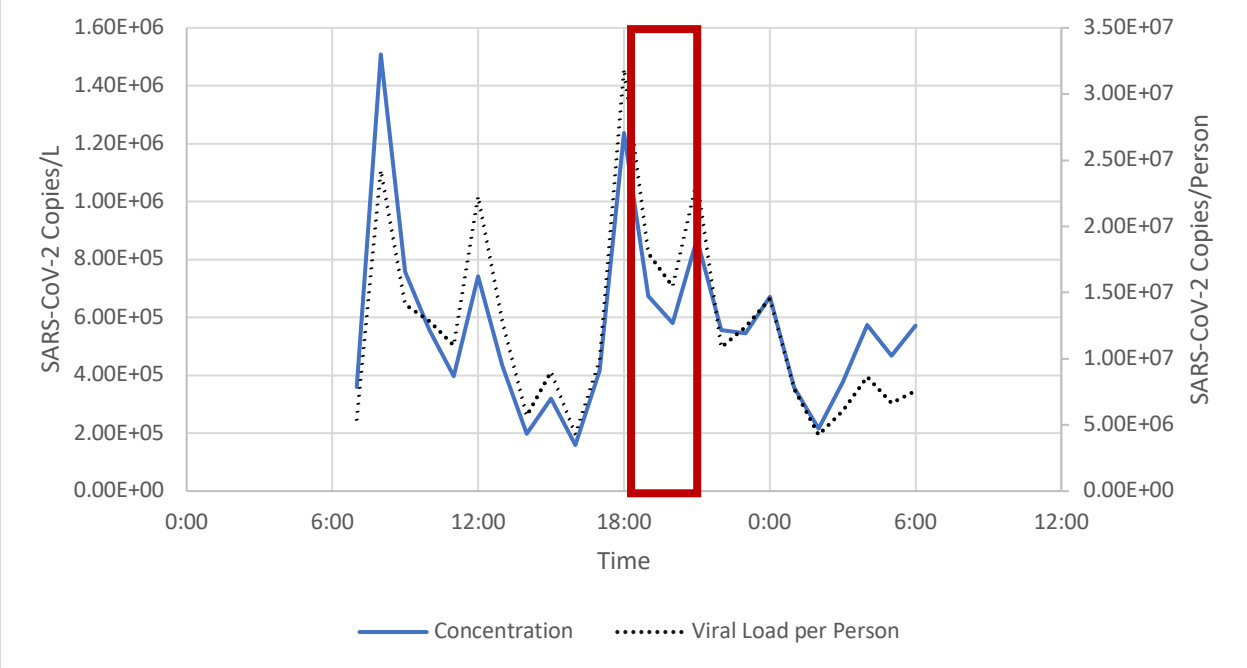

Figure 54: SARS-CoV-2 concentration and viral load per person over time for the Baylor (December 5, 2020) game. Approximate game time is outlined in red.

For the Tulane game, the peaks in the viral load per person before and during the game are much less exaggerated than compared to the evening samples. The SARS-CoV-2

concentration and viral load per person over time for the Tulane game can be seen in Figure 55. Ultimately, the viral load per person gives an accurate depiction of the amount of SARS-CoV-2 in the wastewater by normalizing it by the number of people and flow recorded at the wastewater treatment facility.

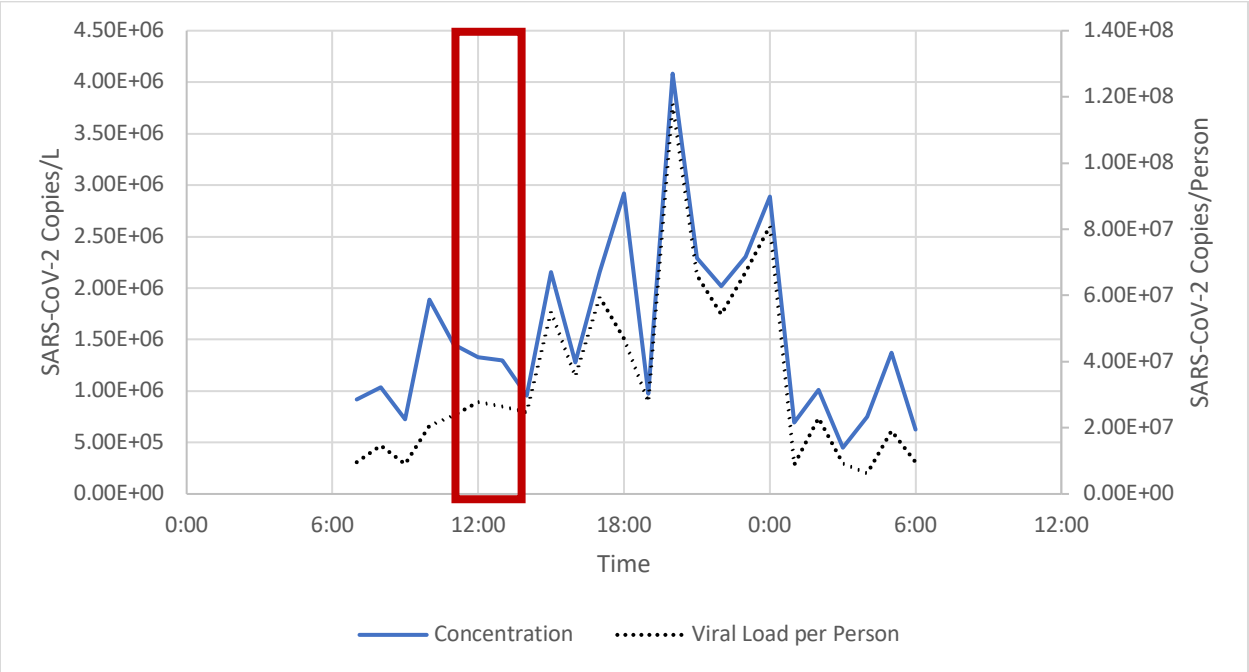

Figure 55: SARS-CoV-2 concentration and viral load per person over time for the Tulane (September 4, 2021) game. Approximate game time is outlined in red.

CHAPTER 5

CONCLUSIONS FOR EVENT-BASED WASTEWATER MONITORING STUDY

The first hypothesis was designed to determine whether the amount of SARS-CoV-2 in the wastewater was greater on gamedays than weekdays. Because there was no population data available for the weekdays, only the concentration was compared between these days. The average concentration from the NWRF composites on weekdays was greater than the average of the gameday samples for the Missouri State (September 12, 2020) and Baylor (December 5, 2020) games for the 2020 season, and all games in the 2021 season, with exception to West Virginia (September 25, 2021). This is the opposite of the hypothesis and could be due to greater dilution on gamedays due to more people being in the sewershed. To determine if dilution was a reason for the gameday samples' average concentration being less than the NWRF composites, the flow for each game was compared. The average daily flow in cfs for the Missouri State was the greatest of all of the games and was significantly greater than all games except the Oklahoma State game. The flow for the Baylor and West Virginia games were not significantly from the rest of the games in their respective seasons. Ultimately, this indicates that dilution was likely not a cause for the gameday samples to be less than the NWRF composites.

The second hypothesis was designed to determine if the amount of SARS-CoV-2 in the wastewater was greater on gamedays than the control days for each season. For the 2020 season, the SARS-CoV-2 concentration for the Missouri State and Kansas (November 7, 2020) games are slightly less than the control (November 14, 2020) and this difference is not significant at the 95% confidence level. The Oklahoma State (November 21, 2020) game had an average concentration greater than the control, though it was not significant. The average concentration

for the Baylor game was significantly greater than the control. The average SARS-CoV-2 viral load per person was significantly greater than the control for each day with a football game. The average relative viral load per person was greater for all gamedays in 2020 than the control, though the difference was significant only for the Baylor gameday. For the 2021 season, the SARS-CoV-2 concentration was significantly greater than the control (November 13, 2021) for all games except the Texas Christian (October 16, 2021) game, which was slightly less than the control (not significant at the 95% confidence level). When using the viral load per person as the metric for SARS-CoV-2 in the wastewater, the viral load per person was greater for every day with a game compared to the control. This difference was significant for all games except Nebraska and Texas Christian. The relative viral load per person on the control day was significantly less than the relative viral load per person for every game. Ultimately, this confirms the hypothesis that the amount of SARS-CoV-2 in the wastewater is greater on gamedays than the control. It also further illustrates that using the viral load per person is a sufficient way to standardize the data to compare days with different populations and circumstances.

The third hypothesis was focused on within day variability in the amount of SARS-CoV-2 in the wastewater, with the amount being greatest before and during the football games. Because for each time category there were only four samples, statistically significant comparisons cannot be made. However, for the 2020 football season, the SARS-CoV-2 concentration was greatest before the game for the Missouri State, Kansas, and Oklahoma State games. The concentration was greatest during the game for the Baylor game. The before game time category had the greatest viral load per person for the Missouri State and Oklahoma State games. The viral load per person was greatest during the game for the Baylor game and after the game for the Kansas game. The relative viral load per person was greatest before the game for

the Missouri State and Oklahoma State games, during the game for Baylor, and after the game for Kansas. The third hypothesis was true for three out of the four games in the 2020 football season when the viral load per person and relative viral load per person were used as the SARS-CoV-2 metric and was true for all of the games when the concentration was used. For the 2021 football season the concentration was greatest during the game for the Western Carolina and Nebraska games. The concentration was greatest after the game for the Tulane and Iowa State games and greatest during the late-night category for the West Virginia and Texas Christian games. The viral load per person was greatest during the game for the Western Carolina and Nebraska games. Again, the viral load per person was greatest after the game for the Tulane and Iowa State games, while it was greatest in the late-night category for the West Virginia and Texas Christian games. The relative viral load per person was greatest in the after category for the Tulane game, the during category for the Western Carolina game, the during category for the Nebraska game, the late-night category for the West Virginia game, the late-night category for the Texas Christian game, and the after category for the Iowa State game. The results of this analysis for this season are far more varied than the first season and the before category did not have the most SARS-CoV-2 for any game, using any metric.

It was hypothesized that there would be more SARS-CoV-2 in the wastewater in the 2021 football season than the 2020 season. With all metrics, this is true. The average concentration and viral load per person for the 2021 season are significantly greater than the 2020 season and the relative viral load per person is greater in the 2021 season, though the difference is not significant.

The final hypothesis was that the population would be greater on gamedays than the control days. For the 2020 football season, this was true for every gameday, and all differences

were statistically significant. The estimated population for each gameday in the 2021 season was significantly greater than the control. This confirms the hypothesis that the population is greater on gamedays than the control game, indicating that more people travel into Norman for gamedays than leave.

This study shows that using an hourly sampling method effectively shows the temporal variation in the SARS-CoV-2 concentration during large events. It also shows that by using the flow and population, a viral load per person can be calculated, which is a good way to normalize the concentration data. Furthermore, using mobile device counting technology such as StreetLight can be used to estimate the population for an entire sewershed.

CHAPTER 6

CLOSING THOUGHTS

Throughout this process, I learned many lessons about properly sampling wastewater for SARS-CoV-2. Compared to the first season, where autosamplers were set up the day of during a range of times, the 2021 season autosamplers were set up the day before and programmed to start at 8:00 am. This method, however, did cause problems. For the 2021 football season, there were many more errors related to the autosampler clogging from being in the sewage too long. This allowed for strainers to fill with toilet paper and other debris from the sewage. Another lesson learned in this process is better time management. To complete this paper, it was challenging to receive data in a timely from StreetLight, which slowed the process to complete this.

Event-based WBE is an important tool to help guide public health decisions. If I were to do this research again or continue it, there are a couple things I would do differently. One of the most important things I would change is that I would sample the wastewater that was leaving the football stadium and other hotspots in town, such as campus corner, which hosts thousands at its bars, restaurants, and shops every gameday, in conjunction to the municipal wastewater treatment plant to determine how much of the SARS-CoV-2 in the wastewater was directly related to the football game. This was not feasible for this project given personnel and funding limitations, though I believe it would improve the results of this study immeasurably.

Another very important thing I would like to do is get a more accurate count of the population in the sewershed at any given moment. Though we tried to account for the decrease in population throughout the 2020 football season, ultimately, there was too much noise in the data to come up with a dynamic baseline population. I think having a more accurate baseline would

be beneficial in determining the role that human movement plays in WBE. One way I think the accuracy of population data could be improved is by setting up nested layers of geofences to capture movement once people entered the sewershed. For instance, setting up another geofence around campus and campus corner, as well as one just capturing the football stadium could account better illustrate people's movement in relation to the football game. Again, this could not be accomplished for this analysis due to funding and personnel shortages. Despite the concerns about the accuracy for the data in this study, it is well within the margin of error, given the large population as well as the high concentration. If the population had not been so large, for instance if the population in the city were only 5,000, 1,000 people leaving the area could drastically impact the results.

Along with the one-time statewide survey, I have also managed the data for numerous other wastewater projects, including 14 manhole sites in the City of Oklahoma City, three manhole dynamic sites in the City of Tulsa, data from wastewater treatment plants across the state, as well as all the sampling we did on campus, which lasted nearly all the 2020-2021 school year during my time as a graduate student. I ran quality assurance analysis to make sure our equipment was performing properly. This included ensuring the autosamplers collected the programmed amount of liquid per sample, the flow measurement devices functioned properly, the autosampler was programmed to collect samples frequently enough that the composite sample was representative of the flow. I also managed the data to compare different experimental sampling methods, such as passive sampling. Throughout this process, I have learned to manage a small team of undergraduates to make sure we kept up to date on our duties, and many other lessons.

I know I will look back on this work fondly and with great pride because I believe this is a very important project. However, as of writing this now, I largely feel frustration. The frustration lies with every decision-maker who had access to the data we, and thousands of scientists and medical professionals, were generating and did not do anything to protect more people from this pandemic, be that the University, municipal governments, state governments, and even the federal government. I am the child of a medical professional – a nurse – who worked in hospitals throughout this pandemic and saw the strain it put on her and listened to her relay stories about what she and her coworkers faced every day. I believe wastewater-based epidemiology has proven itself as a very good way to monitor diseases and I can only hope that as a society, we have learned from these past few years and will be better prepared when the next pandemic occurs.

CHAPTER 7

REFERENCES

2020 Football Season. (n.d.). Retrieved from Soonerstats: http://soonerstats.com/football/seasons/schedule.cfm?seasonid=2020

2020 Game Day Policies & Procedures. (2020, September 3). Retrieved from soonersports.com.

Ahmed, W., Angel, N., Edson, J., Bibby, K., Bivins, A., O'Brien, J. W., . . . Hugenholtz, P. (2020). First confirmed detection of SARS-CoV-2 in untreated wastewater in Australia: A proof of concept for the wastewater surveillance of COVID- 19 in the community. *Science of the Total Environment, 728*.

Ai, Y., Davis, A., Jones, D., Lemeshow, S., Tu, H., He, F., . . . Lee, J. (2022). Wastewater-based epidemiology for tracking COVID-19 trend and variants of concern in Ohio, United States. *medRxiv*.

Albastaki, A., Naji, M., Lootah, R., Almeheiri, R., Almulla, H., Almarri, I., . . . Alghafri, R. (2021). First confirmed detection of SARS-COV-2 in untreated municipal and aircraft wastewater in Dubai, UAE: The use of wastewater based epidemiology as an early warning tool to monitor the prevalence of COVID-19. *Science of The Total Environment, 760*.

Barich, D., & Slonczewski, J. L. (2021, January). Wastewater Virus Detection Complements Clinical COVID-19 Testing to Limit Spread of Infection at Kenyon College. *medRxiv*.

Baz-Lomba, J., Di Ruscio, F., Amador, A., Reid, M., & Thomas, K. V. (2019). Assessing Alternative Population Size Proxies in a Wastewater Catchment Area Using Mobile Device Data. *Environmental Science and Technology, 53*(4), 1994-2001.

Benaglia, L., Udrisard, R., Bannwarth, A., Gibson, A., Been, F., Lai, F. Y., . . . Delemont, O. (2020, April). Testing wastewater from a music festival in Switzerland to assess illicit drug use. *Forensic Science International, 309*.

Betancourt, W. Q., Schmitz, B. W., Innes, G. K., Prasek, S. M., Progreba Brown, K. M., Stark, E. R., . . . Pepper, I. L. (2021). COVID-19 containment on a college campus via wastewater-based epidemiology, targeted clinical testing and an intervention. *Science of the Total Environment, 779*.

Bian, L., Gao, Q., Gao, F., Wang, Q., Wu , X., Mao, Q., . . . Liang, Z. (2021, September 9). Impact of the Delta variant on vaccine efficacy and response strategies. *Expert Reviews of Vaccines*.

Bill Information for SB 658. (2021). Retrieved from Oklahoma State Legislature: http://www.oklegislature.gov/BillInfo.aspx?Bill=sb658&Session=2100

Bivins, A., Lott, M., Shaffer, M., Wu, Z., North, D., Lipp, E. K., & Bibby, K. (2021, May 17). Building-level wastewater monitoring 1 for COVID-19 using tampon 2 swabs and RT-LAMP for rapid SARS-CoV-2 RNA detection. *Preprints.org*.

Bivins, A., North, D., Wu, Z., Schaffer, M., Ahmed, W., & Bibby, K. (2021, March 24). Within-Day Variability of SARS-CoV-2 RNA in Municipal Wastewater Influent During Periods of Varying COVID-19 Prevalence and Positivity. *medRxiv*.

Bliss, C., Musikanski, L., Phillips, R., & Davidson, L. (2020). When Will the Pandemic End? Suggestions for US Communities to Manage Well-Being in the Face of COVID-19. *International Journal of Community Well-Being*, 299-313.

Boogaerts, T., Covaci, A., Kinyua, J., Neels, H., & van Nuijs, A. L. (2016, March 1). Spatial and temporal trends in alcohol consumption in Belgian cities: A wastewater-based approach. *Drug and Alcohol Dependence, 160*, 170-176.

CDC. (2021, July 23). *Guidance for Institutions of Higher Education (IHEs)*. Retrieved from Centers for Disease Control and Prevention: https://www.cdc.gov/coronavirus/2019-ncov/community/colleges-universities/considerations.html

Cevik, M., Kuppalli, K., Kindrachuk, J., & Peiris, M. (2020, October 23). Virology, transmission, and pathogenesis of SARS-CoV-2. *BMJ, 371*.

Chaix, B. (2018). Mobile Sensing in Environmental Health and Neighborhood Research. *Annual Review of Public Health, 39*, 367-384.

Chakraborty, I., & Maity, P. (2020). COVID-19 outbreak: Migration, effects on society, global environment and prevention. *Science of the Total Environment, 728*.

Chen, C., Kostakis, C., Gerber, J. P., Tscharke, B. J., Irvine, R. J., & White, J. M. (2014). Towards finding a population biomarker for wastewater epidemiology studies. *Science of The Total Environment*.

Chen, Y., Chen, L., Deng, Q., Zhang, G., Wu, K., Ni, L., . . . Cheng, Z. (2020, April 3). The presence of SARS-CoV-2 RNA in the feces of COVID-19 patients. *Journal of Medical Virology, 92*(7), 833-840.

City of Norman, OK. (n.d.). *Water Reclamation* . Retrieved from City of Norman, OK: https://www.normanok.gov/your-government/departments/utilities/water-reclamation

Couture, V., Dingel, J. I., Green, A. E., Handbury, J., & Williams, K. R. (2020, July). MEASURING MOVEMENT AND SOCIAL CONTACT WITH SMARTPHONE DATA: A REAL-TIME APPLICATION TO COVID-19. *NBER Working Paper Series*.

Curtis, K., Keeling, D., Yetka, K., Larson, A., & Gonzalez, R. (2020). Wastewater SARS-CoV-2 Concentration and Loading Variablity from Grab and 24-Hour Composite Samples. *medRxiv*.

D'Aoust, P. M., Mercier, E., Montpetit, D., Jia, J.-J., Alexandrov, I., Neault, N., . . . MacKenzie, A. (2021). Quantitative analysis of SARS-CoV-2 RNA from wastewater solids in communities with low COVID-19 incidence and prevalence. *Water Research, 188*.

Devault, D. A., Peyre, A., Jaupitre, O., Daveluy, A., & Karolak, S. (2020). The effect of the Music Day event on community drug use Author links open overlay panel. *Forensic Science International, 309*, April.

Deville, P., Linard, C., Martin, S., Gilbert, M., Stevens, F. R., Gaughan, A. E., . . . Tatem, A. J. (2014, November 11). Dynamic population mapping using mobile phone data. *PNAS, 111*(45), 15888-15893.

Dix, B. (2020, May 27). *Sooners release statement conveying frustration on OU-Nebraska game.* Retrieved from Sooners Wire: https://soonerswire.usatoday.com/2021/05/27/oklahoma-sooners-nebraska-2021-matchup/

Dougherty, K., Mannell, M., Naqvi, O., Matson, D., & Stone, J. (2021, July). SARS-CoV-2 B.1.617.2 (Delta) Variant COVID-19 Outbreak Associated with a Gymnastics Facility — Oklahoma, April–May 2021. *Morbitity and Mortality Weekly Report, 70*(28), 1004-1007.

Egger, F., Faude, O., Schreiber, S., Gärtner, B. C., & Meyer, T. (2021, March 18). Does playing football (soccer) lead to SARS-CoV-2 transmission? - A case study of 3 matches with 18 infected football players. *Science and Medicine in Football*.

Engelbrecht, C. (2020, December 1). OU football: Lincoln Riley announces sooners will not hold senior day festivities due to COVID-19 precautions. *OU Daily*.

Farkas, K., Marshall, M., Cooper, D., McDonald, J. E., Malham, S. K., Peters, D. E., . . . Jones, D. L. (2018). Seasonal and diurnal surveillance of treated and untreated wastewater for human enteric viruses. *Environmental Science and Pollution Research*, 33391-33401.

Frye, L. (2020). *Measures to Ensure the Protection of Public Health in Response to COVID-19.* State of Oklahoma, Oklahoma State Department of Health and Public Health Advisory. Oklahoma State Department of Health.

Gibas, C., Lambirth, K., Mittal, N., Juel, M. A., Bharati Barua, V., Roppolo Brazell, L., . . . Chen, D. (2021). Implementing building-level SARS-CoV-2 wastewater surveillance on a university campus. *Science of the Total Environment, 782*.

Gonçalves, J., Koritnik, T., Mioč, V., Trkov, M., Bolješič, M., Berginc, N., . . . Paragi, M. (2021, February 10). Detection of SARS-CoV-2 RNA in hospital wastewater from a low COVID-19 disease prevalence area. *Science of The Total Environment, 755*.

Gonzalez, R., Curtis, K., Bivins, A., Bibby, K., Weir, M. H., Yetka, K., . . . Gonzalez, D. (2020). COVID-19 surveillance in Southeastern Virginia using wastewater-based epidemiology. *Water Research*.

Graham, K. E., Loeb, S. K., Wolfe, M. K., Catoe, D., Sinnot-Armstron, N., Kim, S., . . . Boe. (2021). SARS-CoV-2 RNA in Wastewater Settled Solids Is Associated with COVID-19 Cases in a Large Urban Sewershed. *Environmental Science & Technology, 55*(1), 488-498.

Greenwald, H. D., Kennedy, L. C., Hinkle, A., Whitney, O. N., Fan, V. B., Crits-Christoph, A., . . . Dow, J. (2021, August). Tools for interpretation of wastewater SARS-CoV-2 temporal and spatial trends demonstrated with data collected in the San Francisco Bay Area. *Water Research X, 12*.

Hata, A., Honda, R., Hara-Yamamura, H., & Meuchi, Y. (2020). Detection of SARS-CoV-2 in wastewater in Japan by multiple molecular assays-implication for wastewater-based epidemiology (WBE). *medRxiv*.

Hayes, E. K., Sweeney, C. L., Anderson, L. E., Li, B., Erjavec, G. B., Gouthro, M. T., . . . Gagnon, G. A. (2021, June 14). A novel passive sampling approach for SARS-CoV- 2 in wastewater in a Canadian province with low prevalence of COVID-19. *Environmental Science Water Research & Technology*.

Hayes, J. (2020, September 11). OU Chief COVID Officer Dr. Dale Bratzler gives updates on cases, warnings for game day. *OU Daily*.

Helsel, D. R. (2005). More Than Obvious: Better Methods for Interpreting Nondetect Data. *Environmental Science and Techonology*, 419A-423A.

Hemalatha, M., Kiran, U., Kuncha, S. K., Kopperi, H., Gokulan, C., Mohan, S., & Mishra, R. K. (2020). Comprehensive Surveillance of SARS-CoV-2 Spread Using Wastewater-based Epidemiology Studies. *medRxiv*.

Hewitt, J., Trowsdale, S., Armstrong, B. A., Chapman, J. R., Carter, K. M., Croucher, D. M., . . . Gilpin, B. J. (2022). Sensitivity of wastewater-based epidemiology for detection of SARS-CoV-2 RNA in a low prevalence setting. *Water Research*.

Honein, M. A., Christie, A., Rose, D. A., Brooks, J. T., Meaney-Delman, D., Cohn, A., . . . Kuhn. (2020, December 11). Summary of Guidance for Public Health Strategies to Address High Levels of Community Transmission of SARS-CoV-2 and Related Deaths, December 2020. *Morbidity and Mortality Weekly Report, 69*(49), 1860-1867.

Hoover, J. E. (2021, August 30). *Update: Oklahoma vs. Tulane Officially Moved to Norman.* Retrieved from FanNation All Sooners :

https://www.si.com/college/oklahoma/football/report-hurricane-ida-forces-oklahomas-opener-at-tulane-to-be-moved-to-norman
Hu, B., Guo, H., Zhou, P., & Shi, Z.-L. (2020, October). Characteristics of SARS- CoV-2 and COVID-19. *Nature Reviews Microbiology*.
Hu, B., Guo, H., Zhou, P., & Shi, Z.-L. (2020, October 6). Characteristics of SARS-CoV-2 and COVID-19. *Nature Reviews Microbiology*.
Izquierdo-Lara, R., Elsinga, G., Heijnen, L., Oude Munnink, B. B., Schapendonk, C. M., Nieuwenhuijse, D., . . . de Graaf, M. (2021). Monitoring SARS-CoV-2 Circulation and Diversity through Community Wastewater Sequencing, the Netherlands and Belgium. *Emerging Infectious Diseases*, 1405-1415.
Jones, B., Phillips, G., Kemp, S., Payne, B., Hart, B., Cross, M., & Stokes, K. A. (2021, February 11). *British Journal of Sports Medicine*.
Kitajima, M., Ahmed, W., Bibby, K., Carducci, A., Gerba, C. P., Hamilton, K. A., . . . Rose, J. B. (2020, April). SARS-CoV-2 in wastewater: State of the knowledge and research needs. *Science of the Total Environment, 739*.
Krizman, I., Senta, I., Ahel, M., & Terzic, S. (2016, October 1). Wastewater-based assessment of regional and temporal consumption patterns of illicit drugs and therapeutic opioids in Croatia. *Science of the Total Environment, 566-567*, 454-462.
Kuhn, K. G., Jarshaw, J., Jefferies, E., Adesigbin, K., Maytubby, P., Dundas, N., . . . Reeves, H. (2022, March 15). Predicting COVID-19 cases in diverse population groups using SARS-CoV-2 wastewater monitoring across Oklahoma City. *Science of The Total Environment, 812*.
Kyncl, J. (2020, September 5). Members of OU Greek life 'embarrassed' by disregard for COVID-19 safety protocols. *OU Daily*.
Lauer, S. A., Grantz, K. H., Bi, Q., Jones, F. K., Zheng, Q., Meredith, H. R., . . . Lessler, J. (2020, May 5). The Incubation Period of Coronavirus Disease 2019 (COVID-19) From Publicly Reported Confirmed Cases: Estimation and Application. *Annals of Internal Medicine*.
Lazuka, A., Arnal, C., Soyeux, E., Sampson, M., Lepeuple, A.-S., Deleuze, Y., . . . Lacroix, S. (2021). COVID-19 wastewater based epidemiology: long-term monitoring of 10 WWTP in France reveals the importance of the sampling context. *Water Sciene & Technology*.
Lee, W. K., Sohn, S., & Heo, J. (2018, March). Utilizing mobile phone-based floating population data to measure the spatial accessibility to public transit. *Applied Geography, 92*, 123-130.
Leidman, E., Duca, L. M., Omura, J. D., Proia, K., Stephens, J. W., & Sauber-Schatz, E. K. (2021, January 13). COVID-19 Trends Among Persons Aged 0–24 Years — United States, March 1–December 12, 2020. *Morbiditiy and Mortality Weekly Report, 70*.
Leidner, A. J., Barry, V., Bowen, V. B., Silver, R., Musial, T., Kang, G. J., . . . Pevzner, E. (2021, January 8). Opening of Large Institutions of Higher Education and County-Level COVID-19 Incidence — United States, July 6–September 17, 2020. *Morbidity and Mortality Weekly Report, 70*(1), 14-19.
Lemas, D. J., Loop, M. S., Duong, M., Schleffer, A., Collins, C., Bowden, J. A., . . . Delcher, C. (2021, April 10). Estimating drug consumption during a college sporting event from wastewater using liquid chromatography mass spectrometry. *Science of the Total Environment, 764*.

Liu, Y., & Rocklöv, J. (2021). The reproductive number of the Delta variant of SARS-CoV-2 is far higher compared to the ancestral SARS-CoV-2 virus. *Journal of Travel Medicine*.

Lu, D., Huang, Z., Zhang, X. (., & Sha, S. (2020). Primary concentration – The critical step in implementing the wastewater based epidemiology for the COVID-19 pandemic: A mini-review. *Science of the Total Environment, 747*.

Mahase, E. (2021). Delta variant: What is happening with transmission, hospital admissions, and restrictions? *BMJ, 373*.

McCourry, C. (2020, November 14). OU football: Sooners' Bedlam match to host College GameDay. *OU Daily*.

McCourry, C. (2020, September 13). 'We need to do better': Sooners' Athletics Director Joe Castiglione responds to game day COVID-19 precautions being ignored. *OU Daily*.

Mehta, S. H., Clipman, S. J., Wesolowski, A., & Solomon, S. S. (2021, August 30). Holiday gatherings, mobility and SARS-CoV-2 transmission: results from 10 US states following Thanksgiving. *Scientific Reports, 11*.

Miura, F., Kitajima, M., & Omori, R. (2021, January 4). Duration of SARS-CoV-2 viral shedding in faeces as a parameter for wastewater-based epidemiology: Re-analysis of patient data using a shedding dynamics model. *Science of the Total Environment, 769*.

Montgomery, A. B., O'Rourke, C. E., & Subedi, B. (2021). Basketball and drugs:Wastewater-based epidemiological estimation of discharged drugs during basketball games in Kentucky. *Science of the Total Environment, 752*.

Monz, C., Mitrovich, M., D'Antonio, A., & Sisneros-Kidd, A. (2019). Using Mobile Device Data to Estimate Visitation in Parks and Protected Areas: An Example from the Nature Reserve of Orange County, California. *Journal of Park and Recreation Administration*.

Nelson, E. D., Do, H., Lewis, R. S., & Carr, S. A. (2010, December 28). Diurnal Variability of Pharmaceutical, Personal Care Product, Estrogen and Alklphenol Concentrations in Effluent from a Tertiary Wastewater Treatment Facility. *Environmental Science and Technology, 45*.

Notari, A. (2021, April 1). Temperature dependence of COVID-19 transmission. *Science of the Total Environment, 763*.

Oklahoma State Department of Health. (2021, October 15). *OSDH Weekly Briefing Recap*. Retrieved from Oklahoma State Department of Health: https://oklahoma.gov/covid19/newsroom/2021/october/osdh-weekly-briefing-recap01.html

OU Announces Calendar Updates to Fall, Spring Semesters . (2020, October 6). Retrieved from University of Oklahoma: https://www.ou.edu/web/news_events/articles/news_2020/ou-announces-calendar-updates-to-fall-spring-semesters

OU Announces Return of Tailgating and Other Game Day Activities for 2021 Football Season. (2021, August 31). Retrieved from The University of Oklahoma: https://www.ou.edu/web/news_events/articles/news_2021/ou-announces-return-of-tailgating-and-other-game-day-activities-for-2021-football-season

Oxford Learner's Dictionaries. (n.d.). *Bedlam*. Retrieved from Oxford Learner's Dictionaries: https://www.oxfordlearnersdictionaries.com/us/definition/english/bedlam?q=bedlam

Pillay, L., Amoah, I. D., Deepnarain, N., Pillay, K., Awolusi, O., Kumari, S., & Bux, F. (2021). Monitoring changes in COVID-19 infection using wastewater-based epidemiology: A South African Perspective. *Science of The Total Environment*.

Polo, D., Quintela-Baluja, M., Corbishley, A., Jones, D. L., Singer, A. C., Graham, D. W., & Romalde, J. L. (2020). Making waves: Wastewater-based epidemiology for COVID-19 – approaches and challenges for surveillance and prediction. *Water Research, 186*.

Prado, T., Machado Fumian, T., Ferreira Mannarino, C., Resende, P. C., Couto Motta, F., Fontes Eppinghaus, A. L., . . . Mar, G. (2021). Wastewater-based epidemiology as a useful tool to track SARS-CoV-2 and support public health policies at municipal level in Brazil. *Water Research*.

Pullen, M. F., Skipper, C. P., Hullsiek, K. H., Bangdiwala, A. S., Pastick, K. A., Okafor, E. C., . . . Boulware, D. R. (2020, July). Symptoms of COVID-19 Outpatients in the United States. *Open Forum Infectious Diseases*.

Radu, E., Masseron, A., Amman, F., Schedl, A., Agerer, B., Endler, L., . . . Kreuzinger, N. (2022). Emergence of SARS-CoV-2 Alpha lineage and its correlation with quantitative wastewater-based epidemiology data. *Water Research*.

Reeves, K., Leibig, J., Fuela, A., Saldi, T., Lasda, E., Johnson, W., . . . Heuer, H. (2021, May 26). High-resolution within-sewer SARS-CoV-2 surveillance facilitates informed intervention. *medRxiv*.

Salgueiro-Gonzalez, N., Rousis, N. I., Gracia-Lor, E., Borsotti, A., Zuccato, E., & Castiglioni, S. (2021, July 1). First comprehensive study of alcohol consumption in Italy using wastewater-based epidemiology. *Science of the Total Environment, 776*.

Sassano, M., McKee, M., Ricciardi, W., & Boccia, S. (2020, May 29). Transmission of SARS-CoV-2 and Other Infections at Large Sports Gatherings: A Surprising Gap in Our Knowledge. *Frontiers in Medicine*.

Schang, C., Crosbie, N. D., Nolan, M., Poon, R., Wang, M., Jex, A., . . . Kolotelo, P. (2021). Passive Sampling of SARS-CoV-2 for Wastewater Surveillance. *Environmental Science & Technology, 55*, 10432-10441.

Schmitz, B. W., Innes, G. K., Prasek, S. M., Betancourt, W. Q., Stark, E. R., Foster, A. R., . . . Pepper, I. L. (2021, December 20). Enumerating asymptomatic COVID-19 cases and estimating SARS-CoV-2 fecal shedding rates via wastewater-based epidemiology. *Science of The Total Environment, 801*.

Scott, L. C., Aubee, A., Babahaji, L., Vigil, K., Tims, S., & Aw, T. (2021). Targeted wastewater surveillance of SARS-CoV-2 on a university campus for COVID-19 outbreak detection and mitigation. *Environmental Research, 200*.

Siegel, D. A., Reses, H. E., Cool, A. J., Shapiro, C. N., Hsu, J., Boehmer, T. K., . . . Adj. (2021, September 10). Trends in COVID-19 Cases, Emergency Department Visits, and Hospital Admissions Among Children and Adolescents Aged 0–17 Years — United States, August 2020–August 2021. *Morbidity and Mortality Weekly Report, 70*(36), 1249-1254.

Siegel, M., Kloppenburg, B., Woerle, S., Sjoblom, S., & Danyluk, G. (2021, March 19). Notes from the Field: SARS-CoV-2 Transmission Associated with High School Football Team Members — Florida, September–October 2020. *Morbidity and Mortality Weekly Report, 70*(11), 402-404.

Silverman, A. I., & Boehm, A. B. (2020). Systematic Review and Meta-Analysis of the Persistence and Disinfection of Human Coronaviruses and Their Viral Surrogates in Water and Wastewater. *Environmental Science and Technology Letters, 7*, 544-553.

State of Oklahoma Department of Health. (n.d.). *Oklahoma COVID-19 Risk Level*. Retrieved from Oklahoma State Department of Health: https://oklahoma.gov/covid19/covid-19-alert-system.html

StreetLight. (2020, July). Our Methodology and Data Sources.
Sunjaya, A. P., & Jenkins, C. (2020, April 30). Rationale for universal face masks in public against COVID-19. *Respirology*.
Symonds, E. M., Rosario, K., & Breitbart, M. (2019, April 18). Pepper mild mottle virus: Agricultural menace turned effective tool for microbial water quality monitoring and assessing (waste) water treatment technologies. *PLoS Pathog, 15*(4).
Tao, K., Tzou, P. L., Nouhin, J., Gupta, R. K., de Oliveira, T., Kosakovsky Pond, S. L., . . . Shafer, R. W. (2021, September 17). The biological and clinical significance of emerging SARS-CoV-2 variants. *Nature Reviews Genetics, 22*, 757-773.
Tarkar, P. (2020). Impact Of Covid-19 Pandemic On Education System. *Impact Of Covid-19 Pandemic On Education System, 29*(9), 3812-3814.
The Lancet Microbe. (2021). COVID-19 vaccines: the pandemic will not end overnight. *Elsevier Public Health Emergency Collection*.
Thomas, K. V., Amador, A., Baz-Lomba, J., & Reid, M. (2017). Use of Mobile Device Data To Better Estimate Dynamic Population Size for Wastewater-Based Epidemiology. *Environmental Science and Technology, 51*(19), 11363-11370.
Tizzoni, M., Bajardi, P., Decuyper, A., Kon Kam King, G., Schneider, C. M., Blondel, V., . . . Colizza, V. (2014). On the Use of Human Mobility Proxies for Modeling Epidemics. *Computational Biology, 10*(7).
Travis, S. A., Best, A. A., Bochniak, K. S., Dunteman, N. D., Fellinger, J., Folkert, P. D., . . . Schuitema, A. J. (2021, March). Providing a safe, in-person, residential college experience d uring the C OVID-19 p andemic. *medRxiv*.
US Census Bureau. (2020, June 18). *Ensuring an Accurate Count of College Students and Towns in the 2020 Census*. Retrieved from United States Census Bureau: https://www.census.gov/newsroom/press-releases/2020/2020-college-students.html
Walke, H. T., Honein, M. A., & Redfield, R. R. (2020, September 29). Preventing and Responding to COVID-19 on College Campuses. *JAMA, 324*(17), 1727-1728.
Whitney, O. N., Kennedy, L. C., Fan, V. B., Hinkle, A., Kantor, R., Greenwald, H., . . . Nelson, K. L. (2021). Sewage, Salt, Silica, and SARS-CoV-2 (4S): An Economical Kit-Free Method for Direct Capture of SARS-CoV-2 RNA from Wastewater. *Environmental Science & Technology*, 4880-4888.
World Health Organizaton. (2021, December 9). *WHO Coronavirus (COVID-19) Dashboard*. Retrieved from World Health Organization: https://covid19.who.int/
Wu, F., Zhang, J., Xiao, A., Xiaoqiong, G., Lee, W. L., Armas, F., . . . Erickson, T. B. (2020, July 21). SARS-CoV-2 Titers in Wastewater Are Higher than Expected from Clinically Confirmed Cases. *mSystems*.
Xu, X., Zheng, X., Li, S., Sze Lam, N., Wang, Y., Chu, D. K., . . . Zhang, T. (2021). The first case study of wastewater-based epidemiology of COVID-19 in Hong Kong. *Science of The Total Environment*.
Yan, T., O'Brien, P., Shelton, J. M., Whelen, A. C., & Pagaling, E. (2018). Municipal Wastewater as a Microbial Surveillance Platform for Enteric Diseases: A Case Study for Salmonella and Salmonellosis. *Environmental Science and Technology, 52*, 4869-4877.
Young, M. (2021, August 13). OU football: Tulane requiring vaccination proof or negative COVID-19 test for attendees of September 4 opener vs Sooners. *OU Daily*.
Yu, X., & Yang, R. (2020, July 14). COVID-19 transmission through asymptomatic carriers is a challenge to containment. *Influenza and Other Respiratory VIruses, 14*(4), 474--475.

Yu, Y., Liu, Y.-R., Luo, F.-M., Tu, W.-W., Zhan, D.-C., Yu, G., & Zhou, Z.-H. (2020). COVID-19 Asymptomatic Infection Estimation. *medRxiv*.

Zhang, X., Huang, R., Li, P., Ren, Y., Gao, J., Mueller, J. F., & Thai, P. K. (2019). Temporal profile of illicit drug consumption in Guangzhou, China monitored by wastewater-based epidemiology. *Environmental Science and Pollution Research, 26*.

Zhang, Y., Cen, M., Hu, M., Du, L., Hu, W., Kim, J. J., & Dai, N. (2021, April). Prevalence and Persistent Shedding of Fecal SARS-CoV-2 RNA in Patients With COVID-19 Infection: A Systematic Review and Meta-analysis. *Clinical and Translational Gastroenterology, 12*(4).

APPENDICES

A. Appendix A – Flow

Table A - 1: Raw flow data for all sampling days in the 2020 and 2021 football seasons at 15-minute time intervals.

Approximate Time	Missouri State	Kansas	Control (2020)	Oklahoma State	Baylor	Tulane	Western Carolina	Nebraska	West Virginia	Texas Christian	Control (2021)	Iowa State
7:00						9.28	9.75	14.08	10.68	9.90	10.06	7.74
7:15						7.43	9.13	12.07	8.97	10.52	9.90	9.44
7:30						8.82	9.90	11.45	8.82	10.37	9.44	10.52
7:45						10.06	9.13	12.53	10.52	9.59	8.97	8.66
8:00	12.82	13.75	12.26	12.63	12.26	12.53	9.75	11.60	7.43	8.66	9.28	8.82
8:15	12.63	11.89	12.45	10.40	13.38	10.99	9.90	12.69	7.58	8.82	10.06	8.82
8:30	14.31	12.45	13.56	12.45	12.63	9.75	9.90	12.07	8.51	9.28	10.06	10.06
8:45	14.49	14.31	11.15	14.12	12.82	11.14	10.37	12.53	10.52	9.44	9.44	9.90
9:00	15.24	14.49	11.89	12.26	14.12	11.14	10.37	12.69	11.91	13.31	10.68	9.44
9:15	15.24	15.98	12.26	12.08	14.12	10.83	8.97	12.22	10.68	12.53	12.22	11.45
9:30	14.31	15.61	13.75	14.12	14.31	11.45	7.58	11.91	11.91	13.00	10.21	10.52
9:45	15.61	14.12	14.68	12.63	15.98	13.15	10.99	14.39	11.45	11.45	9.75	9.59
10:00	15.98	17.09	14.68	14.86	16.91	10.06	10.68	9.13	12.84	11.76	12.69	13.93
10:15	19.14	19.32	11.15	15.61	16.54	12.07	8.36	8.36	12.53	14.85	12.07	10.52
10:30	15.24	18.39	15.79	16.91	18.21	11.29	12.84	7.89	10.83	14.23	14.08	15.32
10:45	18.95	20.62	18.21	16.35	19.32	15.47	16.86	17.64	13.93	14.85	13.62	15.47
11:00	16.91	19.88	18.02	16.54	19.88	16.09	14.85	14.08	10.99	16.71	12.69	16.40
11:15	21.74	20.81	17.28	19.51	21.92	10.21	10.52	10.68	16.56	16.71	10.68	9.75
11:30	23.41	23.41	19.32	18.95	23.23	17.02	19.34	18.72	14.85	19.96	18.72	19.03
11:45	22.11	22.48	21.00	16.72	23.60	21.66	15.01	21.97	18.41	16.40	11.14	21.20
12:00	25.08	23.23	21.92	22.67	23.78	20.89	21.04	19.50	16.71	21.04	8.66	8.51

12:15	26.20	25.83	21.00	22.30	25.08	20.27	21.35	17.02	12.22	21.97	13.15	23.98
12:30	25.45	25.45	23.41	23.04	26.01	20.11	18.26	21.20	21.51	19.80	24.29	24.45
12:45	26.76	26.01	23.97	23.60	25.83	18.72	22.13	21.04	22.90	24.45	21.04	23.98
13:00	27.87	27.68	24.34	26.38	27.68	19.96	21.97	19.80	22.13	23.67	22.13	32.03
13:15	28.24	26.20	24.15	26.01	25.27	20.42	20.58	16.25	22.90	20.42	21.97	15.63
13:30	28.43	26.20	24.34	26.20	25.83	15.78	16.25	19.19	21.97	24.14	22.90	24.60
13:45	26.76	27.87	25.27	25.08	25.08	21.20	23.05	21.51	19.50	24.14	16.56	24.91
14:00	28.06	26.20	25.27	26.57	25.83	24.45	18.72	23.36	21.35	19.34	21.51	23.67
14:15	27.68	27.68	25.83	25.27	26.38	25.37	18.72	23.36	21.82	18.88	23.52	22.74
14:30	29.36	27.50	25.64	26.76	25.64	23.98	13.77	23.98	23.52	23.52	22.74	19.03
14:45	27.50	25.83	24.15	25.27	24.71	22.43	21.97	23.21	21.20	24.29	22.59	21.20
15:00	27.31	25.45	25.64	25.45	24.71	21.20	23.05	22.28	21.82	21.51	21.51	20.89
15:15	29.17	26.76	25.45	25.27	24.53	21.51	23.36	16.09	21.35	23.05	21.04	17.79
15:30	27.13	25.08	24.34	25.08	25.27	22.28	16.40	19.19	21.20	20.58	21.51	18.88
15:45	25.64	23.97	23.97	24.53	24.34	21.82	22.90	17.48	21.51	21.97	21.97	21.66
16:00	26.94	24.34	23.97	24.71	23.41	22.13	19.19	14.08	19.50	11.14	18.10	20.27
16:15	26.76	18.77	23.78	25.45	24.15	19.96	22.90	21.82	21.35	22.74	16.56	19.80
16:30	26.38	24.34	23.60	26.38	23.60	19.34	22.43	12.84	15.63	24.76	14.70	16.86
16:45	26.01	23.97	23.23	21.00	23.23	17.48	18.57	21.35	23.36	24.14	21.35	19.03
17:00	25.45	23.41	23.04	25.08	23.78	21.35	20.27	21.04	16.56	23.36	20.58	18.72
17:15	25.08	23.41	22.48	24.90	22.67	21.66	21.66	19.65	19.03	18.41	22.28	18.72
17:30	25.27	23.60	23.41	24.34	18.77	21.66	22.43	21.04	22.13	22.90	21.66	18.10
17:45	25.64	23.60	22.85	24.34	23.97	21.51	22.74	21.66	17.64	14.08	19.50	18.41
18:00	25.83	23.97	22.48	22.11	22.48	12.38	23.67	18.10	22.28	17.95	19.03	17.95
18:15	25.45	23.41	22.48	24.15	22.85	22.59	23.36	16.56	19.50	22.13	13.31	18.57
18:30	25.08	23.23	18.95	22.11	23.78	21.04	23.67	20.58	23.05	19.03	8.20	18.26
18:45	25.64	22.67	22.48	18.21	20.44	21.66	23.98	19.50	23.36	23.52	14.23	18.26
19:00	25.27	17.28	22.11	19.14	23.97	22.13	22.90	11.76	20.89	23.21	12.69	17.79

19:15	25.45	23.41	22.30	23.97	23.23	23.52	19.19	18.10	20.42	21.66	13.46	17.48
19:30	24.53	23.23	17.84	23.41	21.74	22.43	12.07	13.31	15.16	17.64	11.91	15.63
19:45	24.53	18.02	21.92	23.97	23.04	21.97	21.66	19.65	20.89	21.04	21.20	16.56
20:00	23.60	24.15	22.11	21.55	23.04	22.13	21.04	9.28	20.42	20.27	14.70	18.26
20:15	23.78	24.15	22.30	23.23	23.23	22.13	19.96	17.48	15.47	22.13	20.73	18.72
20:30	21.00	24.15	21.55	22.48	22.67	20.73	22.28	20.89	20.42	19.80	22.28	18.26
20:45	24.71	20.07	21.92	19.69	22.48	21.51	19.19	16.86	20.58	20.42	22.28	17.33
21:00	25.08	23.78	20.44	19.32	21.37	21.97	19.80	20.27	20.42	21.20	21.82	18.57
21:15	25.08	16.35	20.44	23.04	21.00	22.13	20.73	16.86	19.50	20.89	21.97	17.64
21:30	23.78	21.55	20.62	22.85	22.67	22.43	21.04	8.66	20.27	14.70	21.35	17.79
21:45	21.92	24.34	21.18	23.04	18.95	21.97	19.96	21.51	20.42	20.27	19.96	17.48
22:00	24.53	17.65	19.69	18.58	18.39	20.73	21.04	17.64	19.19	20.58	18.57	17.64
22:15	25.45	24.34	23.78	21.00	21.74	20.58	16.25	20.42	12.07	19.34	17.95	17.17
22:30	25.27	23.23	24.15	22.67	16.54	21.66	21.04	10.52	20.89	14.39	17.33	17.02
22:45	17.28	21.37	21.92	23.41	16.54	21.82	19.65	13.31	21.35	15.47	12.53	16.40
23:00	24.90	23.97	19.32	24.34	14.68	22.74	20.58	21.04	18.57	17.95	20.42	17.02
23:15	24.34	23.60	22.11	16.54	21.55	22.13	13.93	9.13	18.88	12.84	20.11	17.02
23:30	24.90	17.47	21.92	21.74	19.69	22.13	21.04	12.38	6.96	19.19	20.42	17.17
23:45	24.34	18.95	20.62	19.51	18.95	19.34	14.08	11.91	20.58	19.19	21.35	14.85
0:00	24.15	23.41	18.58	21.00	18.58	22.28	12.22	12.22	13.77	21.04	16.71	15.47
0:15	24.71	21.92	19.69	21.74	21.37	21.82	12.84	22.13	14.39	19.80	11.14	18.41
0:30	23.23	15.61	18.39	21.55	13.19	21.51	7.43	21.20	8.05	19.80	9.90	16.86
0:45	24.53	23.23	21.00	20.62	20.25	17.02	7.74	10.68	13.31	7.27	20.11	16.56
1:00	24.15	14.49	20.25	20.07	20.07	10.37	20.58	20.42	8.97	19.50	20.73	16.09
1:15	23.78	15.98	16.35	18.21	14.12	11.45	20.73	7.12	10.21	13.93	14.23	15.47
1:30	23.78	22.85	19.88	21.55	19.69	20.89	21.51	20.11	10.99	15.16	12.22	14.85
1:45	20.81	22.11	15.79	15.24	20.25	19.03	18.41	23.05	19.80	11.29	18.26	14.54
2:00	22.85	15.61	19.32	20.62	20.25	18.41	18.72	21.20	15.63	20.27	17.33	14.39

2:15	23.04	20.44	15.24	20.81	18.39	19.34	15.63	21.04	12.38	20.58	16.09	13.77
2:30	22.30	13.38	13.56	20.25	17.09	8.82	14.39	19.65	20.42	19.65	9.59	13.62
2:45	19.32	13.56	12.45	19.14	16.72	19.03	9.28	18.88	17.33	8.51	14.54	13.15
3:00	17.28	20.07	17.84	15.98	15.61	16.40	19.03	14.23	17.17	5.88	15.16	12.69
3:15	13.56	17.84	17.65	19.14	14.68	8.51	18.26	16.86	15.78	19.03	10.68	12.53
3:30	15.24	14.49	16.72	18.77	14.86	15.47	12.22	10.37	17.02	10.83	14.23	11.91
3:45	20.62	15.79	16.91	16.91	14.49	16.56	10.52	14.08	13.31	16.56	13.46	10.06
4:00	17.84	12.63	12.08	16.91	11.52	12.69	15.94	12.84	15.94	16.09	12.53	9.59
4:15	13.94	12.45	13.75	15.61	13.75	15.16	12.69	11.60	12.38	15.63	9.90	9.75
4:30	15.98	14.86	13.56	15.05	13.19	14.70	12.38	12.07	11.45	10.37	12.22	11.60
4:45	15.42	14.68	15.24	15.05	12.63	13.62	10.21	11.45	13.31	16.09	10.06	11.60
5:00	15.42	11.15	13.56	15.42	12.08	11.29	11.45	11.14	11.29	13.00	11.45	10.37
5:15	12.45	13.38	12.82	17.47	12.08	6.19	13.15	11.60	8.66	10.06	10.06	10.37
5:30	14.68	13.01	12.45	10.96	13.19	6.03	12.53	12.53	12.22	12.38	9.75	8.82
5:45	15.98	10.78	10.40	16.54	11.71	11.45	11.45	8.82	11.76	12.38	9.90	8.51
6:00	11.89	12.08	11.52	15.79	11.52	12.22	10.83	9.44	11.29	11.91	10.37	8.51
6:15	11.33	12.82	13.38	15.79	10.59	11.14	10.83	9.13	9.90	11.60	9.44	9.28
6:30	10.96	10.40	9.66	17.65	12.82	11.29	10.52	10.21	8.51	8.05	7.74	9.44
6:45	14.68	14.31	10.78	15.79	11.15	11.29	9.44	10.06	8.97	9.28	7.89	8.82
7:00	12.63	12.45	11.52	16.16	10.96							
7:15	10.03	10.03	10.78	17.84	10.96							
7:30	12.45	11.15	10.78	16.54	12.45							
7:45	11.33	13.01	10.03	17.09	11.15							
8:00	14.49	10.22	10.40	17.84	11.33							

B. Appendix B – Population

Table B - 1: Raw population data for all sampling days in the 2020 and 2021 seasons at the hourly time interval.

Time	Missouri State	Kansas	Control (2020)	Oklahoma State	Baylor	Tulane	Western Carolina	Nebraska	West Virginia	Texas Christian	Control (2021)	Iowa State
7:00						90,117		92,560	88,894	88,560	88,112	89,579
8:00	83,792	83,414	81,829	83,319	82,666	90,076	89,219	99,154	87,481	87,539	88,053	92,171
9:00	82,342	82,911	80,505	82,230	81,644	90,345	87,361	110,986	84,982	85,700	87,374	99,558
10:00	82,323	82,692	78,942	82,239	81,095	93,796	87,348	129,267	84,702	84,353	87,340	106,483
11:00	82,126	82,402	78,871	82,041	80,935	100,183	86,543	133,191	84,800	83,449	88,236	93,154
12:00	83,637	84,892	78,857	81,857	81,249	101,829	88,039	131,529	88,315	85,007	87,304	87,234
13:00	85,404	87,063	78,287	82,609	82,369	99,763	91,705	125,013	92,667	87,982	87,658	82,097
14:00	85,641	93,907	78,120	82,091	83,467	96,818	94,765	94,425	98,322	92,198	86,662	61,241
15:00	85,837	93,227	77,572	84,695	83,591	84,674	100,179	83,539	105,891	100,101	87,833	78,671
16:00	88.,144	88,781	75,768	88,205	83,165	81,131	110,862	78,464	116,376	111,599	86,454	83,215
17:00	96,694	83,210	76,650	90,999	84,019	78,940	126,932	75,316	125,788	123,573	87,903	85,182
18:00	98,970	78,098	76,844	98,006	90,875	78,511	130,532	72,565	135,449	131,328	89,159	86,626
19:00	96,980	78,921	76,836	99,515	92,957	79,127	123,036	71,730	133,990	131,667	86,894	88,279
20:00	89,947	77,654	77,043	98,459	92,148	78,146	103,147	71,408	130,706	128,462	86,662	88,043
21:00	83,933	78,222	77,328	91,689	90,416	77,851	82,646	72,737	117,492	115,058	87,416	88,204
22:00	85,198	79,009	78,015	80,683	79,230	78,680	82,105	73,906	85,785	85,666	89,362	89,903
23:00	86,149	79,626	78,523	82,512	82,098	79,827	82,178	75,736	82,702	82,961	89,302	88,725
0:00	86,699	80,070	79,099	82,957	82,750	80,974	84,552	78,576	87,688	87,727	88,463	89,034
1:00	87,167	80,440	79,495	82,831	83,224	82,447	84,783	78,717	87,812	87,900	88,237	88,039
2:00	87,697	80,918	79,610	83,202	83,349	82,524	83,784	77,785	86,910	87,055	88,533	88,654
3:00	87,662	81,064	79,715	83,331	83,309	82,228	84,256	78,125	87,066	87,340	87,865	87,555
4:00	87,858	81,236	79,777	83,393	83,443	82,286	84,151	78,123	86,928	87,276	87,797	87,708
5:00	87,738	80,800	79,443	83,137	83,152	82,456	83,826	77,743	86,754	86,961	87,608	87,381

6:00	87,372	80,364	79,124	82,963	82,751	82,113	83,556	77,250	86,390	86,784	87,973	87,378
7:00	86,807	80,502	79,356	82,703	82,528		83,365		86,047	86,612	87,827	87,380
8:00	85,326	79,382	79,108	81,711	81,811		82,370		84,606	85,677		86,797

C. Appendix C – Concentration

Table C- 1: Raw SARS-CoV-2 concentration data for all sampling days in the 2020 and 2021 seasons at hourly time intervals.

Time	Missouri State	Kansas	Control (2020)	Oklahoma State	Baylor	Tulane	Western Carolina	Nebraska	West Virginia	Texas Christian	Control (2021)	Iowa State
7:00						918,963		37,817		20,620		
8:00		109,299	53,742	103,458	360,228	1,035,484	1,089,938	177,656	2,795,128	19,685		
9:00		233,693	193,518	85,993	1,508,186	723,495	1,488,757	116,344	1,150,039	99,419		158,840
10:00	81,089	22,396	78,942	96,900	757,831	1,886,427	1,127,511	39,683	738,809	109,941	104,826	28,331
11:00	54,321	41,151	141,543	139,192	556,710	1,451,971	1,305,107	67,848	214,778	123,078	154,048	180,042
12:00	103,019	119,328	79,792	198,232	397,785	1,330,082	935,652	131,467	1,709,780	141,171	179,950	114,639
13:00	169,275	45,148	101,216	52,819	740,820	1,295,057	840,103	1,214,405	844,130	38,186	243,855	128,583
14:00	133,486	62,223	43,568	274,928	432,292	958,157	306,952	71,154	401,452	87,373	91,107	305,112
15:00	170,466	62,238	34,313	379,258	197,504	2,153,799	354,333	70,508	305,112	27,928	31,816	354,685
16:00	157,899	19,234	89,667	547,512	318,692	1,275,597	1,421,955	304,121	557,451	133,390	102,496	733,188
17:00	65,381	07,764	80,975	586,028	159,197	2,155,632	987,710	116,337	508,982	34,283	108,063	945,858
18:00	201,261	77,383	42,979	386,236	416,187	2,919,892	1,488,757	143,052	1,333,563	70,548	127,295	754,422
19:00	247,226	72,033	141,955	371,641	1,237,232	972,815		140,276	629,579	44,736	201,866	791,642
20:00	35,561	135,461	79,875	130,770	673,798	4,082,901		172,532	1,408,659	16,445	46,664	38,127
21:00	01,401	73,708	106,293	191,698	580,423	2,294,790		193,261	597,121	69,223	53,269	54,957
22:00	00,222	85,472	101,869	94,572	870,388	2,016,993		36,460	804,045	133,916	08,874	66,194
23:00	32,481	63,790	82,271	47,992	556,303	2,305,200		453,857	1,499,236	184,751	65,454	16,156
0:00		101,850	179,853	10,301	545,717	2,888,333		141,033	717,111	33,154	109,495	30,766
1:00		55,627	143,316	38,534	671,988	691,951		242,795	677,035	56,448		176,832
2:00		157,649	472,912	37,658	358,077	1,008,322		130,185	761,209			203,770
3:00		192,565	127,748	112,750	215,660	449,271		200,196	1,073,404			641,341
4:00		129,545	159,018	66,214	376,384	753,068		232,423	591,991			453,665

5:00		249,723	216,407	66,114	573,912	1,370,954		116,634	446,788			206,639
6:00		154,427	181,387	63,115	468,614	627,621		215,113	564,636			1,367,803
7:00		181,111	118,097	62,363	571,802			171,214	184,423			430,505
8:00								303,139				

D. Appendix D – Viral Load per Person

Table D- 1: Raw SARS-CoV-2 viral load per person data for all sampling days in the 2020 and 2021 seasons at hourly time intervals.

Time	Missouri State	Kansas	Control (2020)	Oklahoma State	Baylor	Tulane	Western Carolina	Nebraska	West Virginia	Texas Christian	Control (2021)	Iowa State
7:00						9,651,460		586,491		235,058		
8:00		1,680,941	53,742	1,504,693	5,401,582	14,688,245	12,140,472	2,119,740	24,192,452	198,646		
9:00		4,108,486	193,518	1,291,854	24,258,727	9,095,251	18,010,740	1,355,936	16,437,161	1,573,764		1,711,364
10:00	1,452,167	491,781	78,942	1,792,949	14,111,953	20,621,474	14,049,721	285,703	11,420,023	1,562,507	1,098,077	235,032
11:00	1,637,589	1,038,012	141,543	2,905,223	12,848,273	23,776,498	22,836,848	731,231	2,836,632	2,512,655	1,652,389	1,737,797
12:00	3,105,631	3,386,780	79,792	5,283,574	11,012,879	27,815,785	22,799,678	1,986,627	32,982,234	3,562,709	2,113,395	1,181,602
13:00	5,553,809	1,381,011	101,216	1,576,585	22,257,746	26,415,554	20,520,063	19,614,131	20,548,074	1,047,493	2,852,355	1,605,911
14:00	4,382,471	1,796,882	43,568	8,340,588	12,784,010	24,665,397	6,182,429	1,794,893	8,888,185	1,868,608	1,011,582	5,029,757
15:00	5,489,225	1,844,263	34,313	10,730,699	5,703,270	54,970,076	8,313,261	1,917,181	6,408,706	611,731	394,259	4,338,191
16:00	4,799,955	537,782	89,667	14,911,471	9,036,106	35,466,078	25,088,543	5,563,764	9,520,605	1,357,517	1,477,407	10,284,799
17:00	1,929,201	226,306	80,975	16,270,472	4,270,016	59,443,884	16,079,785	3,313,756	6,829,636	660,823	1,279,873	11,910,714
18:00	5,922,468	2,225,368	42,979	8,992,511	9,871,907	46,932,849	27,526,360	3,638,341	22,364,066	982,960	1,418,851	8,517,425
19:00	7,057,717	1,697,905	141,955	9,599,433	31,905,900	27,732,694		2,344,480	10,006,036	803,939	3,004,959	12,731,066
20:00	943,192	3,692,778	79,875	3,341,988	17,978,053	117,855,214		2,286,787	22,440,621	264,541	662,525	464,517
21:00	38,694	1,829,320	106,293	5,323,092	15,429,177	66,026,409		5,490,497	10,582,267	1,300,191	874,726	973,009
22:00	5,887	2,129,747	101,869	2,689,330	23,463,745	54,187,046		887,140	18,333,331	3,279,650	137,842	1,161,434
23:00	917,550	1,544,704	82,271	1,121,076	10,869,649	66,961,752		12,856,016	34,315,143	4,074,942	948,063	304,479
0:00		2,214,228	179,853	252,685	12,391,249	81,024,198		2,236,702	11,481,187	810,752	1,347,202	343,406
1:00		1,231,257	143,316	841,089	14,531,928	8,870,047		6,422,386	7,054,009	1,276,381		3,897,107
2:00		3,070,679	472,912	880,046	7,716,388	22,935,940		3,616,899	13,954,233			4,967,223
3:00		3,391,566	127,748	2,314,199	4,248,696	9,135,776		3,718,802	21,586,808			6,355,082
4:00		1,994,950	159,018	1,203,016	6,062,282	6,211,582		4,764,113	775,205			12,646,727
5:00		3,588,087	216,407	1,162,626	8,636,300	19,145,827		1,703,911	5,930,420			5,893,902
6:00		2,030,451	181,387	1,194,139	6,628,886	9,524,962		2,679,469	7,526,249			38,274,004
7:00		2,331,607	118,097	1,258,701	7,592,701			846,919	2,163,764			16,087,463

8:00								648,278				

E. Appendix E – Relative Viral Load per Person

Table E- 1: Raw relative SARS-CoV-2 viral load per person data for all sampling days in the 2020 and 2021 seasons at hourly time intervals.

Time	Missouri State	Kansas	Control (2020)	Oklahoma State	Baylor	Tulane	Western Carolina	Nebraska	West Virginia	Texas Christian	Control (2021)	Iowa State
7:00						0		0		0		
8:00		0	0	0	0	5,036,785	0	1,533,249	0	-36,412		
9:00		2,427,545	139,776	-212,840	18,857,145	-556,209	5,870,268	769,444	-7,755,290	1,338,705		0
10:00	00,000	-1,189,160	25,200	288,256	8,710,371	10,970,014	1,909,249	-300,789	-12,772,429	1,327,448	0	-1,476,332
11:00	185,422	-642,929	87,800	1,400,529	7,446,691	14,125,038	10,696,376	144,740	-21,355,820	2,277,597	554,312	26,432
12:00	1,653,464	1,705,840	26,049	3,778,881	5,611,297	18,164,325	10,659,206	1,400,136	8,789,782	3,327,651	1,015,318	-529,762
13:00	4,101,642	-299,930	47,473	71,892	16,856,165	16,764,094	8,379,592	19,027,640	-3,644,377	812,434	1,754,278	-105,453
14:00	2,930,304	115,941	-10,174	6,835,895	7,382,428	15,013,937	-5,958,043	1,208,402	-15,304,267	1,633,550	-86,494	3,318,393
15:00	4,037,058	163,322	-19,429	9,226,006	301,688	45,318,616	-3,827,211	1,330,690	-17,783,746	376,673	-703,818	2,626,827
16:00	3,347,788	-1,143,159	35,925	13,406,778	3,634,524	25,814,618	12,948,071	4,977,273	-14,671,847	1,122,458	379,330	8,573,435
17:00	477,034	-1,454,635	27,233	14,765,779	-1,131,566	49,792,424	3,939,313	2,727,265	-17,362,816	425,765	181,796	10,199,349
18:00	4,470,301	544,427	-10,763	7,487,818	4,470,325	37,281,389	15,385,889	3,051,850	-1,828,386	747,901	320,774	6,806,061
19:00	5,605,550	16,964	88,212	8,094,739	26,504,318	18,081,234		1,757,989	-14,186,415	568,881	1,906,882	11,019,702
20:00	-508,975	2,011,837	26,133	1,837,294	12,576,471	108,203,754		1,700,296	-1,751,830	29,482	-435,552	-1,246,847
21:00	-1,413,473	148,379	52,551	3,818,398	10,027,595	56,374,949		4,904,006	-13,610,185	1,065,133	-223,351	-738,355
22:00	-1,446,280	448,806	48,127	1,184,637	18,062,163	44,535,586		300,649	-5,859,121	3,044,592	-960,235	-549,930
23:00	-534,617	-136,237	28,529	-383,618	5,468,067	57,310,293		12,269,524	10,122,692	3,839,884	-150,014	-1,406,885
0:00		533,287	126,111	-1,252,008	6,989,667	71,372,738		1,650,211	-12,711,264	575,694	249,125	-1,367,958
1:00		-449,684	89,574	-663,604	9,130,346	-781,412		5,835,895	-17,138,443	1,041,323	-1,098,077	2,185,742
2:00		1,389,738	419,170	-624,647	2,314,806	13,284,480		3,030,408	-10,238,219			3,255,859
3:00		1,710,625	74,006	809,506	-1,152,886	-515,683		3,132,311	-2,605,644			4,643,717
4:00		314,009	105,276	-301,677	660,700	-3,439,878		4,177,621	-23,417,247			10,935,363
5:00		1,907,146	162,664	-342,068	3,234,718	9,494,367		1,117,420	-18,262,032			4,182,537

6:00		349,510	127,644	-310,554	1,227,304	-126,498		2,092,978	-16,666,203			36,562,639
7:00		650,666	64,355	-245,993	2,191,119			260,428	-22,028,688			14,376,099
8:00								61,787				